ENGINEERING
LIBRARY

JUN 19 1950

NUCLEONICS

TECHNIQUES AND APPLICATIONS OF NUCLEAR SCIENCE AND ENGINEERING

June, 1950

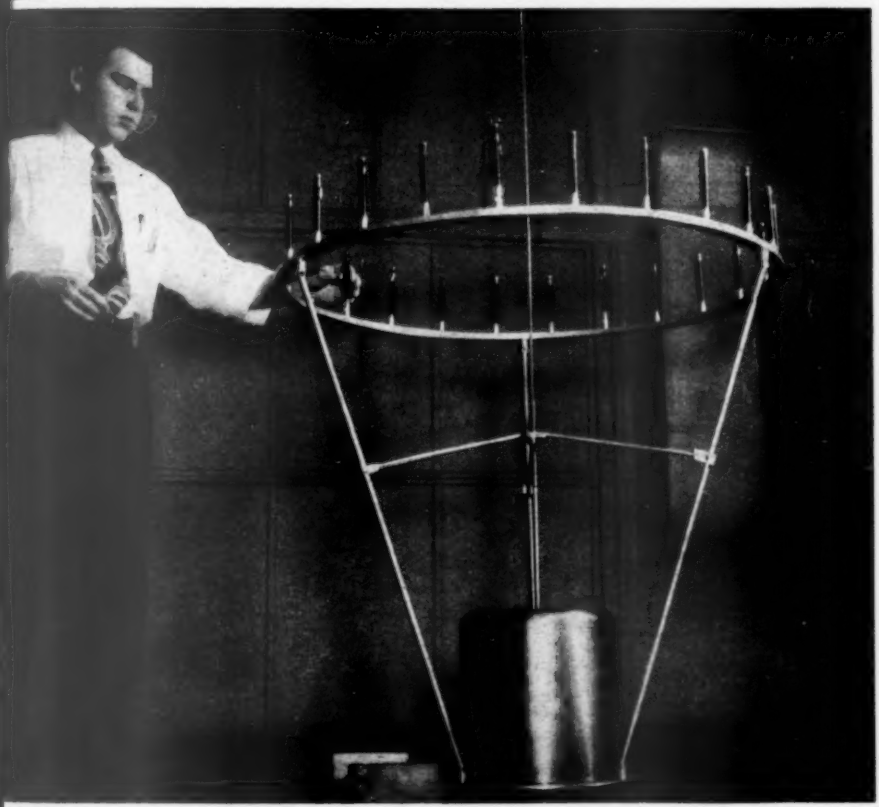

Checking health monitoring instruments; see p. 75

A McGRAW-HILL PUBLICATION

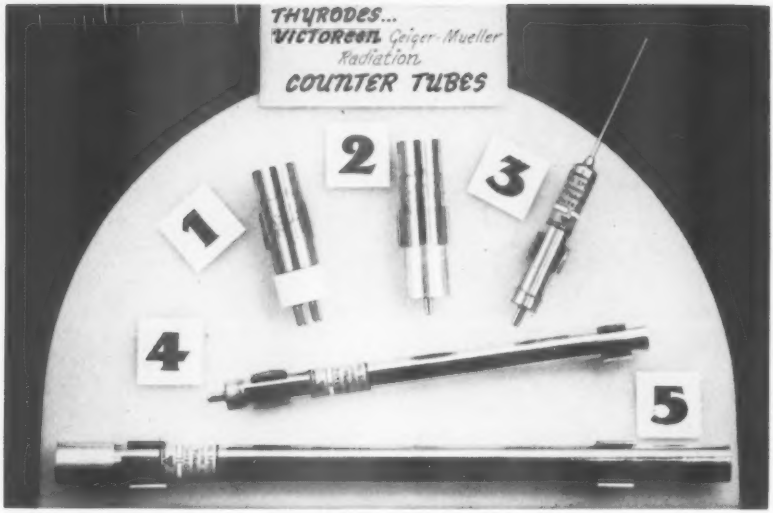

. . . . . *now available*

1. 1B102—Mica window, 2 mg/cm², halogen quenched, operating voltage nominal 900 V, life unlimited by use, four-prong base.

2. 1B106—Mica window, 2 mg/cm², halogen quenched, operating voltage nominal 900 V, life unlimited by use, coaxial base.

3. 1B126—Needle probe type counter, wall thickness 200 mg/cm², operating voltage nominal 900 V, active length 10 mm, coaxial base.

4. 1B124—Cosmic ray counter, wall thickness 300 mg/cm², operating voltage nominal 900 V, active length 16 inches, coaxial base.

5. 1B125—Gamma ray counter, wall thickness 300 mg/cm², operating voltage nominal 900 V, active length 12.5 inches, coaxial base.

THE VICTOREEN INSTRUMENT CO.

5806 HOUGH AVE., CLEVELAND 3, OHIO

NUCLEONICS

JUNE · 1950

Vol. 6, No. 6

Techniques and Applications of Nuclear Science and Engineering

Proportional Counters—I... 5
SERGE A. KORFF

Isotopes in the Study of Chemical Reactions...11
H. R. V. ARNSTEIN and RONALD BENTLEY

Atomic Spectroscopy with Separated Isotopes...28
W. WALCHER

Scintillation Conducting Rods in Tracer Work...37
K. D. TIMMERHAUS, E. B. GILLER, R. B. DUFFIELD, and H. G. DRICKAMER

Irradiation of Small Volumes by Contained Radioisotopes...42
PAUL I. RICHARDS and BENJAMIN A. RUBIN

Pile Neutron Research Techniques—III...50
D. J. HUGHES

Geiger Counter for Civilian Defense Use...56
H. D. LeVINE, H. J. DiGIOVANNI, and M. R. COE

Random Sampling Techniques in Neutron Attenuation Problems—II...60
HERMAN KAHN

INDEX to Volume 6...93

EDITORIAL.....2 CROSS SECTIONS.....66 REFLECTIONS.....72
NUCLEONIC EVENTS....74 BOOKS....79 PRODUCTS AND MATERIALS....82

EDITORIAL STAFF—NORMAN R. BEERS, Editor; JEROME D. LUNTZ, Managing Editor; Ethel Pelzer, Associate Editor; C. J. Mosbacher, Jr., Assistant Editor; Theresa G. Mion, Editorial Assistant; Keith Henney, S. D. Kirkpatrick, P. W. Swain, Consulting Editors; George B. Bryant, Jr., Gladys Montgomery, Washington Office; George C. Tenney, San Francisco Office; Russell F. Anderson, World News

BUSINESS DEPT.—H. W. MATEER, Publisher; WALLACE B. BLOOD, Manager; D. H. Miller, J. Girdwood, New York; Wm. S. Hodgkinson, New England; Warren W. Shew, Philadelphia; C. D. Wardner, Chicago; J. L. Phillips, Cleveland; J. W. Otterson, San Francisco; Carl W. Dysinger, Los Angeles; Ralph C. Maultsby, Atlanta; J. E. Blackburn, Jr., Director of Circulation

NUCLEONICS (with which is consolidated "Atomic Power" and "Atomic Engineering"), June, 1950, Vol. 6, No. 6, Publication Office: 212 East York St., York, Pa. Editorial and Circulation Offices: 330 W. 42nd Street, New York 18, N. Y. Published monthly by McGraw-Hill Publishing Company, Inc. Entered as second class matter December 17, 1947, in the Post Office at York, Pa., under the act of March 3, 1879.

Copyright 1950 by McGraw-Hill Publishing Company, Inc. All rights reserved. Curtis W. McGraw, President; Willard Chevalier, Executive Vice President; Joseph A. Gerardi, Secretary and Treasurer; Paul Montgomery, Senior Vice President, Publications Division; Nelson Bond, Vice-President and Director of Advertising; J. E. Blackburn, Jr., Vice President and Director of Circulation.

Allow at least ten days for change of address. All communications about subscriptions should be addressed to Director of Circulation, 330 W. 42nd St., New York 18, N. Y. Price per copy $1. Subscription rates: United States and U. S. Possessions $10 for 1 year, $16 for 2 years, $20 for 3 years. Canada $15 for 1 year, $25 for 2 years, $30 for 3 years. Latin America $20 a year. All other countries $25 a year. Member A.B.P. Member A.B.C

Education in Atomic Energy

I—IMPLICATIONS OF INDUSTRIAL ATOMIC POWER

ADVANCES IN SCIENCE and technology readily influence our daily lives. But it frequently takes many years before the effect of these advances is felt by that which made them possible—the educational system, the producer of the scientists and engineers.

For example, in the field of electrical engineering, many years passed between the time when it looked as if electronics were here to stay and the time when this fact was acknowledged in the curricula.

There is already evidence in the atomic energy field that this lag will not be duplicated. One prominent university recently announced its plans for an extensive undergraduate curriculum in nuclear engineering. And others are giving it thought. We must be careful, however, that we do not move too fast. What is needed first is some "market research" into the future market for nuclear engineers.

The atomic "industry" is less than a decade old, but already employs about five percent of the nation's technical personnel and has an increasing need for qualified workers. We do not yet know how these additional personnel should be educated. We do not know what their background should be. Should it be broad or should it be specialized? The answer to this question must be dictated by the needs of the field.

Before we can choose our direction in the field of atomic energy education, we must know these needs. One effort to study the situation got under way this month. A five-man regional committee of the American Society for Engineering Education, organized to study the problem, held an exploratory meeting with members of the Atomic Energy Commission in Washington. We hope that this group will learn enough about the needs of the atomic energy field to stimulate intelligent curriculum planning by interested colleges and universities.

Determination of a proper course of action was made more difficult recently when study of the important question of whether or not we are going to have an atomic power industry was, in effect, shelved. The sudden shift in the reactor program of the Knolls Atomic Power Laboratory was evidence of this shelving. The answer to the question of when (or whether) we are to have industrial atomic power is now nowhere in sight.

The importance of atomic power is emphasized by the recent statement of an AEC official:

"We have been convinced from the start that the atomic energy business was either going to be a business, or not, depending upon whether or not reactors turn out to be really useful in the industrial life of the country."

It is obviously important that, before we initiate any extensive program of educating students for ultimate employment in work on reactor technology, we make a serious effort to evaluate whether there is a future in industrial reactors or whether the only future lies in the field of military applications.

All groups interested in this problem—the teachers and the students, both academic and industrial—need this information. Dr. Philip N. Powers, AEC adviser on scientific personnel, recently said:

"Depending upon the amount of specialization, somewhere between four and ten years are required to train a scientist. Decisions as to fields of study may therefore be made as much as eight years before the training is to culminate in professional employment. It is manifestly unlikely that individuals will make all these decisions in proper proportion to the demand developing years ahead—particularly if whole new fields open up in the meantime . . . Students . . . should have the facts that will help them to judge what future demands may be for work in the various fields in which they may be interested."

We fully realize that, had an all-out attack on the problem of industrial atomic power been made since the end of the war, the information needed by educators might still not be available. But placing our direct efforts on the construction of military reactors and indirect efforts on "civilian" reactors does not bring us any closer to the answer.

Commissioner Pike, acting chairman of AEC, recently said:

"In the over-all interest of the American people, it [study of industrial atomic power] has got to be done. You have got to go through this period to see whether you can answer these questions or not."

—Jerome D. Luntz

SCIENCE NEWS FROM GENERAL ELECTRIC

delay lines

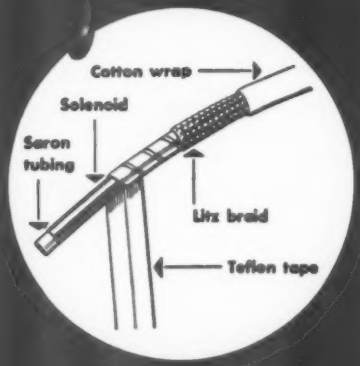

—to aid you in developing special circuits for electronic devices

By enabling you to delay electrical signals for any desired length of time over the range from 0.25 to 3.00 microseconds, General Electric delay lines aid you in developing special circuits. Applications include:

- rendering receivers insensitive for a time-interval following a transmitter signal
- generating pulsed signals of predetermined and definite width
- delaying oscilloscope signals with respect to servo sweep and for single-pulse transients

Write for Bulletin GEC-459. Apparatus Dept., General Electric Co., Schenectady, N.Y.

GENERAL ELECTRIC

687 12D

PROPORTIONAL COUNTERS—I

Detecting one type of radiation and distinguishing it from another—counting alpha particles in the presence of betas, for example—is easily done with proportional counters. The important factors of gas amplification and limited proportionality are clearly described in this article.

By SERGE A. KORFF

Department of Physics, New York University
New York, New York

PROPORTIONAL COUNTING had its inception in 1908 when Rutherford and Geiger, working at the Cavendish Laboratory in Cambridge, England, devised a new means (*1*) for detecting alpha and beta particles. The device they used consisted of a cylinder and an axial wire, a potential difference being applied between these two electrodes. The wire was connected to an electrometer, and changes in the potential of the wire were registered by the needle of the electrometer.

The electrometer needle gave deflections which corresponded to the passage of alpha particles through the device. At somewhat higher voltages these deflections were larger, and the passage of beta particles also produced pulses. At still higher voltages, still larger pulses were produced, and the possibility of distinguishing between alpha and beta pulses disappeared. Thus Rutherford and Geiger discovered, in the early experiments, the main properties of what are called today "proportional counters," and also Geiger counters. Only proportional counters will be considered in this article.

In 1928, Geiger and Klemperer (*2*) further developed the use of proportional counters. Indeed, proportional counters are often referred to, especially in the early literature, as "Geiger-Klemperer counters." It remained to develop the theory of these instruments, and to find the optimum design and operating characteristics. This development is outlined in following paragraphs.

The purpose of a proportional counter is to detect atomic and nuclear particles, and to distinguish one kind from another. These operations are performed by the counter itself, and the results are presented in the form of pulses of voltage on the central wire system. These pulses can be picked up by electronic amplifying systems, and can be further amplified and used to operate various kinds of recording systems.

Different kinds of particles are usually distinguished from each other by the varying size of the pulses they produce. The electronic recording devices are therefore usually made capable of recording the number of pulses of a particular size, or the number occurring within a prescribed size-interval.

In the earliest experiments, and also most generally today, the geometrical arrangement of the electrodes was cylindrical. It is apparent that other geometrical arrangements may also be used. Spherical symmetry has been used, as has a system of parallel plates

between which the field is uniform. These and other geometrical modifications may be made whenever experimental conditions make them desirable. The principle of the operation is the same; for convenience, only the cylindical arrangement will be described here. The counters themselves are the subject of this article. The auxiliary circuitry will be considered in another article.

Theory of Proportional Counting Action

Consider a cylinder with a wire arranged along its axis, the whole contained in a suitable envelope that is filled to a pressure p with a gas or combination of gases, the nature of which will be discussed presently. Let the central wire be connected to a device capable of detecting abrupt changes in its potential, and let a voltage V be applied across the counter, *i.e.*, between the cylinder and the wire. Assume that the wire is positive and the cylinder negative; electrons formed in the gas will drift toward the wire, and positive ions toward the cylinder. Let the device be exposed to a flux of particles, say for example, alpha particles, which it is desired to detect. It is assumed that the envelope is so arranged that the particles can reach the interior of the cylinder.

Certain terms used in the following consideration of the theory should be delineated. Define the term "ionization" as meaning any process whereby a previously uncharged atom or molecule acquires a charge, or whereby electrons are liberated in the counter. Also, define "radiation" as consisting of either electromagnetic radiation, or of streams of charged or neutral particles, such as electrons, alpha particles or neutrons. In addition, define the "primary" as that entity which initiates the counter action in any given case, and the "initial ionizing event" as that event, produced by the primary, in which ionization is produced in the counter. Thus a primary photon may eject a photoelectron from the walls of the device or from an atom of gas; a heavy particle may produce many ions as it passes through the gas or strikes the wall; or a neutron may cause, as its ionizing event, the disintegration of a boron nucleus with the resulting emission of an alpha particle.

According to the theory proposed by Rose and Korff (*3*), proportional counter action can be described as follows: When the primary has produced the initial ionizing event, the electrons and positive ions find themselves in the field produced by the voltage V, and will accordingly start to drift toward the appropriate electrode. Consider first the electrons, which drift toward the central wire. The field at any point defined by a radius r, inside the counter, is given by the relation

$$E = V/r \log (r_2/r_1) \qquad (1)$$

where E is the field, in volts per cm, V the applied voltage, and r_2 and r_1 are the radii of the cylinder and the wire, respectively. It is apparent that this field, increasing as it does with the inverse first power of the radius r, will be of modest proportions except near the central wire. In this region it will increase very fast as the wire is approached, especially if the wire is thin.

A typical case is cited in the table on this page, where the field in a counter is evaluated at various radii. In this

Evaluation of Counter Field

Radius from wire center cm	*Field volts per cm*
5×10^{-3} (wire surface)	37,400
0.01	18,700
0.05	3,740
0.1	1,870
0.5	374
1.0 (at cylinder)	187

table the voltage is assumed to be 1,000 volts across the counter, the cylinder is taken as having a radius of 1 cm, and the wire a radius of 5×10^{-3} cm, corresponding closely to the four-mil wire often used in practice.

It is immediately apparent from the table that the high-field region is very close to the central wire. In this region the electron will experience strong forces, and will acquire a large amount of energy in a short distance. It may be accelerated, in one mean-free-path, by an amount sufficient to enable it to make ionizing collisions and thus to produce new ionization.

At low applied voltages the electrons formed in the counter will drift toward the central electrode without making ionizing collisions as they go, and will arrive and be collected upon the wire. At higher applied voltages, such as the case considered above, the electrons in the high-field region near the wire will make collisions of increasing severity with the target atoms, until finally these are ionized by collision. As soon as ionization by collision starts, two electrons are in evidence—the original one plus that liberated in the collision. These two electrons proceed toward the wire, making further collisions. Since the field increases toward the wire, if any one collision is ionizing, all subsequent collisions will also produce ionization. Since two electrons are available after each collision, there will be progressively more electrons produced as the initial one travels toward the wire, and an "avalanche" of electrons is said to have been formed.

The arrival of this avalanche of electrons on the central wire produces a change in the potential of the wire. The voltage of the central wire will change by an amount given by dV in volts where

$$dV = ANe/C \qquad (2)$$

where N is the number of ion pairs (electrons and positive ions) produced in the initial ionizing event, A is the number of additional electrons produced by collision processes plus the original one, e is the charge of the electron, and C is the distributed capacity of the central wire and those portions of the detecting circuit connected electrically to it. A is called the "gas amplification," and, as indicated previously, may vary from unity to a large value up to many millions. It represents the additional electrons produced by the collision processes. A value of A equal to unity means that the original electrons are collected but no new ones are formed.

If dV is to be in volts, then e should be in coulombs (the charge on the electron is 1.6×10^{-19} coulombs), and C in farads. Both N and A are pure numbers. For example, if A is 1,000, as it might be in the proportional range, and if the particle produces an N of 100 ions during its traversal of the counter, and if the distributed capacity of the counter and circuit is 10 $\mu\mu$f, then the pulse dV will be 1.6×10^{-3} volt. Such a pulse is not at all difficult to detect; it requires no great amount of vacuum-tube amplification to render it usable.

The gas amplification A is well known in gas-discharge phenomena. Townsend's original discussion of the formation of an electron avalanche leading to a spark utilizes basic arguments very similar to those just given. Consider an electron advancing in a gas toward the positive electrode, in a field sufficiently great that the electron will make ionizing collisions. If α is the number of ion pairs per centimeter produced by this electron, the number of new electrons dN formed in a distance dx will be given by:

$$dN = \alpha N dx \qquad (3)$$

This equation can be integrated immediately providing that α is independent of x:

$$N = N_0 e^{\alpha x} \qquad (4)$$

where N_0, the constant of integration,

is the number of original electrons. Now N is the number of electrons arriving at the positive electrode after having gone a distance x through the gas. Starting with a single electron, N_0 is unity, and the number N is, by definition, the same as the gas amplification. Then

$$A = e^{\alpha x}$$

or, more generally, since in a counter α may depend on x, and since the number of ionizing collisions will depend on the energy, which in turn will increase as the electron enters the high-field region near the wire,

$$A = e^{\int \alpha dx} \qquad (5)$$

which serves to relate the first Townsend coefficient to the gas amplification. Numerical values of α for many differing conditions have been evaluated and will be found in the literature (*4*).

Applying this argument to the case of a counter, it has been shown by Rose and Korff (*3*) that A can be evaluated in terms of the parameters usually known in the case of proportional counters. They have shown that A will be given by

$$A = \text{exp. } 2(aNcr_1V)^{1/2}[(V/V_p)^{1/2} - 1] \qquad (6)$$

where N is the number of atoms per cm³ in the counter, c is the capacity of the counter, r_1 is the wire radius, V is the potential applied to the counter, V_p is the threshold voltage for proportional counter action, and a is the rate of increase of ionization cross section with energy, in cm² per volt. Here a has been determined by various observers, and lies between 0.11 (for helium) and 1.81×10^{17} (for argon), with an average value of 0.7 for N_2. It is clear that the exponential approaches zero, i.e., A approaches unity as V approaches V_p. Moreover, we should expect the curves of A against V to be straight lines or semilog plots.

These expectations are well verified by experiment. The actual values of A have been measured by a number of observers and are shown in Figs. 1 and 2. The predicted dependence on wire size, on counter voltage, and on the pressure and composition of the gases in the counter have also been verified experimentally by direct measurement.

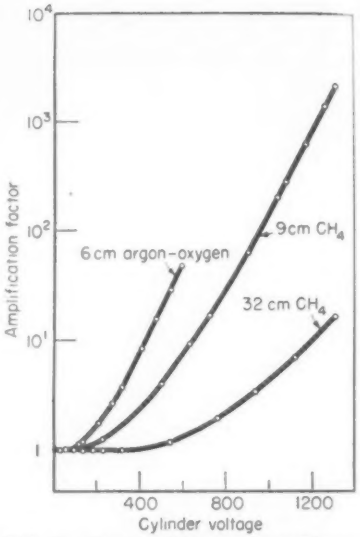

FIG. 1. Gas amplification factor (logarithmic scale) vs cylinder voltage for 6-cm argon-oxygen ($0.94A + 0.06O_2$) and for two pressures of CH_4

Amplification Limit

How far may this theory be carried? That is, what are the experimentally significant limits on the excursions of the variables? The extension to large values of A will be limited by several factors. At large values of A, the assumptions used in deriving Eq. 6 are no longer valid, and this equation no longer correctly expresses the dependence of pulse size on various parameters. The main effect is the increasing role played by space charge in limiting the size which an avalanche can attain. The point is that as the avalanche gets bigger, the effect of the

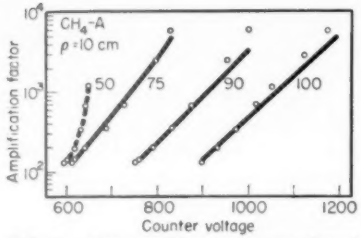

FIG. 2. Gas amplification factor plotted against counter voltage for various relative concentrations in CH_4-A mixtures at 10-cm pressure. Points are experimental; full curves are theoretical. Numbers affixed to curves give relative concentration of CH_4 in percent

cloud of positive ions becomes increasingly important and distorts the field inside the counter.

When only one or two ion pairs are formed, the electrons which have a high mobility move rapidly away from the positive ions, and usually get to the central wire before the heavy positives have had time to drift appreciably. One or a few positives will produce only local fields, and the electron will soon be far enough away that the only field affecting its motion is that produced by the voltage across the counter. If we consider a single electron one mean-free-path (say 10^{-4} cm) from a positive ion, the field at the electron due to the ion will be less by at least two orders of magnitude than the field in the counter produced by the applied voltage. Hence the applied voltage will be the controlling factor.

When, however, many positives are present, they will distort the field; since the positives will be between the electrons and the cylinder, the electrons will be in a field controlled by the positive-ion space charge. This space charge limits the ultimate growth of the avalanche, and indeed is responsible for "quenching" the discharge.

The details of this process have been presented by C. G. and D. D. Montgomery (*5*). As they have pointed out, it is this phenomenon and not the external quenching circuit which terminates the discharge. The counter then stays "quenched" if the discharge is not reinitiated. The mechanism of the reinitiation, and the role played by the organic vapors in this process, have been considered in detail by Korff and Present (*6*).

Consequently Eq. 6 can be expected to break down—to predict relations departing increasingly from those observed—as space-charge effects become increasingly important. In practice, therefore, one expects to find that the pulse size is correctly predicted when the value of A is in the range starting at unity and extending up to 10^4 or 10^5. As the gas-amplification grows to still greater values, we find that the larger pulses, i.e., those starting with a larger original N_0, will not increase as fast with increasing voltage as those of smaller size. In the limit, the pulses will converge in size, and by the time values of A of 10^7 or 10^8 have been reached, the pulse size will be controlled entirely by the space-charge mechanism and will be independent of the number of ions formed in the initial ionizing event. The counter is said then to be operating as a Geiger counter, or in the Geiger region. A counter operating in this manner can no longer be used to distinguish between types of particles or to measure specific ionization. It counts the number of particles producing one or more ions inside its sensitive volume, and presents the total number to the electronic circuitry.

Limited Proportionality

The voltage region of proportional operation does not have an abrupt transition into the Geiger region, but slides gradually into it. The voltage range in which space-charge effects have started to make themselves felt,

but have not assumed complete dominance of the phenomena, is called the region of limited proportionality. This means just what the words suggest—that in this region a large initial ionizing event produces a pulse only a little larger than a small event. If, for example, an alpha particle produces 30,000 ions in the counter and an electron produces ten, then the ratio of the pulse sizes is less than 3,000 to 1. Since it is still possible to distinguish pulses if they differ in size by much less than this ratio, the region of limited proportionality is a useful one, and it is possible to use counters in this region to distinguish between large and small initial events.

A counter's ability to distinguish between sizes of events will diminish as the size of the events increases. The same counter which might not be able to tell an alpha particle producing 30,000 ion-pairs inside it from a proton producing 10,000, might, at the same operating voltage, still be able to separate a slow meson producing 300 ions from a faster one producing 100; the factor of size difference, three, is the same in both cases. The pulses produced by the meson will, of course, be smaller than those produced by the proton. If desired, the pulse size can be increased either by applying additional vacuum-tube amplification, or by increasing the counter voltage. But if the counter voltage is increased, the counter will operate further up in the region of limited proportionality, and may lose the ability to separate the events readily distinguishable at the lower voltage.

Thus the region of limited proportionality is useful, as in this region (*a*) the pulses are quite large, and the vacuum-tube amplification necessary to operate subsequent electronic equipment is modest; and (*b*) the counter retains its ability to distinguish between events. But it must be borne in mind when using a counter in this region that the discriminating property of the counter is not as good as it is at lower voltages.

Dead-time Comparison

One of the important properties of a proportional counter is that it operates very fast, many times faster than an ordinary Geiger counter. To make this statement stronger, let us say that a counter operated in the proportional voltage region operates much faster than the same counter operated with a higher voltage across it in the Geiger region. The increase in speed is a factor between ten and a hundred, depending on such parameters as geometry, voltage, filling-gas, and where the initial ionizing event takes place in the counter.

Most Geiger counters have a dead-time and a resolving-time of the order of 100 or 200 μsec. This time is determined by the time taken by the positive ion sheath to move out, first to a distance such that the field near the wire starts to recover, and finally all the way to the cylinder. Since the velocity of these ions in the counter is of the order of 10^4 cm/sec, it takes of the order of 100 μsec for them to move a centimeter or two. Now, in a proportional counter, especially when operating at low values of A, the start of the development of the pulse on the central wire does not depend on the motion of the positive ions, but on that of the electrons. These have been discussed in detail by Korff (*7*) and have been estimated as producing a pulse on the central wire in between $\frac{1}{10}$ μsec and 10 μsec after the initial ionizing event. Moreover, in the proportional counter, the field near the wire is disturbed by the count only in one small region, and the rest of the wire is ready to receive additional counts at all times. Hence a second

(*Continued on page 36*)

Isotopes in the Study of Chemical Reactions

This review summarizes a great many reaction mechanisms investigated with isotopes over the past thirty years and cites significant contributions which the tracer technique with deuterium, heavy nitrogen, and isotopic carbon has made to our better understanding of chemical reactions as a whole.

By H. R. V. ARNSTEIN and RONALD BENTLEY

National Institute for Medical Research
Mill Hill, London, England

STUDY OF CHEMICAL REACTIONS with the aid of isotopes was begun as early as 1920. In that year, Hevesy and Zechmeister used thorium B to label lead; with the use of this tracer, they demonstrated that there was no exchange between lead ions and the lead atoms of lead tetraphenyl in amyl alcohol solution (*1*).

When the stable isotopes of hydrogen, oxygen, nitrogen and carbon were made available in the 1930's, it became possible to investigate many more reactions in considerable detail. Under the usual laboratory conditions, the added isotopic atoms were not separated from the normal atoms; since the isotope could be detected by reason of its different physical properties (mass or radioactivity), a particular atom could be simply and beautifully traced by its isotope label.

Although the major application of both stable and radioactive isotopes has been in biochemical research, the isotope technique has been used (to quote a few examples) to study structures of compounds, mechanisms of reactions and the activity of surfaces.

In this paper, those reaction mechanisms will be discussed that have been studied with the following tracers: deuterium (D), heavy nitrogen (N^{15}), and three carbon isotopes (C^{11}, C^{13} and C^{14}). For the sake of convenience, the reactions have been grouped under the particular isotope used.

Before proceeding to these detailed descriptions, consideration of an early application of O^{18} to the study of reaction mechanisms will introduce the subject more generally and illustrate a number of fundamental principles. Since reaction mechanisms studied with O^{18} have recently been discussed in NUCLEONICS and elsewhere (*2*), the use of this tracer will not be discussed further in this review.

In the saponification of an ester, the oxygen atom of the alcohol could be derived by either of the following processes:

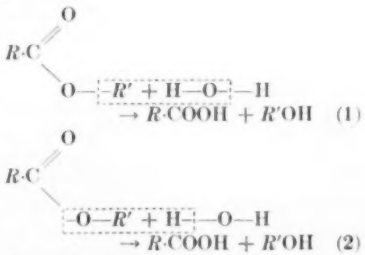

Independent evidence (e.g., the retention of optical activity in R') suggested that the mechanism of Reaction 2 prevailed. Direct proof that this was the case was provided by the alkaline

hydrolysis of *n*-amyl acetate in H_2O^{18}. No excess O^{18} was detected in the amyl alcohol (*3*).

$$CH_3COOC_5H_{11} + H_2O^{18} \rightarrow C_5H_{11}OH + CH_3COO^{18}H$$

Conversely, it was shown that during esterification, the oxygen atom of the alcohol was not eliminated as water (*4*).

$$C_6H_5COOH + CH_3O^{18}H \rightarrow C_6H_5COO^{18}CH_3 + H_2O$$

These investigations serve to exemplify the two main methods of utilizing the technique. Either (as in the latter case) a labeled compound is prepared, or (as in the study of saponification) the reaction is carried out in the presence of an isotope-containing solvent. In either case, account must be taken of the fact that many organic and inorganic compounds take up D or O^{18} when dissolved in water containing an excess of these isotopes. In this way, their own H or O atoms may be exchanged with those of the solvent.

Thus, for example, the hydrogen of carboxylic acids is rapidly replaced by D when the acid is dissolved in D_2O (*5*):

$$R\text{·}COOH + D_2O \rightarrow R\text{·}COOD + HDO$$

Exchange reactions can therefore complicate the interpretation of many experiments, and careful control experiments are almost always essential. By themselves, exchange reactions can be used to provide information about the nature of chemical bonds, the reactivity of particular atoms, and the structure of a compound. They can also be used to obtain labeled compounds (*6*).

So that hydrogen atoms will exchange under mild conditions, some kind of "activation" is necessary. The hydrogen atoms of saturated hydrocarbons do not exchange with water; the highly unsaturated acetylene, however, exchanges hydrogen atoms in alkaline solution, but not in water alone or in *N* phosphoric acid (*7*). The hydrogen atom of the aldehyde group exchanges slowly with water (*8*).

Hydrogen of carbon atoms adjacent to ketone groups also undergoes exchange, the reaction being markedly catalyzed by alkali. The mechanism of this reaction involves the rapid exchange of the acidic hydrogen of the enol form, coupled with the mobile equilibrium between the keto (*I*) and enol (*II*) tautomer (*9*), as shown in the reaction at the bottom of this page. For such base-catalyzed reactions, the activating factor is often the presence of unsaturation (as in the case of acetylene) or a high concentration of positive charges on an adjacent carbon atom (e.g., ketones). Acid-catalyzed hydrogen exchange reactions (e.g., introduction of deuterium into the benzene ring) are facilitated by the presence of adjacent electron-repelling substituents (*10*).

Carbon-bound deuterium atoms are usually classified as (a) *stable*, (b) *semilabile*, and (c) *labile*. A similar classification can be applied in the case of oxygenated compounds. In considering the replacement of a hydrogen or oxygen atom, it is therefore necessary to consider at the same time the stability of the atom to ordinary exchange processes of the type just discussed.

Reaction mechanisms are discussed on the following pages for studies involving deuterium, heavy nitrogen, and isotopic carbon (radioactive as well as stable). These are the isotopes which have found the widest applications.

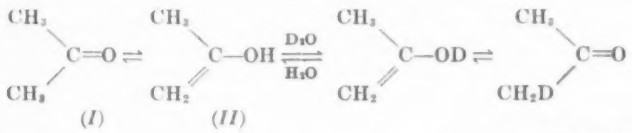

Study of surface reactions: Closely following its isolation, deuterium was used to investigate surface reactions. The equilibrium reaction between hydrogen and deuterium was studied on a variety of surfaces (*11*). Glass and mercury surfaces did not catalyze the reaction, nor did charcoal at liquid air temperature. Equilibration took place over palladium at 270° C and with chromium oxide and nickel catalysts at much lower temperatures (−190° to 110° C). It was concluded that an activated adsorption of atomic hydrogen had occurred, rather than a molecular adsorption. The interpretation of these results may be summarized by a quotation from H. S. Taylor. "The acceleration is not merely due to concentration of the reactants by van der Waals adsorption since charcoal which shows large van der Waals adsorption is inactive. There are therefore areas of low activation energy and low binding energy, capable of producing chemical reactions, which are not revealed by the ordinary processes of study of adsorption phenomena because their existence is obscured by the preponderant van der Waals specific adsorption occurring at the low temperatures in question." (*12*)

The reaction between benzene and HD was investigated. It was found to take place over platinum black and nickel catalysts, and was more rapid than the hydrogenation of benzene (*13*).

$$C_6H_6 + HD \rightleftharpoons C_6H_5D + H_2$$

Similarly, the speed of reaction of HD with ethylene over a nickel catalyst (at 120° C) was found to be comparable to that of the hydrogenation of ethylene to ethane (*14*).

$$C_2H_4 + HD \rightleftharpoons C_2H_3D + H_2$$

It was suggested in this case that a radical, $=C=C=$, was adsorbed on the catalytic surface, and that reaction took place with H or D atoms as the C_2H_3D molecule was reformed. A second possibility was that the adsorbed molecule was $C_2H_2^-$ (or $C_6H_5^-$ in the case of benzene).

An exchange of deuterium takes place between methane and deuteromethane on nickel catalysts at temperatures as low as 138° C (*15*). It has more recently been found that the same reaction takes place on silica-alumina cracking catalysts at temperatures > 345° C (*16*). This finding supports the theory that in cracking petroleum hydrocarbons on such catalysts the process is initiated by breaking at least one C-H bond. Unless this takes place, it is difficult for the hydrocarbon carbon core to come sufficiently close to the catalytic surface. It seems probable therefore, that the initial reaction is rupture of C-H bonds, followed by that of C-C bonds.

Photochemical reactions: Deuterium has found a rather limited application in the study of photochemical reactions. It was used in 1934 to demonstrate the reversibility of the first step in the photolysis of ammonia (*17*). This initial reaction is as follows:

$$NH_3 + h\nu = NH_2 + H$$

However, a low quantum yield was obtained, and this was thought to be due to the back reaction. Since the ultraviolet absorption spectra of ammonia and the deuteroammonias (NH_2D, NHD_2 and ND_3) are easily distinguished, a means was available to investigate this possibility.

When NH_3 was decomposed in the presence of deuterium, the spectra changed from that of NH_3 to that of an equilibrium mixture of NH_2D, NHD_2 and ND_3. A possible explanation was that ammonia itself reacted with atomic deuterium: this

reaction was shown to be of a low probability compared to the back reaction $NH_2 + D = NH_2D$.

The photolysis of acetic acid to methane and carbon dioxide was studied with CH_3COOD dissolved in D_2O; light of wavelengths between 2,000 and 2,400 A.U. was used (*18*). The formation of methane by hydrogenation of methyl groups with a hydrogen atom derived from the carboxyl group or the solvent took place to the extent of about 30%. In a second process which was also discovered, the ultraviolet energy was used to split C-C bonds; the methyl radicals formed reacted with carbon-bound hydrogen to form methane. The decomposition of the double molecules of acetic acid proceeded mainly by this latter mechanism.

Study of tautomeric changes: Deuterium has perhaps found its most valuable application as an indicator in the study of tautomeric changes where the migration of hydrogen atoms is involved.

In 1935, it was shown that while butyric and crotonic acids did not exchange carbon-bound hydrogen atoms with D_2O, there was considerable exchange with vinylacetic acid (*19*). Further, there was a parallelism between the exchange and extent of tautomerization. (Crotonic acid tautomerized to the extent of 2% only; with vinylacetic acid, the extent was 98%.) It was suggested, therefore, that a proton was removed from the α carbon atom of vinylacetic acid by a protophilic solvent. Following an internal electronic rearrangement, a deuteron re-entered in the γ position, in a statistical ratio which was determined mainly by the composition of the solvent (but which could be subject to isotope discrimination). Since the solvent plays an important part, the tautomerism must be intermolecular.

It was later shown that the exchange reaction of vinylacetic acid proceeds at a faster rate than the tautomerism, indicating that the isomerization is a bimolecular process (*20*).

Experiments on the isomerization of cyclohexenyl acetonitrile (*III*) showed that this also was a bimolecular process (*21*).

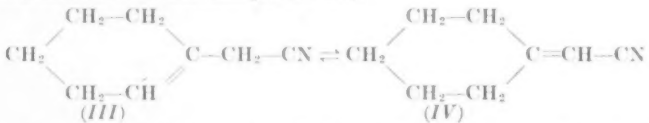

(*III*) (*IV*)

When the $\beta\gamma$ isomer (*III*) was dissolved in D_2O, the exchange of two hydrogen atoms was much more rapid than the isomerization to the $\alpha\beta$ isomer (*IV*). However, when the $\alpha\beta$ compound (*IV*) was similarly dissolved in D_2O, a very small uptake of deuterium took place initially and was ascribed to the presence of an impurity; no further deuterium was taken up after several hours [a period of time which would have allowed a considerable conversion of (*III*) to (*IV*)]. These results were explained by assuming that the initial process was the removal of the α hydrogen atom from (*III*). The rate at which the ion so produced reverted to the less stable $\beta\gamma$ form (*III*) must have been much greater than that at which it was converted to the more stable $\alpha\beta$ compound (*IV*).

The *cis* and *trans* glutaconic acids provide an example of tautomerism in which, owing to symmetry, the tautomeric individuals are identical.

$$X{\cdot}CH_2{\cdot}CH{=}CH{\cdot}X \rightleftharpoons X{\cdot}CH{=}CH{\cdot}CH_2{\cdot}X \quad (X = CO_2H)$$

The exchange between these acids and D_2O in the presence of excess alkali showed that three H atoms were involved in accordance with the modern views on tautom-

erism (*22*). The reaction was considered to proceed through a mesomeric ion (*V*).

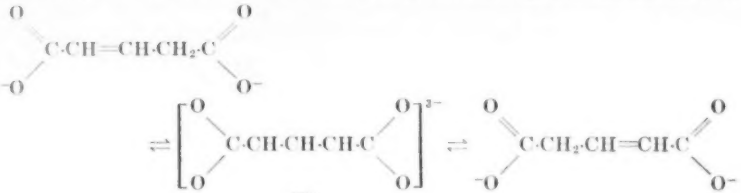

(*V*)

At equilibrium, the interchange was identical for both the *cis* and the *trans* compound. At 20° C and in one hour, the *cis* acid exchanged four times more rapidly than the *trans* acid under the same conditions. To explain this fact, the authors suggested that ionization of the H of the methylene group could take place through hydrogen bond formation (*VI*).

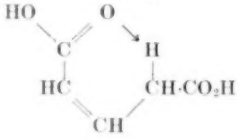

cis
(*VI*)

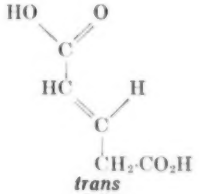

trans
(*VII*)

Important information about tautomerism has been obtained by measurement of the rate of deuterium exchange and the rate of a simultaneous isomerization. The rate of deuterium exchange is a measure of the rate of ionization by loss of a proton. It is often found that the rate of ionization and isomerization are the same. This leads to the conclusion that, in these cases, loss of a proton is the first step in the rearrangement.

Thus, in 1938 it was shown that the rate at which *l*-phenyl β-*n*-butyl ketone exchanged its H atom was nearly the same as the rate of racemization under the same conditions (*23*). (Dioxan-D_2O was used as the solvent, and OD^- as catalyst.) It was concluded, therefore, that racemization and the exchange reaction were controlled by the same fundamental process, ionization of the ketone.

A similar study was the racemization of phenyl *p*-tolylacetic acid (*24*). When optically active phenyl *p*-tolyldeuteroacetic acid was racemized with excess alkali in aqueous solution, loss of optical activity occurred at the same rate as loss of deuterium. With phenyl *p*-tolylacetic acid in 3% D_2O, loss of optical activity was more rapid than in the previous case, and faster than the accompanying exchange reaction. The rate of racemization could be identified with the rate of ionization of the α D and H atoms, respectively, and it was concluded that the reaction proceeded by this ionic mechanism.

A more elaborate study of this nature was that of the mechanism of the Wagner-Meerwein isomerization (*25*). The rearrangement of camphene hydrochloride (*VIII*) to *iso*-bornyl chloride (*X*) (chloroform as solvent) was studied with DCl labeled with radiochlorine. By comparison of the rates of rearrangement and exchange of D and Cl*, it was shown that there were two steps to the reaction: first, a rapid establishment of ionic equilibrium by separation of Cl^-, taking place

under conditions (20° C) where no rearrangement occurred; and, secondly, a slow bimolecular reaction between the ion (*IX*) and a molecule of HCl.

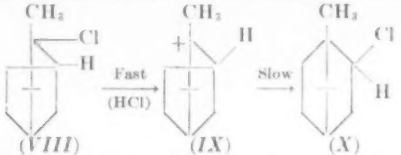

(*VIII*) (*IX*) (*X*)

A more general discussion of this rearrangement has been given by Dostrovsky, Hughes, and Ingold (*25*).

A study of the tautomerism of azomethines used the measurement of rates of ionization and of deuterium exchange under uniform conditions (EtOH-EtOD mixtures containing NaOEt) (*27*).

$$p\ MeOC_6H_4CH_2{-}N{=}CHPh \rightleftharpoons p\ MeOC_6H_4CH{=}NCH_2Ph$$
(*XI*) (*XII*)

Earlier (optical) evidence had suggested that the interconversion was due to a simultaneous abstraction and addition of a proton. This would have produced exchange at each act of isomerization. However, the exchange in (*XII*) [and possibly (*XI*)] was greater than could be accounted for by isomerization alone. The authors suggested an additional exchange mechanism (simultaneous proton transfer at the same carbon atom) to account for direct replacement without isomerization:

In 1940, the method was extended to a system where the isomerides were present in commensurate amounts—the earlier studies usually involved systems where one isomer predominated (*28*). Kinetic data established that Δ^{α}-pentenoic acid came into equilibrium with the Δ^{β} acid (and β-hydroxyvaleric acid) by reversible pseudo-unimolecular reactions: Each acid was in direct equilibrium with the other two. Isomerization was mainly by direct prototropic change (and to a lesser extent via β-hydroxyvaleric acid as intermediate). With the Δ^{α}-pentenoic acid in D_2O, it was shown that a bimolecular mechanism was involved in the direct prototropic isomerization.

In concluding this section, reference must be made to the comprehensive discussion of isotope exchange and the mechanisms of heterolytic substitution given by Ingold and his colleagues in 1948 (*29*).

Condensation reactions: During aldol condensation of acetaldehyde in D_2O solution, no D is taken up in combination with carbon (*30*). The rate of reaction is first order with respect to acetaldehyde and nearly proportional to [OH]. The probable mechanism is:

$$CH_3CHO + B \rightleftharpoons [H_2C{\cdot}CHO]^- + BH^+ \quad (1)$$
$$[H_2C{\cdot}CHO]^- + CH_3CHO \rightleftharpoons [CH_3CH(O)CH_2CHO]^- \quad (2)$$

If Reaction 2 were the rate-determining step, Reaction 1 would be expected to be rapid and reversible, and uptake of D into C-D bonds would be faster than the condensation. Reaction 1 is therefore rate-determining. Similarly, there is no D uptake during hexose formation from glyceraldehyde or a mixture of glyceraldehyde and dihydroxyacetone.

In the case of acetone, although only a small amount of diacetone alcohol is

present at equilibrium, it has been calculated that the rate of aldolization is about $\frac{1}{1000}$ the rate of D exchange (*31*). The rate of the exchange-determining reaction,

$$CH_3COCH_3 + OH^- \rightleftharpoons [CH_3CO\,CH_2]^- + H_2O$$

is much larger than that of the second rate-determining process:

$$[CH_3COCH_2]^- + CH_3COCH_3 \rightleftharpoons \left[\begin{array}{c} CH_3COCH_2C(CH_3)_2 \\ | \\ O \end{array}\right]^-$$

In the Cannizaro reaction (with benzaldehyde, formaldehyde, or glyoxal) in D_2O, the alcohols produced did not contain D (*32*). Hydrogen transfer from one aldehyde group to the other, therefore, takes place without interchange with the solvent. The probable mechanism is

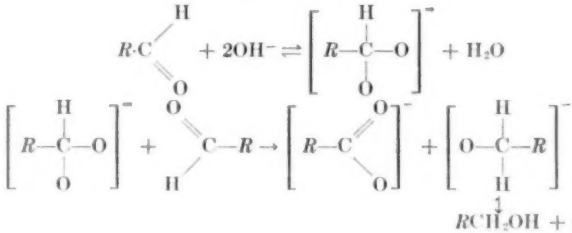

Claisen rearrangement: In the mechanism proposed for the rearrangement of allyl ethers, it was assumed that the displaced hydrogen atom migrated to the oxygen atom of the resulting phenol by an intramolecular process. Direct evidence supporting this proposal has been provided by two studies with deuterium as tracer.

In the first of these investigations, the deuterium labeled allyl ether (*XIII*) and similar compounds were used (*33*).

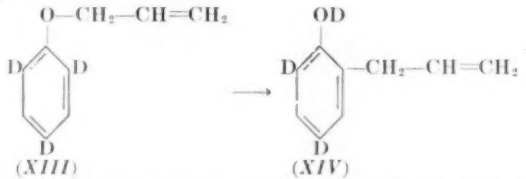

After rearrangement to (*XIV*), the latter compound still contained all the deuterium originally present. The displaced *ortho* deuterium atom must, therefore, have migrated to the oxygen atom of (*XIV*).

Further evidence was provided by the rearrangement of allylphenyl ether in the presence of 3,5-deuteriophenol; the allylphenol produced contained no D (*34*). The rearrangement was therefore confirmed to be intramolecular. In the latter experiment, rearrangement with the formation of allyl ions (bimolecularly) would have provided opportunity for production of a deuterium-containing allyl phenol molecule.

Oxidation of alcohols: To determine the point of attack of chromic acid on *iso*-propanol, a product containing 55% 2-deuteropropanol-2 was prepared (*35*). Since the C-H and C-D bonds differ in their reactivities, the deuterium compound

would be oxidized less rapidly if the removal of the secondary hydrogen atom were rate-determining. The rate of oxidation, even of the mixture, was less than that for pure *iso*propanol, and it was concluded that the rate-controlling step was the attack on the secondary hydrogen atom.

In a study of the oxidation of ethyl alcohol with chromic acid, ethyl alcohol was prepared containing 40 atom % deuterium on the two α hydrogen atoms. Thus it was a mixture of CH_3CH_2OH, CH_3CHDOH and CH_3CD_2OH. On oxidation, the surprising observation was made that 60% of the acetaldehyde was CH_3CDO. Additional evidence showed, in fact, that CH_3CHO was oxidized more rapidly than CH_3CDO by chromic acid, thereby leading to accumulation of CH_3CDO. This effect is probably responsible for the deuterium enrichment in the acetaldehyde formed during the oxidation of alcohol (*36*).

Decomposition of hypophosphite solutions: In the heterogeneous, metal-catalyzed decomposition of sodium hypophosphite in D_2O, half of the evolved hydrogen was derived from phosphorus-bound hydrogen atoms and half from water or OH groups (*37*). A second reaction, favored by high concentrations of hypophosphite and probably by the presence of D_2O itself, was one in which both hydrogen atoms were derived from phosphorus-bound hydrogen.

Hydrolysis of chloral: The alkali fission of chloral yields chloroform and alkali formate. By studying the reaction in D_2O, it was demonstrated that the hydrogen atom of the formate ion is most probably the same as that in the aldehyde group of the original chloral (*38*). The initial reaction

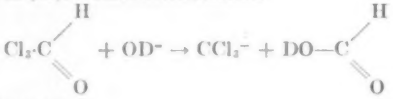

is followed by the reactions

$$OD^- + H{-}COOD \rightarrow DOD + H{-}COO^-$$
$$CCl_3^- + DOD \rightarrow DCCl_3 + OD^-$$

A small amount of D found in the formate was assumed to be from the initial exchange into the aldehyde group of chloral. The exchange between formate ion and D_2O was certainly too slow to account for this result. It was also shown that subsequent hydrolysis of the $DCCl_3$ did not occur to any appreciable extent:

$$DCCl_3 + 4NaOH \rightarrow DCOONa + 3NaOH$$

Transamination reaction: Two possible routes for the *in vitro* transamination reaction can be represented as follows:

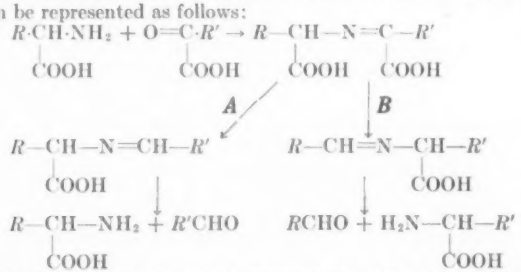

Using α-aminophenylacetic acid and pyruvic acid ($R = C_6H_5$; $R' = CH_3$), the

reaction proceeds via route ***B*** to yield benzaldehyde and alanine ($R = C_6H_5$; $R' = CH_3$). If carried out in D_2O, two possibilities arise:

a) If the α H is not involved in the reaction, RCHO would be without D, but $R'CHNH_2CO_2H$ would pick up D in the α-position.

b) If the α H were reactive, the aldehyde should contain deuterium (RCDO) and the new amino acid might or might not contain it. In fact, no deuterium was found in the benzaldehyde, but the alanine contained two atom equivalents of deuterium, probably in the methyl group (*39*), due to this tautomeric shift:

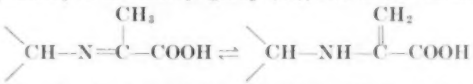

When the transamination is carried out starting with the α deuteroamino acid in H_2O, there are also two alternatives:

a) If the α deuterium atom of the amino acid reacted, the aldehyde would not contain D. The amino acid would contain D provided that no exchange with the solvent took place during the shift across the methylene azomethine bridge.

b) If the α deuterium atom were not involved, the aldehyde would be RCDO, and the new amino acid would not contain deuterium. This was the case.

The *in vitro* transamination reaction, therefore, involves decarboxylation of the intermediate Schiff's base, probably accompanied by simultaneous shift of the double bond, followed by addition of a proton from the medium to a carbonium ion.

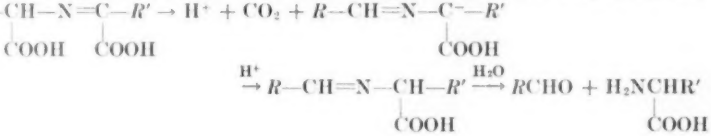

Hydrocarbon isomerization: In a study of butane isomerization, it was shown that by treating *n*- or *iso*-butane with a 10 mole % of DBr-$AlBr_3$ catalyst (20 hours, 25° C), no isomerization took place and only 6 and 9.5%, respectively, of deuterium was exchanged (*40*). However, when 0.1 mole % of *n*-butenes was present under the same conditions, 40% of the butane isomerized and 92% of the deuterium exchanged. Decreasing the contact time to 7 hours only slightly diminished the D exchange. Using deuteroxyaluminum dibromide (DOAlBr) as catalyst, only very little exchange took place. The following mechanism was proposed:

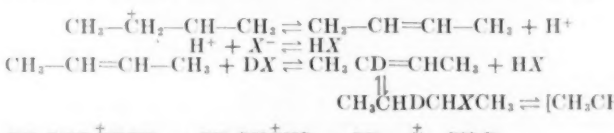

NITROGEN-15

Fischer indole synthesis: Aniline containing N^{15} was synthesized and converted to acetophenone phenylhydrazone (*XV*). When the Fischer synthesis was carried out on this compound the 2 phenylindole obtained (*XVI*) contained all the

excess N^{15} (*41*). This observation provided confirmation for Robinson's representation of the synthesis, in which it was assumed that the nitrogen atom farthest from the ring was lost.

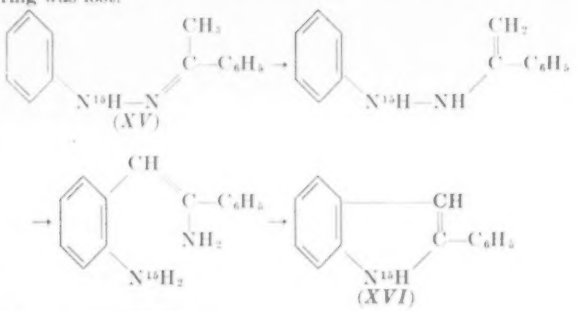

Synthesis and oxidation of uric acid: In the synthesis of uric acid by the method of Grimaux (*42*), N^{15}-labeled urea was used. One equivalent of $N^{15}H_3$ was lost in the course of the reaction, and the uric acid contained one N^{15} atom derived from the urea (*43*).

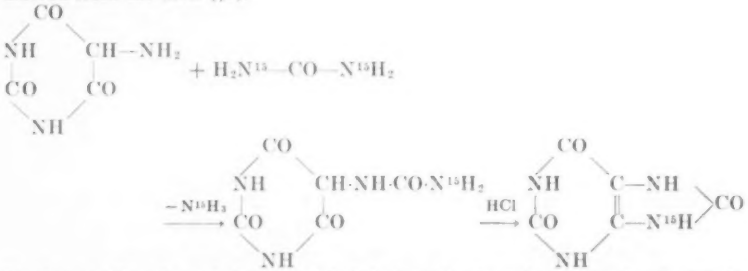

Further studies showed that the labeled atom in the uric acid molecule was in position 9; the analogous reaction of 2,6-dioxy-4,5-diaminopyrimidine was carried out using labeled urea. The uric acid in this case did not contain any N^{15}:

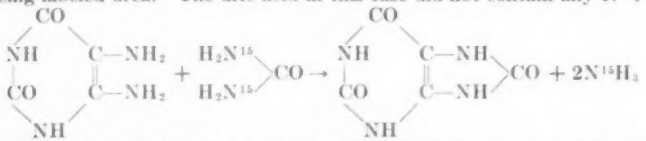

A study of the oxidation of uric acid (labeled with N^{15} in the 1 and 3 positions) showed that when nitric acid or chlorine was used as the oxidizing agent, alloxan was formed from the pyrimidine ring alone (*44*).

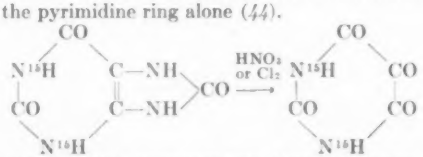

In the oxidation with alkaline permanganate (allantoin being formed), evidence

was obtained showing that the reaction proceeded through a symmetrical intermediate, such as (*XVII*), with a resulting randomization of the nitrogen atoms.

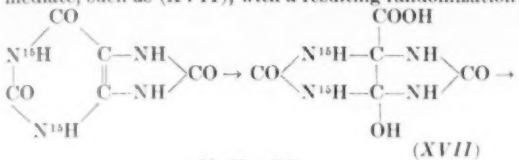

(*XVII*)

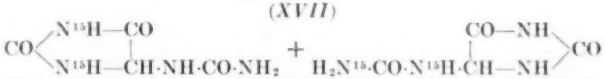

This conclusion was reached by further degradation of the allantoin, as follows:

a) Oxidation of a portion with potassium permanganate to potassium oxonate (*XVIII*).

b) Reduction of a second portion to hydantoin (*XIX*).

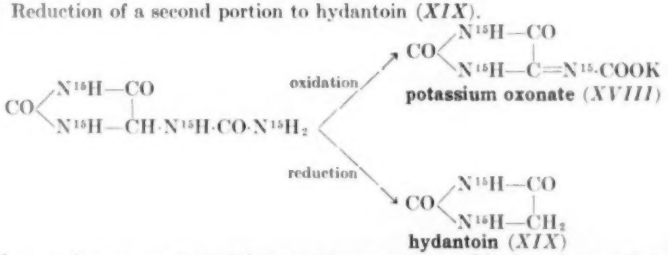

The heavy nitrogen content of the potassium oxonate and hydantoin was the same as that of the allantoin. This meant that there had been a random distribution of N^{15} between the urea and imidazolone moieties in the formation of the allantoin and that the isotope in the urea moiety was equally distributed between the two nitrogens.

Production of nitrous oxide : Apparently N^{15} has been used only once in the study of inorganic reactions. Ammonium nitrate ($N^{15}H_4NO_3$) was decomposed to nitrous oxide; the latter was reduced to nitrogen by means of a reduced iron catalyst (*45*). From the distribution of the isotope, it was shown that the decomposition proceeded by bond formation between the two nitrogen atoms of the different radicals present, i.e.,

$$N^{15}H_4NO_3 \rightarrow N^{15}NO + 2H_2O$$

There was little or no production of $N^{15}N^{16}O$ or $NN^{15}O$.

CARBON-11, 13, and 14

Fatty acid oxidation : The oxidation of propionic acid has been studied under a variety of conditions. Wood *et al.* studied its oxidation to oxalic acid and sodium carbonate with alkaline permanganate. They found that only 37% of the C^{13}, originally present in the carboxyl group, was found in the sodium carbonate. Some C^{13} was also present in the oxalic acid (*46*).

$$CH_3CH_2COONa \xrightarrow[KMnO_4]{\text{alkaline}} \begin{matrix} COONa \\ | \\ COONa \end{matrix} + Na_2CO_3$$

This reaction, and also the oxidation of the hydroxypropionic acids, was further

studied with C^{11}-labeled acids (*47*). Again the results indicated that the carbon dioxide was derived mainly from the β carbon atoms, rather than from the carboxyl carbon atom. The main conclusions were as follows:

a) In sodium hydroxide solutions of 10^{-4} to 2*N* concentration, about 71% of the carbonate was formed from the β carbon atom of propionic acid. At higher alkalinities, the α-β bond was split even more preferentially.

$$CH_2CH_2C^{11}OONa \rightarrow Na_2CO_3 + \begin{matrix} C^{11}OONa \\ | \\ COONa \end{matrix}$$

b) It was established that no isotope exchange took place between $CO_3^{=}$ and $C_2O_4^{=}$.

c) In the case of sodium lactate and sodium β-hydroxypropionate, 70% of the carbonate was derived from the β carbon atom. This value was unchanged on changing the concentration of sodium hydroxide from 2 to 12*N*.

d) The α-β carbon bond of propionic acid was broken in strongly basic solution without either α- or β-hydroxypropionic acids being formed as intermediate products.

In contrast to these results, it has been shown that the oxidation of propionic acid with acid dichromate solutions yields carbon dioxide and acetic acid where all the former is derived from the carboxyl group of the propionic acid (*48*).

$$CH_2CH_2C^{11}OOH \xrightarrow[K_2Cr_2O_7]{\text{acid}} CH_3COOH + C^{11}O_2$$

The oxidation of butyric acid with hydrogen peroxide yields carbon dioxide, acetic acid, and acetone. Using carboxyl-labeled butyric acid, no label was found in the acetone—as expected. The isotope content of the carbon dioxide was diluted to some extent by the oxidation of other intermediates (*49*).

Oxidation of propene: The oxidation of 1-C^{14}-propene-1 by alkaline permanganate was found to proceed mainly according to the following scheme (*50*):

$$\underset{3}{CH_3}\underset{2}{CH}=\underset{1}{C^{14}H_2} \rightarrow \underset{3}{CH_3}\underset{2}{CO_2H} + \underset{1}{C^{14}O_2}$$

Oxalic acid was isolated after its addition as a carrier; in this secondary reaction, the CH_2-CH bond was also split to the extent of about 15 to 20%. In the oxidation, a high yield of carbon dioxide of low specific activity was obtained. It was calculated that about half of the propene was converted directly to carbon dioxide, a third to acetic acid and carbon dioxide, and a sixth to oxalic acid and carbon dioxide. The presence of a low but significant activity in the acetic acid suggested the involvement of a symmetrical intermediate, such as *iso*propanol or acetone, in which the methyl group was retained.

In this work, the preparation of 1-C^{14}-propene-1 was of importance. Dehydration of 1-C^{14}-propanol-1 with reagents such as metaphosphoric acid or alumina led to varying degrees of rearrangement. Pure 1-C^{14}-propene-1 could be prepared only by pyrolysis of the quaternary base, $CH_3{\cdot}CH_2{\cdot}C^{14}H_2{\cdot}N(CH_3)_3{\cdot}OH$.

Decarbonylation of ethyl pyruvate: By the use of α C^{14}-labeled ethyl pyruvate, it was demonstrated that the carbon monoxide evolved on heating (110–130° C) was derived from the carboxyl group (*51*). There was no C^{14} in the carbon monoxide (obtained in 90% yield) or in the trace of carbon dioxide which was also formed.

$$\underset{3}{CH_3}\underset{2}{C^{14}O}\underset{1}{COOC_2H_5} \rightarrow \underset{1}{CO} + \underset{3}{CH_3}\underset{2}{C^{14}OOC_2H_5}$$

Rearrangement of unsymmetrical diketones: It has been shown that the rearrangement of phenylglyoxal to mandelic acid, $C_6H_5COCHO \rightarrow C_6H_5CHOHCOOH$, takes place in D_2O without deuterium being taken up into stable C-D bonds (*52*). If the aldehydic hydrogen atom migrates, it must therefore do so by an intramolecular process. In this study, it was shown further that C^{13}-carbonyl-labeled α,α-dibromoacetophenone with aqueous base gave $C_6H_5C^{13}HOHCOOH$. Phenylglyoxal was formed as an intermediate.

$$C_6H_5C^{13}OCHBr_2 \rightarrow C_6H_5C^{13}OCHO \rightarrow C_6H_5C^{13}HOHCOOH$$

At the same time, the reaction was studied with C^{14}-labeled phenylglyoxal (*53*). The following mechanism was proposed and no rearrangement of the carbon skeleton took place.

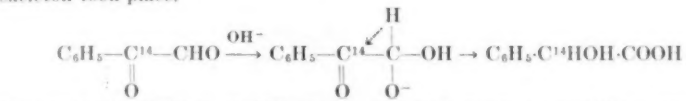

The reversible addition of OH^- at one carbonyl group seemed likely from the study of benzilic acid rearrangement (*54*).

Arndt-Eistert synthesis: A ketene (*XX*) was proposed as intermediate by Eistert (*55*) in this procedure for converting an acid to its next higher homolog:

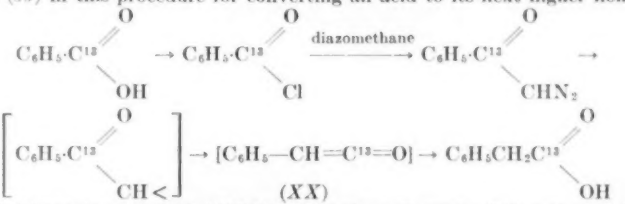

Labeled benzoic acid, $C_6H_5C^{13}OOH$ (2.51 atom % excess C^{13}) was used in the reaction; the phenylacetic acid produced was decarboxylated with copper chromite in quinoline to yield carbon dioxide of 2.53 atom % excess C^{13} (*56*). Further evidence for this reaction mechanism was provided in a study of the Willgerodt reaction (see below). [For a comparison of this reaction with the similar rearrangement of the acid azides (Curtius), see Lane *et al.* (*57*).]

Willgerodt reaction: In this unusual transformation, an amide is formed by heating an aromatic ketone with yellow ammonium sulfide.

A modification (Kindler-Willgerodt) consists in the use of a high-boiling amine (e.g., morpholine) and sulfur. In this case, the initial reaction product is the thioamide which is readily hydrolyzed to the acid. Under the latter conditions, acetophenone ($C_6H_5{\cdot}C^{13}O{\cdot}CH_3$) was converted to phenylacetic acid. No excess C^{13} was present in the carboxyl group, showing that the carbon skeleton was retained (*58*). Kindler's hypothesis involving migration of an acyl group (*59*) was therefore incorrect.

At the same time, a Willgerodt reaction (i.e., using the yellow ammonium sulfide process) was carried out on C^{14}-carbonyl-labeled acetophenone, and phenylacetamide was isolated along with some phenylacetic acid as a by-product (*60*).

Carbon dioxide obtained by Hofmann degradation of the phenylacetamide contained only 3% of the starting specific activity; the amide was formed by oxidation-reduction along the chain, without migration of carbon atoms.

Carbon dioxide derived from the phenylacetic acid produced as a by-product contained 75% of the specific activity of the starting material; the acid therefore was apparently formed by an entirely different mechanism. The dilution of the activity was probably due to contamination with phenylacetic acid produced from the amide.

$$C_6H_5C^{13}OCH_3 \xrightarrow[6\text{ hr, }170^\circ]{NH_4OH,\ S,\ \text{pyridine}} \begin{matrix} \nearrow\ C_6H_5C^{14}H_2CONH_2 \\ \searrow\ C_6H_5CH_2C^{14}OOH \end{matrix}$$

For a recent discussion of these reaction mechanisms, see McOmie (*61*).

Incidentally, during these investigations it was found that the carbon dioxide obtained from the labeled phenylacetic acid by the use of copper chromite and quinoline contained rather less isotope than was expected. It was shown subsequently (*62*) that this was due to further oxidation of the toluene, and that this did not take place when iron or copper powder was used.

Synthesis of uvitic acid: A reaction which has been known for a long time (*63*) is the formation of uvitic acid (*XXI*) from sodium pyruvate. During work leading to the synthesis of ring-labeled toluene, uvitic acid was prepared from carbonyl-labeled sodium pyruvate. By analysis of the end products (oxalic acid is also formed), the following reaction sequence was proved (*64*).

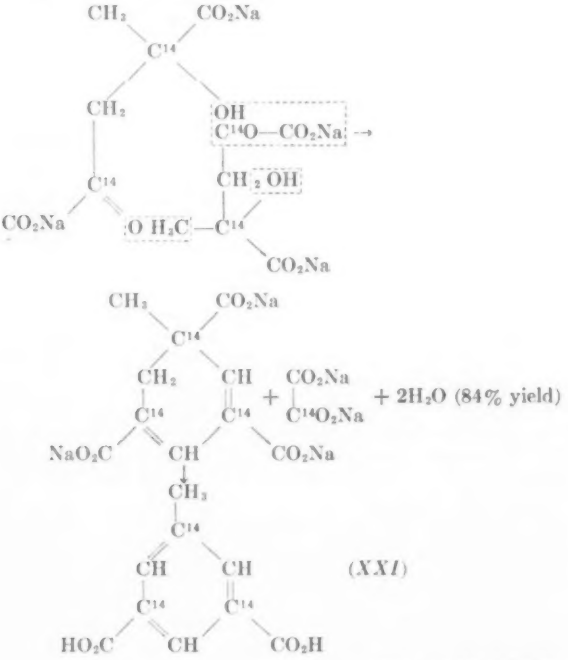

Decomposition and structure of aldoketene dimers: An ingenious application of C^{14} has been to study the structure of ketene dimers. For diketene, five structures are possible; only (*XXV*) has two equivalent carbonyl groups.

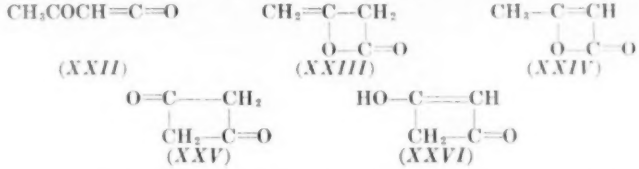

(*XXII*) (*XXIII*) (*XXIV*)

(*XXV*) (*XXVI*)

Higher aldoketene dimers have chemical and physical properties analogous to those of diketene, and probably present the same structural problem. A mixed dimer was therefore prepared from $CH_3CH_2C^{14}OCl$ and $C_7H_{15}COCl$ (*65*). If this had the cyclobutanedione 1:3 structure [analogous to (*XXV*)], it would yield the following products on alcoholysis.

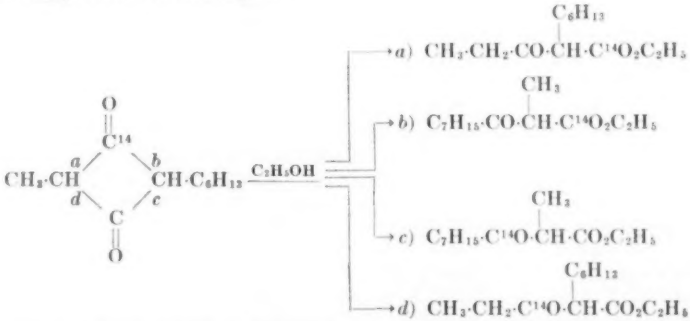

On reaction of this β-keto ester mixture with $NaOC_2H_5$, a C^{14}-labeled ethyl caprylate would be obtained; if all the dimer had the proposed structure, all the C^{14} would be equally distributed between the ethyl propionate and ethyl caprylate fractions. It was found, however, that the activity of the caprylic acid was 1.5% of the activity per labeled carbon atom of the mixed dimer. Therefore, the maximum amount of the proposed structure, convertible to acetoacetic ester with C_2H_5OH is 3%. The authors suggest that structure (*XXIII*) or (*XXIV*) is most nearly in accordance with the known facts.

Fischer-Tropsch synthesis: In this important synthesis, carbon monoxide is hydrogenated over various metal catalysts. The possibility that the metal carbide may be involved as an intermediate has been investigated by using a surface layer of metal carbide containing C^{14} (*66*).

It was expected that if this theory were valid, C^{14} would be incorporated into the initial hydrocarbon products. Conversely, using a normal carbide surface and H_2-$C^{14}O$ mixture, the first formed hydrocarbons should have a lower specific activity than the $C^{14}O$. It was, in fact, found that the greater part of the reaction mixture was formed by processes other than the reduction of an intermediate carbide. Only about 10% of the products were so formed on iron catalysts, at or below 260° C, and on cobalt catalyst at 200° C.

Isomerization of hydrocarbons and their derivatives: Preliminary studies on the isomerization of hydrocarbons have been reported. In particular, 1-C^{13}-propane was found to be reversibly converted to 2-C^{13}-propane by an exclusively intramolecular mechanism in the presence of a water-promoted aluminum bromide catalyst at 25° C (*67*). Similar experiments have been made with 1-C^{13}-butane (*68*).

The rearrangement of *t*-butyl and amyl compounds has been studied. The *t*-amyl chloride (*XXVII*) was rearranged over aluminum chloride to give a product containing 64% of the starting material, 35% of (*XXVIII*) and 1% (*XXIX*).

$$\underset{(XXVII)}{(CH_3)_2C^{14}ClCH_2CH_3} \rightleftharpoons \underset{(XXVIII)}{(CH_3)_2CClC^{14}H_2CH_3} \rightleftharpoons \underset{(XXIX)}{(CH_3)_2CClCH_2C^{14}H_3}$$

The recovered chloride was degraded according to the following reaction scheme, where no rearrangement takes place during the individual steps (*69*).

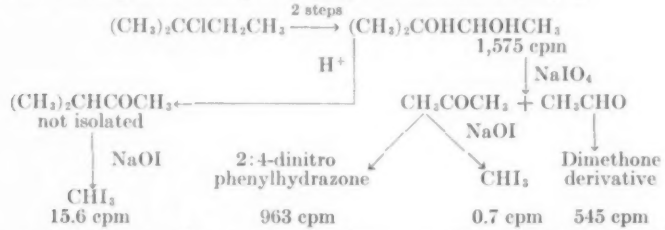

(All counts are expressed as counts per minute per milligram of $BaCO_3$.) These results showed that rearrangement may occur between the 2 and 3 positions of the *t*-amyl group, but that the rate of interchange is very slow between the terminal carbon atoms and those in the middle of the chain.

Exchange of a formamido group: In work directed to the synthesis of labeled adenine, the sulphate of (*XXX*) was heated in formamide. Unexpectedly, extensive exchange took place with the formamide and only 25% of the C^{13} originally present was found in the resulting adenine. The probable mechanism was considered to be ammonolysis of the formyl group, since formamide is known to yield ammonia and carbon monoxide on heating (*70*).

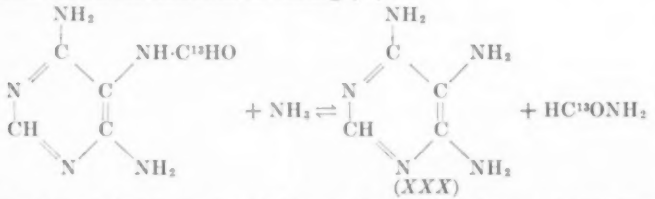

Confirmatory evidence was provided by the finding that the 4,5,6-triaminopyrimidine gave a high yield of adenine when heated with formamide.

BIBLIOGRAPHY

1. G. v. Hevesy, L. Zechmeister, *Ber.* **53**, 410 (1920)
2. R. Bentley, NUCLEONICS **2**, No. 2, 18 (1948); Cold Spring Harbor Symp. Quant. Biol. **13**, 11 (1948)
3. M. Polányi, A. L. Szabo, *Trans. Farad. Soc.* **30**, 508 (1934)
4. I. Roberts, H. C. Urey, *J. Am. Chem. Soc.* **60**, 2391 (1939)
5. M. Harada, T. Titani, *Bull. Chem. Soc. Japan* **10**, 554 (1935); **11**, 465 (1936)
6. H. R. V. Arnstein, R. Bentley, *Quarterly Reviews (Chem. Soc. London)* (currently in press)

7. L. H. Reyerson, S. Yuster, *J. Am. Chem. Soc.* **56,** 1426 (1934)
8. R. Klar, *Z. physik. Chem.* **B26,** 335 (1934)
9. K. F. Bonhoeffer, R. Klar, *Naturwissenschaften* **22,** 45 (1934); J. O. Halford, L. C. Anderson, J. R. Bates, *J. Am. Chem. Soc.* **56,** 491 (1934)
10. C. K. Ingold, C. G. Raisin, C. L. Wilson, *J. Chem. Soc.* 1637 (1936)
11. A. J. Gould, W. Bleakney, H. S. Taylor, *J. Chem. Phys.* **2,** 362 (1934); A. J. Gould, W. Bleakney, *J. Am. Chem. Soc.* **56,** 247 (1934)
12. H. S. Taylor, *J. Franklin Institute* **218,** 1 (1934)
13. J. Horiuti, G. Ogden, M. Polányi, *Trans. Farad. Soc.* **30,** 663 (1934); *Nature* **134,** 377 (1934)
14. A. Farkas, L. Farkas, E. K. Rideal, *Proc. Roy. Soc.*, **A146,** 630 (1934)
15. K. Morikawa, W. S. Benedict, H. S. Taylor, *J. Am. Chem. Soc.* **58,** 1445 (1936)
16. G. Parravano, E. F. Hammel, H. S. Taylor, *J. Am. Chem. Soc.* **70,** 2269 (1948)
17. H. S. Taylor, J. C. Jungers, *J. Chem. Phys.* **2,** 452 (1934)
18. K. Clusius, W. Schanzer, *Ber.* **75B,** 1795 (1942)
19. D. J. G. Ives, H. N. Rydon, *J. Chem. Soc.* 1735 (1935)
20. D. J. G. Ives, *J. Chem. Soc.* 91 (1938)
21. C. K. Ingold, E. de Salas, C. L. Wilson, *J. Chem. Soc.* 1328 (1936)
22. E. M. Evans, H. N. Rydon, H. V. A. Briscoe, *J. Chem. Soc.* 1673 (1939)
23. S. K. Hsû, C. K. Ingold, C. L. Wilson, *J. Chem. Soc.* 78 (1938)
24. D. J. G. Ives, G. C. Wilks, *J. Chem. Soc.* 1455 (1938)
25. T. P. Nevell, E. de Salas, C. L. Wilson, *J. Chem. Soc.* 1188 (1939)
26. I. Dostrovsky, E. D. Hughes, C. K. Ingold, *J. Chem. Soc.* 192 (1946)
27. E. de Salas, C. L. Wilson, *J. Chem. Soc.* 319 (1938)
28. D. J. G. Ives, R. H. Kerlogue, *J. Chem. Soc.* 1362 (1940)
29. S. K. Hsû, C. K. Ingold, C. G. Raisin, E. de Salas, C. L. Wilson, *J. chim. physique* **45,** 232 (1948); P. B. D. de la Mare, B. D. England, L. Fowden, E. D. Hughes, C. K. Ingold, *ibid.* 236; E. D. Hughes, C. K. Ingold, *ibid.* 241.
30. K. F. Bonhoeffer, W. D. Walters, *Z. physik. Chem.* **A181,** 441 (1938)
31. W. D. Walters, K. F. Bonhoeffer, *Z. physik. Chem.* **A182,** 265 (1938)
32. H. Fredenhagen, K. F. Bonhoeffer, *Z. physik. Chem.* **A181,** 379 (1938)
33. G. B. Kistiakowsky, R. L. Tichenor, *J. Am. Chem. Soc.* **64,** 2302 (1942)
34. A. S. Fomenko, G. P. Miklukhin, E. A. Sadovnikova, *Doklady Akad. Nauk. U.S.S.R.* **62,** 91 (1948); *Chem. Abstracts* **43,** 602i (1949)
35. F. H. Westheimer, A. Nicolaides, *J. Am. Chem. Soc.* **71,** 25 (1949)
36. J. W. Cornforth, G. Popják *Nature* **164,** 1053 (1949)
37. W. Franke, J. Mönch, *Ann. Chem.* **550,** 1 (1942)
38. I. Lauder, S. E. Wright, *Nature* **158,** 381 (1946)
39. R. M. Herbst, D. Rittenberg, *J. Org. Chem.* **8,** 380 (1943)
40. H. Pines, R. C. Wackher, *J. Am. Chem. Soc.* **68,** 2518 (1946)
41. C. F. H. Allen, C. V. Wilson, *J. Am. Chem. Soc.* **65,** 611 (1943)
42. E. Grimaux, *Bull. soc. chim. Paris* **31,** No. 2, 535 (1879)
43. L. F. Cavalieri, V. E. Blair, G. B. Brown, *J. Am. Chem. Soc.* **70,** 1240 (1948)
44. L. F. Cavalieri, G. B. Brown, *J. Am. Chem. Soc.* **70,** 1242 (1948)
45. J. T. Kummer, *J. Am. Chem. Soc.* **69,** 2559 (1947)
46. H. G. Wood, C. H. Werkman, A. Hemingway, A. O. Nier, C. G. Stuckwisch, *J. Am. Chem. Soc.* **63,** 2140 (1941)
47. P. Nahinsky, C. N. Rice, S. Ruben, M. D. Kamen, *J. Am. Chem. Soc.* **64,** 2299 (1942)
48. P. Nahinsky, S. Ruben, *J. Am. Chem. Soc.* **63,** 2275 (1941)
49. H. G. Wood, R. W. Brown, C. H. Werkman, C. G. Stuckwisch, *J. Am. Chem. Soc.* **66,** 1812 (1944)
50. B. A. Fries, M. Calvin, *J. Am. Chem. Soc.* **70,** 2235 (1948)
51. M. Calvin, R. M. Lemmon, *J. Am. Chem. Soc.* **69,** 1232 (1947)
52. W. v. E. Doering, T. I. Taylor, E. F. Schoenewaldt, *J. Am. Chem. Soc.* **70,** 455 (1948)
53. O. K. Neville, *J. Am. Chem. Soc.* **70,** 3499 (1948)
54. I. Roberts, H. C. Urey, *J. Am. Chem. Soc.* **60,** 880 (1938)
55. B. Eistert, *Ber.* **68,** 208 (1935)
56. C. Huggett, R. T. Arnold, T. I. Taylor, *J. Am. Chem. Soc.* **64,** 3043 (1942)
57. J. F. Lane, J. Willenz, A. Weissberger, E. S. Wallis, *J. Org. Chem.* **5,** 276 (1940); J. F. Lane, E. S. Wallis, *ibid.* **6,** 443 (1941)
58. E. M. Schantz, D. Rittenberg, *J. Am. Chem. Soc.* **68,** 2109 (1946)
59. K. Kindler, *Ann. Chem.* **431,** 193, 222 (1923)
60. W. G. Dauben, J. C. Reid, P. E. Yankwich, M. Calvin, *J. Am. Chem. Soc.* **68,** 2117 (1946)
61. J. F. W. McOmie, *Ann. Reports on Progress Chem. (Chem. Soc. London)* **45,** 210 (1948)
62. W. G. Dauben, P. Coad, *J. Am. Chem. Soc.* **71,** 2928 (1949)
63. L. Wolff, *Ann. Chem.* **305,** 125 (1899)
64. D. M. Hughes, J. C. Reid, *J. Org. Chem.* **14,** 516 (1949)
65. J. D. Roberts, R. Armstrong, R. F. Trimble, M. Burg, *J. Am. Chem. Soc.* **71,** 843 (1949)
66. J. T. Kummer, T. W. De Witt, P. H. Emmett, *J. Am. Chem. Soc.* **70,** 3632 (1948)
67. O. Beeck, J. W. Otvos, O. P. Stevenson, C. D. Wagner, *J. Chem. Phys.* **16,** 255 (1948)
68. J. W. Otvos, D. P. Stevenson, C. D. Wagner, O. Beeck, *J. Chem. Phys.* **16,** 745 (1948)
69. R. E. McMahon, J. S. Hine, *J. Am. Chem. Soc.* **71,** 1896 (1949)
70. L. F. Cavalieri, G. B. Brown, *J. Am Chem. Soc.* **71,** 2246 (1949)

Atomic Spectroscopy with Separated Isotopes

Analysis of a hyperfine structure pattern discloses spin and magnetic moment, as well as composition of the isotope mixture. But because of possible multiplicity of HFS components, unequivocal determination of the nuclear properties to be measured is often practicable only by means of artificially separated isotopes. Spectroscopic analysis, on the other hand, allows a kind of optical mass spectrometry.

By W. WALCHER*

Physics Institute, University of Marburg
Marburg, Germany

THERE ARE various measurable properties by which the nucleus of an atom can be characterized: its charge Z, its mass M, its radius R, perhaps by the quadrople moment defining the deviation from spherical shape, and finally, its mechanical moment (spin) I, and its magnetic moment μ.

Z, M, and R are generally found from scattering and transmutation interactions of various nuclei, or from deflection experiments in electric and magnetic fields (mass spectrograph). The spin and the magnetic moment can be determined from the forces acting upon the atoms in inhomogeneous magnetic fields, but they are especially evident in the so-called hyperfine structure (HFS) of the atomic spectra. The size and mass of the nucleus are also revealed by the HFS in the so-called isotope-displacement effect.

It is the purpose of the following exposition to report on this type of atomic spectroscopy with separated isotopes.

Principles and Observation of Atomic HFS Spectra

When we observe yellow sodium light with the usual spectroscope, we see two narrow adjacent lines, a so-called fine structure. This is due to the fact that the spin of the orbital electron (quantum number s) has two possible values relative to the angular momentum of the orbit (quantum number l; resultant quantum number $j = l \pm s$).

The interaction between the magnetic moment of the electron and the magnetic field of the orbit produces a small additional energy for each atomic state. However, there are two different possible spin orientations with different energy values. This causes a splitting of the term and a doublet structure in the lines.

The mechanical and magnetic moments of the nucleus show similar effects (I); they are oriented with respect to the magnetic field originated by the orbital electron at the nucleus.

The angular momentum of the nucleus (quantum number I) and the resultant angular momentum of the electron envelope (quantum number J) are added vectorially to obtain the integral resultant angular momentum F of the particular atomic state.

The coupling between the nuclear magnet and the magnetic field produces an additional energy and, thus, a term

* Translation of this paper from German was made by P. H. Lowry, Brookhaven National Laboratory, Upton, New York.

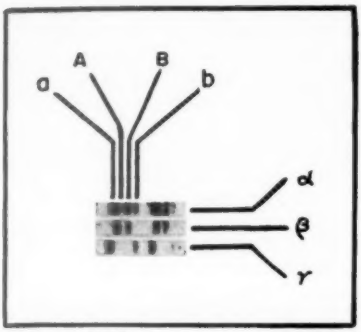

FIG. 1. HFS photographs of the Rb *I* resonance line 7,800 A.U.: α) natural Rb mixture (Rb^{85}: Rb^{87} = 2.68 : 1); β) electromagnetically separated Rb^{85}; γ) electromagnetically separated Rb^{87}. [From Walcher (2)]

splitting. The number of possible states of the nuclear magnet, which is the number of possible "hyperfine structure" terms, is either $(2I + 1)$ or $(2J + 1)$, depending on whether $J \geq I$ or $I \geq J$. The amount of the hyperfine-structure separation is about three powers of ten smaller than that in the case of fine-structure separation, since the magnetic moment of the nucleus is, in order of magnitude, 1/1,836 of the electron moment.

An interferometric spectroscope is needed to observe such a fine structure in the spectral lines. Much use has been made of the so-called Fabry-Pérot etalon. It consists of two partially transparent silvered optically flat quartz plates placed parallel to each other at a fixed distance apart.

If these plates are put in a parallel beam between two lenses, an interference system of concentric rings is produced in the focal plane of the second lens by light from a source at the focal plane of the first lens, provided monochromatic light is used. If the light consists of two or more very narrow adjacent lines (HFS), two or more rings will appear in each order of the ring system. If there is a mixture of spectral lines with HFS, a further separation will be needed.

The ring system is projected on the slit of a spectroscope so that the ring elements cut by the relatively broad slit are perpendicular to the length of the slit. The individual spectral lines with their HFS are then observed on a photographic plate.

Figure 1 shows one of the resonance lines of rubidium (7,800 A.U.; corresponding to the Na resonance line 5,890 A.U.). The relatively broad spectrograph slit is shown horizontal in the figure; it is cut through vertically by the interference rings, which can be recognized by their slight curvature.

HFS of Rubidium Resonance Line 7800 A.U.

The upper photograph (α) in Fig. 1 was made from natural rubidium. Characteristically, 4 HFS components are present in each interference order, although the two at the left are not resolved. The explanation of this HFS pattern is given in Fig. 2, where the term scheme of the transition

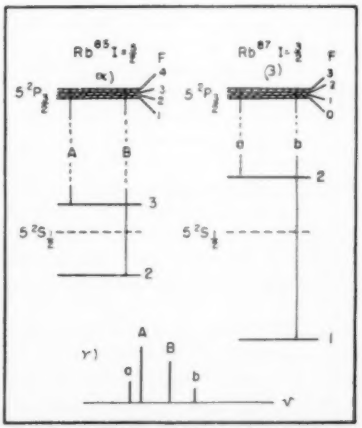

FIG. 2. Term scheme of the Rb *I* resonance line 7,800 A.U. ($5\,^2P_{3/2} - 5\,^2S_{1/2}$)

$5\ ^2P_{3/2} - 5\ ^2S_{1/2}$(7,800 A.U.) is shown.

The upper term of the Rb^{85} (Fig. 2α), with $J = 3/2$, splits into four HFS terms with quantum numbers $F = 4, 3, 2, 1$. The degree of separation is so small that the corresponding lines cannot be resolved. The lower term, $J = 1/2$, splits into two HFS terms with $F = 3$ and 2 ($\Delta\nu = 0.096$ cm^{-1}, corresponding to $\Delta\lambda = 0.061$ A.U.). The selection rule $\Delta F = \pm 1.0$ holds for the possible spectral lines. Only the two lines, A and B, appear in the foregoing case because of the small amount of the separation. Their intensity ratio is 7 to 5, according to the intensity rule.

The HFS pattern in Fig. 1, however, shows four components in each order, which can be explained by rubidium isotopes. For every 2.7 Rb^{85} atoms with $I = 5/2$, there is one Rb^{87} atom with $I = 3/2$, whose term scheme is given in Fig. 2β. Here, the lower term ($^2S_{1/2}$) has the greater separation ($\Delta\nu = 0.220$ cm^{-1}, corresponding to $\Delta\lambda = 0.14$ A.U.), while the upper term ($^2P_{3/2}$) is again not measurable, so that the transitions a and b have an intensity ratio 5 to 3.

The isotope mixture thus emits the line 7,800 A.U. with the HFS shown in Fig. 2γ. The components pairs A,B and a,b are so close that their centers of gravity coincide; as will be explained later, there is no isotope displacement. The HFS pattern in Fig. 2γ was determined from the spacing and intensities of the spectrogram in Fig. 1α. The accuracy of the isotope relationships of the components is shown in Fig. 1β and γ, where the same lines have been photographed with about 50 μg of electromagnetically separated Rb^{85} and Rb^{87}.

The HFS pattern of Rb shows that the multiplicity of the components is further increased by different I- and μ-values belonging to each isotope, so that, under certain conditions, reliable results can be obtained only by an isotope separation. The multiplicity of the component patterns can be increased, too, when elements are used that produce an isotope displacement in addition to the "magnetic HFS," which was considered previously. In this connection, an important result of HFS research should be kept in mind: that all isotopes with even mass numbers show no magnetic HFS and thus will not split on the basis of the effects described before ($I = 0$, or small μ).

Isotope-displacement Effect

In Fig. 3, a HFS photograph of the Pb *II* line 5,372 A.U. is reproduced. There are four components in each order, which belong to the various isotopes. Natural lead consists of the isotopes 204, 206, 207, 208 with the abundance ratio

1.54:22.62:22.62:53.22.

According to the rule given above, only one component has been shown for the isotopes 204, 206, and 208. The isotope 207, on the other hand, for the line in question, has a magnetic HFS with two components, whose center of gravity falls between 206 and 208. The

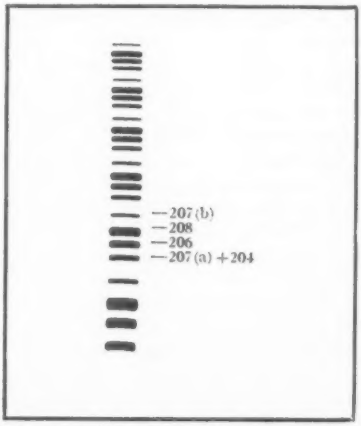

FIG. 3. HFS photograph of isotope displacement in the Pb *II* line 5,372 A.U. [From Rose and Stranathan (3)]

components with their isotopes are shown in Fig. 3.

It is apparent, therefore, that the components of different isotopes (or the centers of gravity of the magnetic HFS patterns) are usually displaced with respect to each other. There can be various causes for this displacement (*1*).

For the lighter elements (up to argon, say), it is a question of the effect of the relative motion of the nucleus. The electron and the nucleus, as is well known, revolve about their common center of gravity, whose position varies according to the mass of the nucleus. Thus the energy of a given quantum state differs slightly for each isotope of an element. For quantum states where many electrons are concerned, there are phase relations such that electrons with the same or opposite sense of rotation affect the relative motion of the nucleus in a different manner.

For the heavy elements, differences in nuclear radii become important. The "optical electron" will be found in the nucleus with a certain probability described by its ψ-function, according to the laws of quantum mechanics. Although a coulomb field prevails outside the nucleus, it is substantially decreased within. The decrease begins at the nuclear radius. Therefore, as the mean coupling energy between the electron and the nucleus differs for each isotope, so do the term values.

For elements in the middle range (*viz.*, Rb), there is no observable isotope displacement.

HFS Analysis with Separated Isotopes

In analyzing hyperfine structures (*1*), general use is made of the HFS laws, particularly the intensity and interval rules. In this connection, a knowledge of the isotope mixture is beneficial. In doubtful cases, the use of separated isotopes may be valuable. A few examples should be given to show how these rules can be corroborated (by the use of separated isotopes), and how problems, insoluble by other methods, can be clarified.

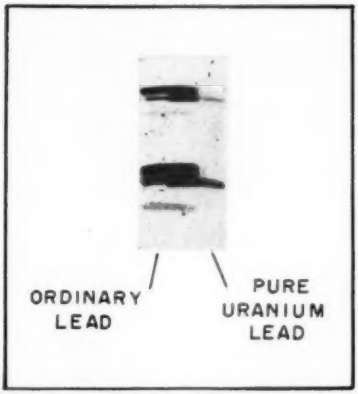

FIG. 4. HFS photograph of the Pb *I* line 4,058 A.U. for ordinary lead (left) and pure uranium lead (right). The uranium lead consists of about 93% Pb^{206} and 7% Pb^{207}. The Pb^{207} line is weak and does not appear in the photograph. [From Kopfermann (*4*)]*

Fig. 1 offers an example of how to control the analysis of the components. Fig. 4, a photograph of pure uranium lead, obtained from pure uranium ore, shows clearly that the relationships within the Pb HFS are correct, as determined on the basis of relative intensity. The HFS of an ordinary lead mixture is shown beside the HFS of uranium lead, which—as was required above and will be proved here—consists of only one component identical with that of ordinary lead, as found by analysis of Pb^{206}.

Another example of valuable aid in HFS analysis with separated isotopes is given in Fig. 5, where a number of interferometer photographs (γ) of various thallium mixtures are shown beside the HFS term scheme (α) and the separation pattern (β) of the green thal-

*Permission to reproduce this illustration from the text "Kernmomente" has been granted by the publisher, J. W. Edwards, Ann Arbor, Michigan.

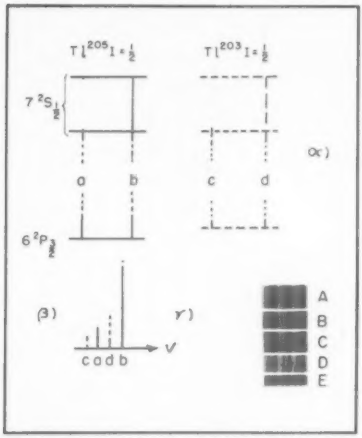

FIG. 5. α) **HFS term scheme;** β) **separation pattern;** γ) **interferometer photographs of various thallium mixtures with the green line 5,351 A.U. of Tl** I**; A) natural mixture 29% Tl^{203}, 71% Tl^{205}; B) 56% Tl^{203}, 44% Tl^{205}; C) 50% Tl^{203}, 50% Tl^{205}; D) 10% Tl^{203}, 90% Tl^{205}; E) 4% Tl^{203}, 96% Tl^{205}. [From Kopfermann and Walcher (5)]**

lium line 5,351 A.U. Natural thallium consists of the isotopes Tl^{205} and Tl^{203} with an abundance ratio 2.39:1.

The green line is formed by a transition from the upper term $7\ ^2S_{1/2}$—which splits twice because of the spin $I = 1/2$ of the Tl^{205} nucleus—to the $6\ ^2P_{3/2}$ term whose separation cannot be measured. The upper term consists of two components a and b. If Tl^{203} had exactly the same term values as Tl^{205}, its HFS pattern would consist of only the two components a and b, where b must have three times the strength of a, according to the intensity rule.

In reality, four components are observed in Fig. 5γ (A). Their formation can be most readily explained by the fact that the $6\ ^2P_{3/2}$ state of the Tl^{203}, which also must have $I = 1/2$, is displaced slightly, as indicated in Fig. 5α, so that the c and d components appear in the HFS, which must be weaker according to the abundance ratio (2.39), as is shown in Fig. 5γ (A). Thus, the nuclear spin of the isotope, its abundance ratio, and the HFS laws are brought into agreement.

This analysis, however, shows a discrepancy with our conception of the isotope-displacement effect. One would expect the terms of the lighter isotopes with smaller nuclear radii to be deeper than those of heavier isotopes, since the interaction in the coulomb field is stronger than within the nucleus. The opposite is the case in our example; term values are inverted, and the question arises whether an error exists in the analysis of the HFS components. (That the upper S-state of Tl^{203} cannot be displaced downward is shown by research on lines which terminate at this state.) Electromagnetic separation of the Tl isotopes, in this case, can prove the accuracy of the HFS analysis.

The spectra of various Tl mixtures are shown in Fig. 5γ, photographs B to E. The intensity ratios $b:a$, as well as $d:c$, agree within a few per cent with the abundance ratios obtained from an analysis of the current distribution curve of the electromagnetic separation given in the legend of Fig. 5. The accuracy of this HFS analysis is therefore proved, despite our incomplete knowledge of the isotope-displacement effect. It is an open question whether the "isotope-spin effect," recently discovered in helium will serve to clarify this point (6).

Weak Isotopes

In optical determination of nuclear moments, it is assumed that the HFS components can be resolved. Fig. 6 gives an example in which this is not the case with natural isotope mixtures.

The magnetic splitting of the Sr^{87} isotope (6.96%) is partially masked by the isotopes $Sr^{86} + Sr^{88}$ (9.75% + 82.74%), so that the three components ABC cannot be resolved. To determine the mechanical moment

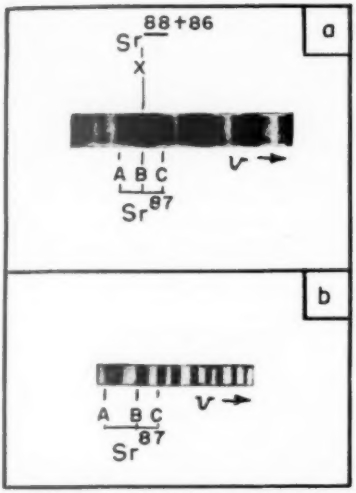

FIG. 6. HFS photographs of a natural strontium mixture: *a*) (Sr^{88}: Sr^{87}: Sr^{86} = 82.74 : 6.96 : 9.75); *b*) pure Sr^{87}. [From Heyden and Kopfermann (7)]*

(spin I), it is necessary to know either the intensity ratio $A:B:C$ (intensity rule), or the separation ratio $AB:BC$ (interval rule); to determine the magnetic moment of the nucleus, it is necessary to know the absolute amount of the separations AB and BC.

Fig. 6*a*, showing natural Sr, indicates clearly that none of the necessary measurements can be carried out with this HFS. Here, a spectroscopic examination of pure Sr^{87} will be successful. Fig. 6*b* shows its spectrum.

The pure isotope can be obtained from a micaceous rubidium ore free from natural strontium. It is known that Rb^{87} is a β-emitter with a half-life of 6.0×10^{10} years, decaying into Sr^{87}. In geologically old Rb ore, this process has produced so much Sr^{87} that several milligrams can be chemically extracted from a few kilograms of ore, making an HFS investigation possible.

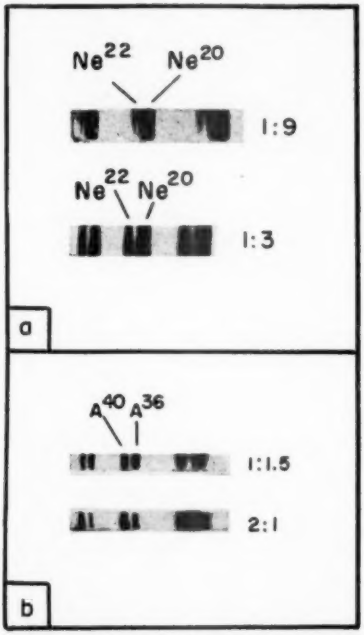

FIG. 7. Isotope displacement: *a*) normal neon (Ne^{22}: Ne^{20} = 1 : 9.8) and neon enriched by diffusion (Ne^{22}: Ne^{20} = 1 : 3) [from Hertz (8)]; *b*) argon enriched by by diffusion (A^{40}: A^{36} = 1 : 1.5 or 2 : 1) [from Kopfermann and Krüger (9)]*

Spectral photographs are best evaluated when the lines to be measured are of equal blackening. Evaluation becomes difficult for a blackness ratio of 10 to 1; for a ratio of 100 to 1, it is possible only in special cases.

If the isotope displacement of a very rare and a very abundant isotope is to be measured, it can only be done by enriching the rare isotope.

Two characteristic cases are shown in Fig. 7. Normal neon consists of:

$$Ne^{20}:Ne^{21}:Ne^{22} = 90.51:0.28:9.21$$

and normal argon of

$$A^{40}:A^{38}:A^{36} = 99.57:0.08:0.35.$$

The spectrum of natural neon is shown

*Permission to reproduce this illustration from the text "Kernmomente" has been granted by the publisher, J. W. Edwards, Ann Arbor, Michigan.

FIG. 8. Isotope displacement of uranium lines (grating spectrum) A = 4,242 A.U.; B = 4,244 A.U. Reading down: 1) U^{238}; 2) $U^{238} + U^{235}$; 3) U^{235}; 4) $U^{235} + U^{233}$; 5) U^{233}; and 6) $U^{238} + U^{233}$. [From Burkhart, Stukenbroeker and Adams (*10*)]

in Fig. 7*a*. Each order of interference consists of two components. We are concerned, here, with the slightly displaced components of the non-splitting isotopes Ne^{20} and Ne^{22} (Ne^{21} is too weak to appear).

An exact measurement of the separation of the components is very difficult in this case, but it can be carried out with greater accuracy after an enrichment to a ratio of 1:3. Such a measurement would be wholly impossible with natural argon, whose HFS pattern always consists of a single component. Enrichment to a ratio of about 1:1 (Fig. 7*b*), using a Hertzian diffuser, allows the isotope displacement between A^{40} and A^{36} to be measured; A^{38} is still insufficiently enriched to appear. The measured values of the isotope displacement obtained from these photographs are consistent with the conception of the isotope-displacement effect previously discussed.

Another good example of the measurement of isotope displacement with separated isotopes is given in Fig. 8, showing artificially produced uranium. Details are given in the legend.

Optical Identification of Nuclear Transformations

If pure gold is bombarded with thermal neutrons, the reaction

$$_{79}Au^{197} + {}_{0}n^{1} = {}_{79}Au^{198} \xrightarrow[2.7d]{\beta} {}_{80}Hg^{198}$$

occurs. Au^{198}, originated by neutron capture, decays to isotopically pure mercury. If the reaction is allowed to continue for a sufficiently long time and a gold sheet sealed in a quartz cylinder is exposed to a sufficiently intense neutron source and heat is applied to evaporate the resulting Hg out of the Au, a "quartz mercury lamp" filled with Hg^{198} is obtained.

The HFS spectrum of the line 5,461 A.U. is compared to the spectrum of natural mercury in Fig. 9. Natural mercury consists of a mixture of

$$Hg^{196}:Hg^{198}:Hg^{199}:Hg^{200}:Hg^{201}:Hg^{202}:Hg^{204} = 0.15:10.12:17.04:23.25:13.18:29.54:6.72.$$

The odd-numbered isotopes show a magnetic HFS splitting, while the components of the even-numbered isotopes and the centers of gravity of the odd-numbered isotopes are displaced toward one another. In this manner, the complicated HFS pattern of Fig. 9 can be understood.

The component of Hg^{198} is to be expected at position *II*; that of Hg^{200} at position *III*. The HFS spectrum of

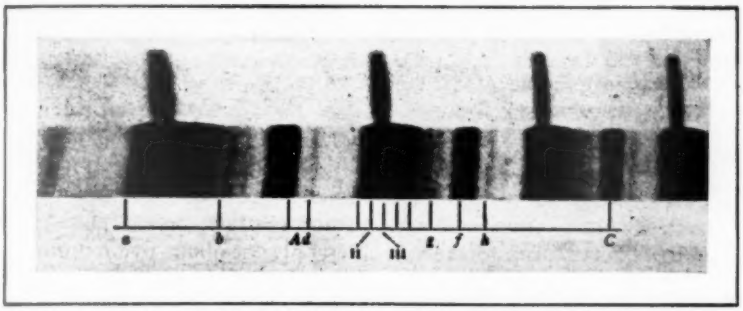

FIG. 9. HFS of the Hg *I* line **5,461 A.U.**; lower, natural Hg mixture; upper, pure Hg^{198} produced by nuclear transmutation. [From Wiens (*11*)]

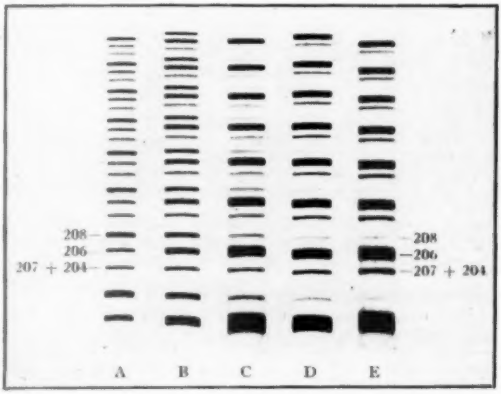

FIG. 10. HFS spectra of lead samples containing uranium of the Pb *II* line 5,372 A.U.; A) normal lead; B) Colorado carnotite; C) Wilberforce uranite; D) pitchblende from Great Bear Lake; E) Katanga pitchblende. [From Rose and Stranathan (*3*)]

the same line of the pure isotope is found to consist of only one component which is at the position expected from the HFS analysis.

On the one hand, Fig. 9 proves once more the accuracy of HFS analysis and HFS laws; on the other hand, it furnishes for the first time a means of optical identification for nuclear reactions.

Such an isotopically pure mercury is particularly suitable for associating an optical wavelength with the meter. As is shown in Fig. 9, the width of this line is especially small and this increases the accuracy of measurement.

Optical Mass Spectrometry

It has already been stated that an important part of HFS analysis has to do with the fact that the intensities of the HFS components are in the same ratio as the isotope abundances. This fact may serve to determine the isotope ratios in different samples, e.g., in Fig. 5. It can therefore be naturally used as a kind of "optical mass spectrometry," if one defines mass spectrometry as determination of isotope abundances.

This technique has been applied to a modest extent. An especially good example is given in Fig. 10, where the

HFS spectra of the line 5,372 A.U. of several lead samples are shown. The same line was shown in Fig. 3, where there were 4 components in each order. In this case the distance between the Fabry-Pérot plates is so chosen that one of the two components of Pb^{207} coincides with that line of the next interference order, which corresponds to both the other component of Pb^{207} and that of Pb^{204}.

Thus reproduced in each order is a complete mass spectrum consisting of three lines: 208, 206, and 207 + 204. Photograph A shows an average "normal lead." (The abundance ratio of "normal lead" varies to a greater degree than does that of other elements because of the radioactivity to be discussed below.) Photographs B to E show the spectra of lead samples containing uranium. It is easily seen that these samples, compared to those of normal lead, Pb^{206}, the end-product of the U^{238}-Ra series, and Pb^{207}, the end-product of the U^{235}-Ac series, are more or less strongly enriched, though in differing amounts.

It follows that different amounts of "radiogenitive" lead are formed in minerals of different ages because of the differing lives of U^{238} and U^{235}. Working backwards, the age of the mineral can be determined from the abundance ratio. These "optical" methods have advantages over the usual mass spectrometer. In the latter instrument hydride formation may falsify the abundance ratio, while such errors do not occur in the former method.

BIBLIOGRAPHY

1. H. Kopfermann, "Kernmomente" (J. W. Edwards, Ann Arbor, Mich., 1945)
2. W. Walcher, *Z. Physik* **108,** 376 (1938)
3. J. Rose, R. Stranathan, *Phys. Rev.* **49,** 916 (1936), *ibid.* **50,** 792 (1936)
4. H. Kopfermann, *Z. Physik* **75,** 363 (1931)
5. W. Walcher, *Z. Physik* **122,** 401 (1944); H. Kopfermann, W. Walcher, *ibid.* **122,** 465 (1944)
6. M. Fred, F. S. Tomkins, J. K. Brody, *Phys. Rev.* **75,** 1772 (1949)
7. M. Heyden, H. Kopfermann, *Z. Physik* **108,** 232 (1938)
8. G. Herts, *Z. Physik* **79,** 108 (1932)
9. H. Kopfermann, H. Krüger, *Z. Physik* **105,** 389 (1937)
10. L. E. Burkhart, G. Stukenbroeker, S. Adams, *Phys. Rev.* **75,** 83 (1949)
11. J. H. Wiens, *Phys. Rev.* **70,** 910 (1946)

Proportional Counters *(Continued from page 10)*

count can occur within 10 μsec and still be recorded as a full-sized swing in the potential of the wire. As the value of A is increased, the avalanche becomes larger, spreads over more and more of the wire, and the ultimately attainable counting speed diminishes.

Thus, to increase the speed of operation of a counter, the voltage should be as low as feasible, and the vacuum-tube amplification high. The amplifier must have a short rise-time. The counter is then operated in the proportional region. The circuit connecting the counter to the amplifier must have a short recovery-time; for example, 10,000 ohms and 10 $\mu\mu$f capacity. The circuit differentiates the pulse, and the recording circuit should be designed to record the rapid initial rise. With this arrangement, 10^5 evenly-spaced pulses per second can be counted, a rate at least ten times higher than that obtainable with Geiger counters operated in the conventional way.

BIBLIOGRAPHY

1. E. Rutherford, H. Geiger, *Proc. Roy. Soc.* **81A,** 141 (1908)
2. H. Geiger, O. Klemperer, *Z. Physik* **49,** 753, (1928)
3. M. E. Rose, S. A. Korff, *Phys. Rev.* **59,** 850 (1941)
4. S. A. Korff. "Electron and Nuclear Counters" (D. Van Nostrand, New York, N.Y., 1946)
5. C. G. and D. D. Montgomery, *Phys. Rev.* **57,** 1030 (1940)
6. S. A. Korff, R. D. Present, *Phys. Rev.* **65,** 274 (1944)
7. S. A. Korff, *Phys. Rev.* **72,** 477 (1947)

Scintillation Conducting Rods in Tracer Work

Successful use of light-conducting media with scintillation counters in tracer work is time-saving. Lucite has been found most useful by the authors. Results presented here will help anyone interested in designing such circuitry.

By K. D. Timmerhaus, E. B. Giller, R. B. Duffield,* and H. G. Drickamer

Department of Chemistry, University of Illinois
Urbana, Illinois

DEVELOPMENT of the scintillation counter made feasible a number of tracer experiments which were formerly either impossible or extremely difficult. In tracer experiments it is frequently desirable to conduct the light from the crystal to the photomultiplier tube along some sort of light conducting rod. By placing the crystal inside the system it is then possible to analyze without sampling. Such procedure is particularly advantageous in high pressure or flow systems.

The use of light-conducting media mirrors, hollow tubes of polished metal, and solid plastic or quartz rods is discussed by Collins (*1*, *2*) and by Jordan and Bell (*3*) in a review article. The use of tapered rods has also been mentioned. While these are important for energy measurements, they are not so useful for tracer work, since it is usually desirable to have as small a crystal as feasible inside the system.

This investigation was primarily concerned with the properties of various light conducting rods as they affect scintillation counting. Among the variables studied were type of rod, rod length, rod diameter, energy and type of radiation, type of crystal, and effect of bending the rod.

In all the experiments a type 1P28 photomultiplier tube cooled to dry ice temperature was used. The tube was mounted within a light-tight brass box, Fig. 1, of $\frac{3}{32}$-in. wall thickness. The box was divided into two compartments. The lower section contained the photomultiplier tube in an inverted position and the upper compartment all the wiring essential to the operation of the tube. The direct-current voltage supply was brought into the brass box through a seven-pronged Cannon plug. The signal pulse from the tube was brought out of the box through a single-pronged Cannon plug. Both of these cable connections were tightly wrapped in water-proof tape and then covered with ceresine wax. The tube circuit was a modification of one proposed by Sherr (*4*) and by Marshall, Coltman, and Bennett (*5*).

The brass box was held inside another box, this one made from bakelite with $\frac{3}{32}$-in. wall thickness, by four evenly spaced brass struts. The outside of the bakelite box was covered with $\frac{1}{4}$-in. cork sheets. The top of the outer box was made removable to allow the addition of dry ice to the apparatus at two-hour intervals. This cooling of the photomultiplier tube was necessary to reduce the background noise.

A $\frac{3}{4}$-in. hole was cut in the light-tight brass box on the side directly facing the photosensitive portion of the

* Also member of Department of Physics.

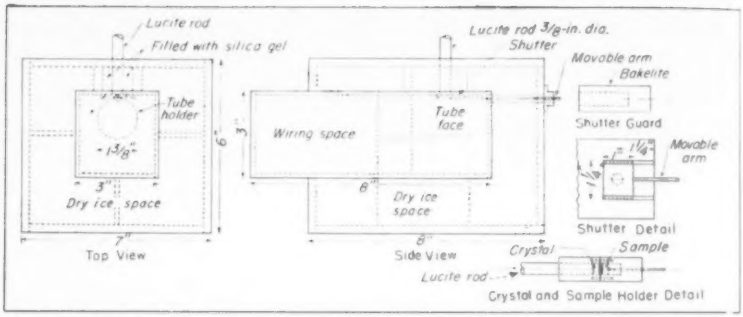

FIG. 1. Apparatus for using scintillation counter with light-conducting media. All pieces are 1/8-in. brass plate except outer wall which is of 1/4-in. bakelite

tube. Another 3/4-in. hole was cut in the outside bakelite box which was directly in line with the hole in the brass box. To make a light-tight seal between the inner brass box and the outer brass box a 1½-in. brass cylinder was inserted in the gap and secured after being centered around the two holes. The outside of the brass box and cylinder were then covered with glyptal to insure a light-tight seal. For the purpose of measuring dark current, a brass shutter was installed inside the brass box so that the photomultiplier could be shielded from scintillations in the crystal.

A linear amplifier was used in all of these experiments. The pulses were counted by a standard scale unit. The high voltage supply for the photomultiplier tube was a battery pack (820 volts was used for the major portion of the experiment).

Preparation of Rods

Most of this work was done with plastic rods. All the rods were cut and then polished, first with varying grades of sandpaper, and finally with finely powdered calcium carbonate. Great care was exercised to insure uniform polishing from rod to rod.

Lucite was used for the bent-rod experiment. The rods were bent by heating the 12-in. rods in 94° C water until the rods were quite pliable and flexible. One rod was made with a gradual curvature using the whole length of the rod. The same angle was used in the other except that the bend was made as sharp as possible. The rods were then polished in the same manner as described previously.

Preparation of Samples

The radioactive materials used in these tests are listed in Table 1 along with their type and energy of radiation. All samples were thin and mounted on thin backing. They were obtained from the Atomic Energy Commission.

Preparation of Crystals

Rough commercial naphthalene and anthracene crystals were obtained and cut into usable shapes. The calcium

TABLE 1

Material	*Type and Energy of Radiation*
P^{32}	β 1.72 Mev
Tl^{204}	β 775 kev
Sr^{90}	β 600 kev
Ca^{45}	β 260 kev
C^{14}	β 154 kev
Fe^{59}	β 260 kev; γ 1.1 Mev
	β 460 kev; γ 1.3 Mev
Ag^{110}	β 100 kev; γ 0.3 to 1.4 Mev
Po^{210}	α 5.30 Mev

tungstate crystals were obtained in the form of ¼-in. cylinders. These were cut up and pieced together to obtain the desired size crystal. One crystal of thallium-activated sodium iodide was also used.

For a permanent installation any of the above crystals is best fastened to a light-conducting rod with a slow drying mixture made from Lucite shavings dissolved in a solution of ethylene dichloride. This eliminates a surface and gives better efficiency of light transmission.

Experimental Results

Except where otherwise noted, all data were obtained with the use of anthracene crystals.

Table 2 shows a comparison of three types of plastic rods of different length. It can be seen that at any length the Lucite is considerably superior to the Plexiglas, and the polystyrene is inferior to both, regardless of the type of radiation. At 6 inches the number of counts is approximately in the ratio 5:4.2:3.8, although it varies somewhat, being higher in the case of weak beta radiation. On increasing the length the transmission falls off much less rapidly for the Lucite than for the other type rods. For Lucite the transmission of light from beta radiation of any energy is about 75% as great at 12 inches as it is at 6 inches. Figure 2 shows the relative transmission of the three types of rods as a function of wavelength measured spectroscopically on 9 cm rods. Qualitatively the com-

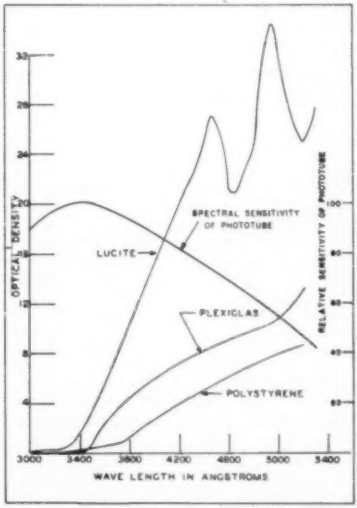

FIG. 2. Relative transmission of Lucite, Plexiglas, and polystyrene

TABLE 2

Effect of Varying Lengths of ⅜-inch Dia Rods of Lucite, Plexiglas, and Polystyrene

Sample	*Rod length*	*Counts per min*		
		Lucite	*Plexiglas*	*Polystyrene*
P^{32}	3	5191	4256	3949
	6	4745	3138	2754
	9	4003	2075	1314
	12	3633	1505	533
Ca^{45}	3	3319	2861	2643
	6	2988	2037	1743
	9	2489	1327	816
	12	2207	1169	496
Fe^{59}	3	1083	1021	981
	6	1019	847	788
	9	897	669	580
	12	847	581	487

parison is similar to that obtained from the crystals, especially in the near ultraviolet region.

A comparison made between 9 inch quartz and Lucite rods indicates that the quartz is equivalent to Lucite for anthracene crystals and about 40% superior to Lucite for calcium tungstate crystals.

Table 3 shows the effect of rod diameter on counting rate. There is a definite increase in counting rate with increase in rod diameter below ½ inch. Above this diameter the increase is not so effective. This is to be expected since the photosensitive surface is only about ½ inch wide. In tracer work, it is frequently desirable to use as small a diameter crystal and rod as possible.

Table 4 compares the counts obtained from an Sr^{90} source with various crystals. The variation in crystal quality is about as great as could reasonably be expected, and still the counting rate varies only by a factor of two. Variations among photomultiplier tubes have been found to be much greater than this.

In Table 5 four different types of crystals are compared using various sources and a 6-in. Lucite rod ½ in. in diameter. All crystals were quite clear, and in the case of the anthracene, naphthalene, and sodium iodide they were of approximately the same thickness and roughly the size of the end of the rod. It was not possible to obtain a calcium tungstate crystal ½ in. in diameter, as it was necessary to piece together a mosaic out of smaller pieces. This makes the comparison somewhat unfair in the case of this type of crystal.

The results show that anthracene is superior for beta counting as has been found by other investigations. For alpha sources there is not so much to choose, particularly between anthracene and calcium tungstate. For the alpha sources used, the thallium-impregnated sodium iodide was by far the best.

TABLE 3
Effect of Rod Diameter on Counting Length for Sr^{90}

Rod Dia In Inches	*Photo Multiplier Count (cpm)*
⅜	1323
½	1560
¾	1721

TABLE 4
Effect of Varying Quality of an Anthracene Crystal, Using a Constant Beta Source (Sr^{90})

Crystal Diam In Inches	*Photomultiplier Counts (cpm)*	*Quality of Crystal*
½	1945	cloudy and scarred
½	2650	fairly clear
½	3663	most clear

TABLE 5
Effect of Various Types of Crystals of Same Diameter with Fixed-dia Sources*

Source	*Counts per min*			
	Anthracene	*Napthalene*	*Calcium Tungstate*	*NaI-Tl*
P^{33}	44,772	39,811	21,791	32,791
Tl^{204}	37,429	29,650	9,352	9,791
Fe^{59}	3,120	2,621	2,678	2,154
Fe^{59}†	564	441	863	899
Ag^{110}	9,499	6,555	8,874	6,299
Ag^{110}†	1,294	1,106	1,340	1,366
Po^{210}	10,560	8,351	16,050	41,130

* A ½-in. dia. 6-in. Lucite rod was used throughout this investigation.
† With 600 mg/cm² of aluminum absorber.

TABLE 6

Effect of Different Bends with ⅜-in. Dia, 12-in. Lucite Rod. (For the gradual bends the whole rod was utilized in forming the bend, whereas for the sharp bends the minimum length of rod was used to effect the bend.)

Source	*Angle*	*Counts Per Minute*		
		Gradual	*Sharp*	*No Bend*
P^{32}	0°	.....	.....	26,743
	45°	24,307	14,998	
	90°	17,426	13,646	
	180°	14,599	9,208	
Tl^{204}	0°	.....	.....	1,740
	45°	1,357	869	
	90°	1,075	617	
	180°	614	295	

For many tracer uses it would be convenient to bend the light-transmitting rod between the crystal and the tube. In Table 6 the effect of bending is shown for a 12-in. Lucite rod, ⅜ in. in diameter. It is important to make the bend as gradual as possible, but it is quite possible to make even a 180° bend without losing more than 50% of the counts.

Conclusions

The authors have found the scintillation counter with Lucite rod a very useful and flexible tool in tracer work. A successful device for counting radiation under pressures as high as 2,000 psi without sampling has been used, and is described elsewhere (*6*). It is certain that many other uses will develop in the future.

BIBLIOGRAPHY

1. Conference on scintillation and crystal counters, U. of Rochester (July, 1948)
2. Conference on scintillation counters, Oak Ridge, Tenn. (June, 1949)
3. W. H. Jordan, P. R. Bell. Scintillation counters, NUCLEONICS **5**, No. 4, 30 (1949)
4. R. Sherr, *Rev. Sci. Instr.* **18**, 767 (1947)
5. J. W. Coltman, F. H. Marshall, A. I. Bennett, *Rev. Sci. Instr.* **19**, 744 (1948)
6. K. D. Timmerhaus, L. H. Tung, E. B. Giller, R. B. Duffield, H. G. Drickamer, *Rev. Sci. Instr.* **21**, 210 (1950)

RADIATION has gained a permanent foothold in modern science and industry, and society is presently struggling to learn to live with it. Health protection of radiation workers has been remarkably successful in atomic energy installations. It has been possible, for the most part, to keep exposures not only at tolerance levels but considerably below them, and the general health of the workers has been better than that in most other industries. The attitude of alarm which has been so commonly associated with the idea of radiation work can safely be discarded, provided it is replaced by one of healthy respect for protective rules.

—*From a paper by M. Ingram,* Science **111**, 103 (1950)

Irradiation of Small Volumes by Contained Radioisotopes*

Calculations of radiation dosage from internal radioactive substances are important to those who would study the biological effects of radioactive decay within a living organism, and to those who wish to irradiate tiny particles in a small volume of radioactive solution. Such dosage calculations may also be important in tracer studies where there is great selective concentration in a small sensitive area. Solutions are presented here for several useful geometric types that may be encountered.

By PAUL I. RICHARDS and BENJAMIN A. RUBIN

Brookhaven National Laboratory
Upton, New York

Biological effects of selectively absorbed unstable isotopes have frequently appeared to be unexpectedly high (*1, 2, 3, 4*). In particular, radioactive disintegrations which result in chemical transmutation (and considerable recoil) *in vivo*, may produce changes which seem *not* to be explainable solely on the basis of ionization (taken here to include all types of energy loss associated with emitted elementary particles). In attempting to decide whether these effects could possibly result from increased ionization density, or whether some other mechanism is involved, it became necessary to devise a method for determining the local radiation dosage resulting from the selective concentration of β-emitting isotopes.

Previous internal dosage studies (*5, 6, 7*) have dealt chiefly with the problems of γ-radiation, and with the portions of the β-problem where average path length was very small compared to the dimensions of the volume being considered. For such cases it was safe to assume that all the energy of the β-particles was dissipated in the irradiated volume. This type of solution was obviously inadequate in studies of microorganisms (*1, 2*) or of important accumulations in very small areas (*8*). In a recent consideration of the internal radiation dosage calculations, Marinelli et al. (*5*) have noted the problem thus:

"Many organs in small animals used in experiments dealing with isotopes emitting high energy beta-rays are not small in comparison to the range of the beta-particles. Proper estimate of the dose in these instances is, in general very complicated and must be left to the future."

In another paper (*6*) they stated:

"It is recognized that, with the use of P^{32} in mice these determinations [using total energy absorption] are not as accurate as one would wish because the linear dimensions of most organs are smaller than the range of a considerable portion of the beta-particles emitted by P^{32}. Similar information in larger animals would yield more reliable figures. Conversely this type of calculation would be fairly accurate even in a small animal if soft beta-ray emitters (H^3, C^{14}, S^{35}, etc.) were used."

The present study attempts to fill this gap in a manner which may be useful in problems where the average path

* Research was carried out at Brookhaven National Laboratory under the auspices of the U. S. Atomic Energy Commission.

of the emitted particle is a significant fraction of the dimensions of a volume being internally irradiated.

Before going into the calculations, it may be interesting to note the scope of the need for corrections of the type to be described. Consider a solution of P^{32} which is being used to irradiate some suspended microorganisms. If one used a convenient volume of say 1.5 ml, in a tube with an inside diameter (i.d.) of 1 cm (as was actually used), the specific radiation dose is 21% less than expected if the calculation assumed that the β-particles dissipated all their energy within the tube. If on the other hand a 16-mm i.d. tube was used, the loss would be 17%. Evidently it is not only necessary to realize that there is a substantial escape of radiation even in what seems a simple operation, but that the size and shape of the vessels used may seriously affect the conditions of the experiment. For problems of dosage measurements in the study of mouse organs, corrections of the same order of magnitude are required. But it is not necessary to utilize an otherwise inconvenient isotope in order to circumvent calculation difficulties.

To illustrate the solution of a problem at the other end of the geometric scale, consider concentrating P^{32} in a microorganism whose volume is 1×10^{-12} ml. The energy dissipated within the organism by the β-particles comes to 1 part in 1.5×10^{-4} of their total energy. This is a most significant observation when it is seen that the biological effect increases at a rate proportional to the internal disintegrations, while, at the same time, there is almost no increase of ionizing energy in the cell.

No attempt will be made here to redescribe aspects of the internal dosage problem which have been defined previously. No account will be taken of the factors of radioactive or biological decay, or of the questions of radiation dose units and measurements. These questions may be evaluated in a manner described by Siri (*10*), by Bush (*7*) and by Marinelli, et al (*5, 6*).

The central approach to the present radiation-dosage calculations is the evaluation of the fraction of "ionizing" energy *escaping* from a volume containing a radioisotope. The radiation will be presumed to arise from a uniformly distributed radioemitter in a volume that is homogeneous and isotropic in regard to its absorption properties. This preliminary supposition is sufficiently satisfied in many experimental situations. Great deviations from uniform distribution may seriously affect the dosage.

Secondly, it is assumed that there is no backscattering from the surrounding media. While this is often not true, the correction involved can be made separately. In general, backscattering cannot increase the fraction of energy which escapes, and this may be sufficient information in some cases. The effects of the scattering within the volume should cancel to first order, since it may be seen that approximately as many particles will be scattered into the interior of the volume as are scattered out. By similar reasoning, β-particles may be treated as monochromatic and as having straight paths.

For initial purposes of analysis, consider an infinite slab of thickness $S \leq$ the radiation range R (Fig. 1), containing an isotope whose "rays" lose energy uniformly along their path. (This will be approximately correct for γ-rays and for ultra-relativistic* particle radiation). Let ρ equal the number of rays originating from a unit volume during a unit time, and let E equal the energy of the radiation and R its range. Referring to Fig. 1, consider radiation leaving a small volume

* *Ultra-relativistic* indicates that the particle has an energy $>2mc^2$. See reference *11*.

V. Lindy

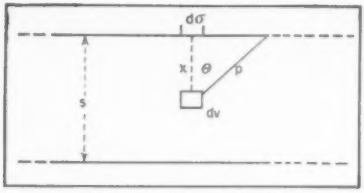

FIG. 1. "Infinite" slab

dV which is located a distance x below the surface. If a ray leaves dV at a polar angle θ, the length of its path within the volume is $p = x/\cos\theta$. If this length is less than the range R, then, by our assumption of uniform rate of ionization, the energy escaping from the volume is $E(1 - p/R) = E(1 - x/R\cos\theta)$. The solid angle subtended by radiation having angles θ to $\theta + d\theta$, is $2\pi \sin\theta\, d\theta$, while the radiation arising from dV is $\rho\, dV/4\pi$ per unit solid angle. Thus, of the total radiant energy arising from the volume dV, the amount which escapes from the top face is

$$\frac{E\rho dV}{2}\int_0^{\cos^{-1}\frac{x}{R}}\left(1-\frac{x}{R\cos\theta}\right)\sin\theta d\theta = \frac{E\rho dV}{2}\left(1-\frac{x}{R}+\frac{x}{R}\log\frac{x}{R}\right)$$

Now, to integrate this over x, note that $dV = d\sigma dx$ where $d\sigma$ is an element of the area of the face. The energy from below $d\sigma$ which escapes from the top face is then

$$\frac{E\rho d\sigma}{2}\int_0^S\left(1-\frac{x}{R}+\frac{x}{R}\log\frac{x}{R}\right)dx = \frac{E\rho S d\sigma}{2}\left\{1-\frac{3}{4}\left(\frac{S}{R}\right)-\frac{1}{2}\left(\frac{S}{R}\right)\log\frac{R}{S}\right\}$$

But the quantity $E\rho S d\sigma$ is the total radiant energy arising from emitters located below $d\sigma$. Hence the fraction F_2 of energy escaping from both faces is

$$2F_1 = F_2 = 1 - \frac{3}{4}\left(\frac{S}{R}\right) - \frac{1}{2}\left(\frac{S}{R}\right)\log\frac{R}{S} \quad (1)$$

A second problem differs from the first only in that the radiation is not considered to lose energy at a constant rate. For low-energy radiation $E < 2mc^2$ (the biologically useful α- and β-rays), the rate of energy loss is more accurately taken as (*11*)

$$\frac{d\epsilon}{dp} = \frac{-\alpha}{\epsilon} \quad (2)$$

where α is a constant which may be related to the range R and initial energy E as follows. The solution of Eq. 2 is: $\frac{1}{2}\epsilon^2 = -\alpha p + C$

Evaluating the constant from the condition that $\epsilon = E$ at $p = 0$,

$$2\alpha p = E^2 - \epsilon^2 \quad (3)$$

Since $\epsilon = 0$ at $p = R$, then $2\alpha R = E^2$; Eq. 3 may be put in the form

$$\epsilon = E\sqrt{1 - p/R} \quad (4)$$

which implies that if the particle escapes from V after traversing a path of length $p < R$, it leaves with the energy $E\sqrt{1 - p/R}$. Hence, in the second problem, by arguments similar to those employed in treating the first, the energy lost out of the top face from radiation arising in the volume dV is

$$\frac{E\rho dV}{2}\int_0^{\cos^{-1}\frac{x}{R}}\sqrt{1-\frac{x}{R\cos\theta}}\,\sin\theta d\theta = \frac{E\rho dV}{2}\left\{\sqrt{1-\frac{x}{R}} - \frac{x}{R}\log\left(\sqrt{\frac{R}{x}}+\sqrt{\frac{R}{x}-1}\right)\right\}$$

Again noting that $dV = d\sigma dx$, the energy lost through the top face out of that arising below $d\sigma$ is, setting $y = x/R$,

$$\frac{E\rho S d\sigma R}{2}\cdot\frac{1}{S}\int_0^{S/R}\left\{\sqrt{1-y} - y\log\left(\sqrt{\frac{1}{y}}+\sqrt{\frac{1}{y}-1}\right)\right\}dy$$

This is best integrated by noting that the logarithm is equal to $-\frac{1}{2}\log y + \log(1+\sqrt{1-y})$. The first of these is easily integrated, and the second may be integrated by setting $u = 1 + \sqrt{1-y}$. The final result is

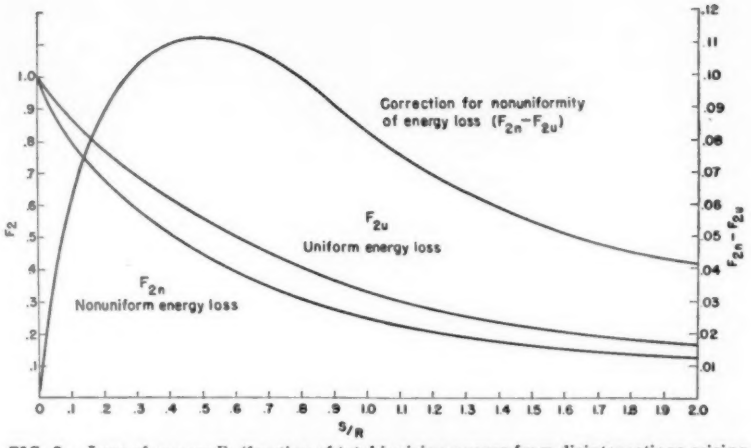

FIG. 2. Loss of energy F_2 (fraction of total ionizing energy from disintegrations arising within a slab) as a function of S/R—other dimensions considered "infinite." The correction may be used for geometric figures in which the calculations are provided only for uniform ionization loss (F_{2u})

$$2F_1 = F_2 = \frac{2}{3}\frac{R}{S}\left[1 - \left(1 - \frac{S}{R}\right)^{3/2}\right] - \frac{S}{4R}\log\frac{R}{S} - \frac{S}{2R}\log\left(1 + \sqrt{1 - \frac{S}{R}}\right) - \frac{1}{6}\left(1 - \sqrt{1 - \frac{S}{R}}\right) - \frac{R}{6S}\left(1 - \sqrt{1 - \frac{S}{R}}\right)^2 \quad (5)$$

The results of these two analyses are plotted in Fig. 2. (Note that Eqs. 1 and 5 hold only for $S \leq R$.)

Several useful formulas can be derived with the aid of these results. If the dimensions of a volume are very much greater than the range R, only radiation arising within a distance $\leq R$ from the surface can escape and be lost. If the surface is everywhere nearly flat (radius of curvature $\gg R$), the preceding formulas for F_1 with $S = R$ indicate that the fraction of energy lost from this surface "skin" is $\frac{1}{8}$ for high energy radiation and $\frac{1}{6}$ for low energies. The total radiative energy arising in the "skin," however, is $E\rho AR$, where A is the surface area. Thus the energy lost is $\frac{1}{8}E\rho AR$ or $\frac{1}{6}E\rho AR$ in the two cases. Dividing by the total radiative energy $E\rho V$ where V is the volume of the body, the fraction F of energy lost is

$$F_{1u} = AR/8V \text{ for high energy} \quad (6)$$

$$F_{1n} = AR/6V \text{ for low energy} \quad (7)$$

Equation 6 has been previously derived by F. Bush (*7*), but he recommends its application to β-rays, whereas this analysis shows that it is precisely for β-rays that Eq. 7 should be used. While Eqs. 6 and 7 are exact for an infinite slab of thickness $S > R$, the derivation would seem to imply that this relationship breaks down rapidly as R becomes comparable to the smallest linear dimension of V. While this is true, the error is no more than 20% as long as R is no greater than the smallest dimension. To see this, note that the worst possible shape satisfying this condition on R would be a sphere of radius $R/2$. Using the high-energy formula (where uniform ionization was assumed), Eq. 6 predicts $F = 3/4$. The mean path $\bar{p}$ within a sphere is known to be 3/4 radius (*9*); in this case $\bar{p} = 3R/8$. Since the maximum path in the sphere is R, the fraction of energy

lost, if the ionization is uniform, is simply $1 - (p/R) = 5/8$.

Under most conditions, slabs of uneven thickness S can be handled easily. In cases where S is always $\geq R$, the absolute value (rather than the fraction) of the loss will remain constant. Where $S < R$, a good approximation can be made by finding a simple average value for S. That this holds, except for the most extreme variations, may be seen from the approximate linearity of the curves presented in Fig. 2. Should cases of very great variation arise, sections of the slab may be considered separately.

While the relations already discussed can be applied to a great many situations, there are cases which are not well approximated in this manner. Unfortunately, in none of the problems which follow has it been found practicable to carry out the appropriate integrations for low-energy radiation. The correction due to nonuniformity of ionization can be estimated however, from Fig. 2 or from comparison of Eqs. 6 and 7, by considering effects in roughly comparable situations.

Equations 6 and 7 are valid for any volume, all of whose dimensions are of the order of R or greater. If the volume is very small and roughly spherical, the fact that the mean path for a sphere equals three-fourths of its radius indicates that

$$F = 1 - \frac{3}{4R}\sqrt[3]{\frac{3V}{4\pi}} = 1 - 0.435\sqrt[3]{\frac{V}{R}}$$

The infinite slab formulas, Eqs. 1 and 5, will be of use for a slab whose lateral dimensions are very large compared to R but whose thickness is less than R. As a next approximation to the *finite* slab, an edge correction can be derived (analogous to the surface corrections of Eqs. 6 and 7 for large volumes).

Consider a very thin strip of width $b < R$ and infinite length. The internal path length for radiation which leaves a small volume dV located at a distance x below the top edge will be $x \cos\theta$ where θ is the angle between the radiation and the vertical direction. (See Fig. 1 where now $S = b$, the width of the strip.) Since we are now considering only radiation within the "plane" of the strip, the relative amount of radiation between θ and $\theta + d\theta$ is $d\theta/2\pi$. Thus, of the energy leaving dV, the amount lost out the top edge is

$$\frac{E\rho dV}{\pi}\int_0^{\cos^{-1}\frac{x}{R}}\left(1 - \frac{x}{R\cos\theta}\right)d\theta$$
$$= \frac{E\rho dV}{\pi}\left\{\cos^{-1}\frac{x}{R} - \frac{1}{2}\frac{x}{R}\log\frac{1+\sqrt{1-(x/R)^2}}{1-\sqrt{1-(x/R)^2}}\right\}$$

Now, noting that $dV = d\sigma dx$, that $\frac{1}{2}\log[(1+x)/(1-x)] = \tanh^{-1}x$, and that the total energy arising below $d\sigma$ is $E\rho b d\sigma$, the fraction lost becomes

$$\frac{1}{\pi}\frac{R}{b}\int_0^b \cos^{-1}\frac{x}{R}\,d\left(\frac{x}{R}\right) - \frac{1}{\pi}\frac{R}{b}$$
$$\int_0^b \frac{x}{R}\tanh^{-1}\sqrt{1-\left(\frac{x}{R}\right)^2}\,d\left(\frac{x}{R}\right)$$

The latter integral may be evaluated by setting $u = \sqrt{1-(X/R)^2}$. The final result is that the fraction F_{e1} of energy lost out of one edge is

$$F_{e1} = \frac{1}{\pi}\cos^{-1}\frac{b}{R} + \frac{R}{2\pi b}\left(1 - \sqrt{1-\frac{b^2}{R^2}}\right)$$
$$- \frac{b}{2\pi R}\tanh^{-1}\sqrt{1-\frac{b^2}{R^2}} \quad (9)$$

This equation, in conjunction with Eq. 1 or 5, should be useful in treating rectangular strips long compared to R but of width $b < R$ and thickness $S \ll b$.

To evaluate this edge correction for finite slabs, consider a band of width R running around the edge of the slab (Fig. 3). From Eq. 9, setting $b = R$, the energy lost from the outer edge is $1/2\pi$ times the energy carried by radiation which travels in the "plane" of the slab; this, in turn, is $(1/2\pi)(1 - F_2)$ times the energy liberated from the

V. Cindy

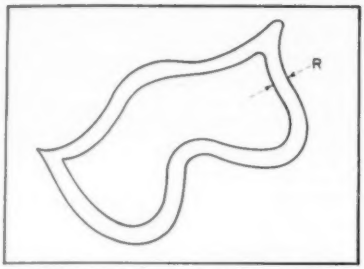

FIG. 3. Surface of a "finite" slab

band. If P is the perimeter of the slab and S its thickness, the energy lost out the edges is $(E\rho SPR)(1 - F_2)/2\pi$. The energy escaping from the two faces is $F_2(E\rho SA)$, where A is the area of the slab and F_2 must be found from Eq. 1 or 5. Adding these and dividing by the total energy,

$$F = F_2 + \frac{PR}{2\pi A}(1 - F_2) \qquad (10)$$

Once again, Eq. 10 is actually more accurate than its derivation might indicate. One might expect Eq. 10 to hold only for slabs whose lateral dimensions are large compared to R and whose thickness $S \ll R$. To test this observation, consider a short cylinder of height R and radius $R/2$. Evaluation of F by Eq. 10 gives (using Eq. 2 for F_2) the value 0.683. Evaluation by Eq. 8, which should hold only for *smaller* diameters, gives the value 0.60, while Eq. 6, which should hold only for *larger* thickness, yields 0.625.

Thus Eq. 10 gives reasonably reliable answers even for fairly thick slabs with quite small lateral dimensions. However, as these dimensions become very small compared to R, Eq. 10 cannot be expected to be at all accurate, nor, because of the strong deviation from sphericity, can Eq. 8 be used.

This leads to consideration of a thin circular disk of thickness $S \ll$ (radius) $r < R$. It can be shown that the average path from points within a circle is $8r/3\pi$. Thus, of the radiation which stays between the faces of the disk, a fraction $(1 - p/R) = 1 - 8r/3\pi R$ will be lost. The radiation traveling between the faces is in turn given by $(1 - F_2)$ times the total energy. Thus, the energy lost out of the edge is $(1 - F_2)(1 - 8r/3\pi R)$ times the total energy, and the fraction lost in all ways is $F = F_2 + (1 - F_2)(1 - 8r/3\pi R)$.

For a roughly circular slab

$$F = F_2 + (1 - F_2)\left(1 - \frac{8\sqrt{A/\pi}}{3\pi R}\right) \qquad (11)$$

To test the range of validity of Eq. 11, consider a circular slab with radius $R/2$; Eq. 10 then gives $F = F_2 + (1/\pi)(1 - F_2)$, while Eq. 11 yields $F = F_2 + (4/3\pi)(1 - F_2)$. The agreement will depend on the value of F_2, but even with the thickness equal to the diameter ($F_2 = 1/8$), the two values are 0.403 and 0.497.

There remains, finally, the cases where (a) one dimension of the body is large compared to R but the other two are R or less, and, corresponding to this, where (b) all dimensions are small but the deviation from sphericity is an elongation rather than a flattening.

Consider, therefore, an infinite circular cylinder of radius a. Let t be the path length of a ray originating a distance r from the axis and traveling at an angle θ to the transverse plane and at an angle ϕ from the plane containing the axis and point of origin (Fig. 4). From the figure

$$t = \frac{p}{\cos\theta}$$

$$p = \sqrt{a^2 - r^2\sin^2\phi} - r\cos\phi$$

Since the element of solid angle is $\cos\theta d\theta d\phi$, the energy lost is given by

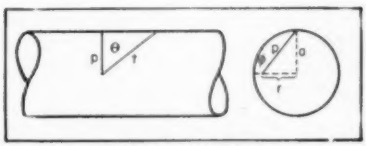

FIG. 4. Cylinder

$$\frac{E\rho dV}{4\pi}\int_0^{2\pi}d\phi\int_{-\cos^{-1}\frac{p}{R}}^{\cos^{-1}\frac{p}{R}}\left(1-\frac{t}{R}\right)\times$$

$$\cos\theta d\theta = \frac{E\rho dV}{\pi}\int_0^{\pi}d\phi$$

$$\int_0^{\cos^{-1}\frac{p}{R}}\left(\cos\theta-\frac{p}{R}\right)d\theta = \frac{E\rho dV}{\pi}\times$$

$$\int_0^{\pi}d\phi\left\{\sqrt{1-\left(\frac{p}{R}\right)^2}-\frac{p}{R}\cos^{-1}\frac{p}{R}\right\}$$

Since this integral is difficult to evaluate exactly, consider the approximation $a \ll R$, which implies $p \ll R$. It will later be seen that the result is less critical to this assumption than might be expected. Expanding the integrand in series and dropping terms of sixth or higher order in (p/R), we get

$$\frac{E\rho dV}{\pi}\int_0^{\pi}d\phi\left\{1-\frac{\pi}{2}\left(\frac{p}{R}\right)+\frac{1}{2}\left(\frac{p}{R}\right)^2+\frac{1}{24}\left(\frac{p}{R}\right)^4\right\}$$

Introducing the expression for p, and noting that terms in $\cos\phi$, $\cos 2\phi$, etc., will not give any contribution, one finds that the energy leaving dV and lost to the cylinder is

$$E\rho dV\left\{1+\frac{1}{2}\left(\frac{a}{R}\right)^2+\frac{1}{24}\left(\frac{a}{R}\right)^4+\frac{1}{3\pi}\left(\frac{ar}{R^2}\right)^2\int_0^{\pi/2}\cos^2\phi d\phi-\int_0^{\pi/2}d\phi\sqrt{\left(\frac{a}{R}\right)^2-\left(\frac{r}{R}\right)^2\sin^2\phi}\right\}$$

$$= E\rho dV\left\{1+\frac{1}{2}\left(\frac{a}{R}\right)^2+\frac{1}{24}\left(\frac{a}{R}\right)^4+\frac{1}{12}\left(\frac{ar}{R^2}\right)^2-\frac{a}{R}\boldsymbol{E}\left(\frac{r}{R}\middle/\frac{a}{R}\right)\right\}$$

where $\boldsymbol{E}$ is the complete elliptic integral of the second kind.

Now $dV = 2\pi r dr dz$ (where dz is a small length along the axis of the cylinder), and the total energy arising in a cross section dz thick is $E\rho\pi a^2 dz$. Thus, integrating the preceding expression and dividing by this total energy, the fraction lost is found to be

$$F_4 = 1-\frac{4}{3}\left(\frac{a}{R}\right)+\frac{1}{2}\left(\frac{a}{R}\right)^2+\frac{1}{12}\left(\frac{a}{R}\right)^4 \quad (12)$$

To indicate the accuracy of Eq. 12, note that the last term contributes only 1% even for $a = R/2$. For this value of a, Eq. 12 yields $F_4 = 0.463$; the first part of Eq. 6 yields 0.500; and double the value of Eq. 1 (since there are four flow directions in which loss can occur) also yields 0.500.

For finite cylinders, a correction for end effects must be made. Consider a length, equal to the range R, located at one end. Since the average internal path of radiation traveling out the end will be $R/2$, the average loss will be $\frac{1}{2}$ of the radiation traveling toward the end or $\frac{1}{4}$ of the axial radiation. The axial radiation, in turn, is $(1 - F_4)$ times the total radiation $E\rho(\pi a^2 R)$ emitted from this end segment. Thus, the energy lost out the two ends is $\frac{1}{2}(1 - F_4)E\rho(\pi a^2 R)$. Adding the loss $F_4 \times$ (total) out the sides, the total fraction lost for a cylinder of length L is

$$F = F_4 + \frac{1}{2}(1-F_4)\left(\frac{R}{L}\right) \quad (13)$$

Again, this result is useful for smaller L than might be suspected (see following).

Finally, for very small cylindrical bodies, since the average path of the axial radiation is $L/2$, the average fractional loss for such radiation is $1 - L/2R$. The total fractional loss is

$$F = F_4 + (1-F_4)(1-L/2R) \quad (14)$$

Note that Eqs. 13 and 14 agree for the intermediate situation, $L = R$.

Finally, the circular cylinder is a poor approximation to a cylinder of rectangular cross section. This case can, however, be easily treated by Eq. 9. First, if the thickness S, width b, and length L are in the relations $S \ll b < R$, $L > R$, the fraction lost out of the faces is F_2 (from Eq. 1 or 5); the remaining "planar" radiation is then $1 - F_2$. Of this fraction $2F_{e1}$ (from Eq. 9) is lost out the lateral edges, leaving a fraction $1 - F_2 + (1 - F_2)2F_{e1} = (1 - F_2)(1 - 2F_{e1})$ remaining "axial" radiation. Finally, considering one end-segment of length R, one-

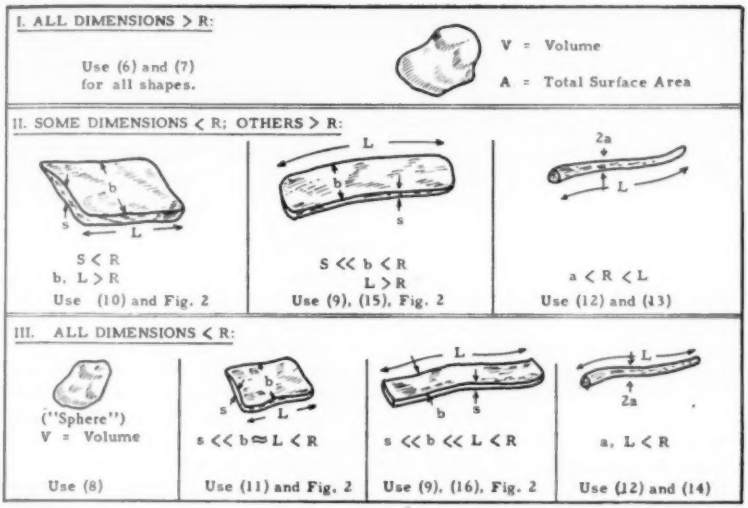

Notes

(a) R = "range" of radiation.

(b) *For β-radiation:* All β-rays at present biologically useful are "low energy" ($E < 2mc^2$). This case is actually covered only in Eqs. 5 and 7 and Fig. 2, but other shapes and sizes can be treated by first using the other entries of the table and then estimating the correction for non-uniformity of ionization from Fig. 2. In particular, if all dimensions are $\ll R$, this correction is negligible.

(c) *For γ-radiation:* In biological work, the range is effectively infinite but the essential point is that the energy given to the organ is proportional to the internal path length. Thus, correct results are obtained by setting $R = E/\eta$ where E = initial γ-ray energy and η is the energy given up per γ-quantum per centimeter of internal path. The entries of the last row are then used with no further correction.

---

quarter of the *axial* radiation arising in this segment will be lost (see the preceding treatment). Thus, from both ends, a fraction $R/2L$ of the total axial radiation is lost and

$$F = F_2 + (1 - F_2)\left[\frac{R}{2L} + 2F_{e1}\left(1 - \frac{R}{2L}\right)\right] \quad (15)$$

If the dimensions stand in the relationship $S \ll b \ll L < R$, the analysis is the same except that, as for the short circular cylinder, the loss out the ends is $1 - (L/2R)$ times the axial radiation. One finds

$$F = F_2 + (1 - F_2)\left(1 - \frac{L}{2R} + F_{e1}\frac{L}{R}\right) \quad (16)$$

Note that Eqs. 15 and 16 agree if $L = R$.

The applications of the various derived results are summarized in the table at the top of this page.

BIBLIOGRAPHY

1. E. L. Powers, Jr., *Genetics* **33**, 120 (1948)
2. B. A. Rubin, *Genetics* **35**, 133 (1950)
3. R. C. King, *Genetics* **35**, 118 (1950)
4. T. J. Arnason, *Cold Spring Harbor Symposia Quant. Biol.* **13**, 1 (1948)
5. L. D. Marinelli, E. H. Quimby, G. J. Hine, NUCLEONICS **2**, No. 4, 56; No. 5, 44 (1948)
6. L. D. Marinelli, E. H. Quimby, G. J. Hine, *Am. J. Roentgenol. Radium Therapy* **59**, 26 (1948)
7. F. Bush, *Brit. J. Radiology* **22**, 96 (1949)
8. R. S. Russel, P. R. Martin, *Nature* **163**, 71 (1949)
9. S. C. Lind. "The Chemical Effects of Alpha Particles and Electrons," page 94 (Am. Chem. Soc. Monograph Series, New York, N.Y., 1928)
10. W. E. Siri, "Isotopic Tracers and Nuclear Radiations," chapter 16 (McGraw-Hill Book Co., New York, N.Y., 1949)
11. F. Bloch, E. Teller, MDDC-1175, pages 26–33 (1947)

PILE NEUTRON RESEARCH TECHNIQUES—III*

Because comparison is easier than absolute measurement, standards play an important part in pile research. Evaluation of present-day "neutron standardization" is discussed here in terms of source strength, flux, and temperature.

By D. J. HUGHES†
Brookhaven National Laboratory
Upton, New York

IT HAS BEEN pointed out, in the description of many of the experimental techniques in this report,§ that relative values of the quantities involved can usually be measured much more accurately than absolute values. Cross sections of all kinds, as well as neutron velocities and fluxes, are measured relative to some standard cross section, velocity, or flux particularly suited to an absolute measurement. Little has been said about the methods of evaluating these standards, and the way in which this "neutron standardization" is performed will now be described. The main emphasis will be on neutron source strength, flux and "temperature" (velocity), because these quantities are of major importance in pile research.

Source Strength

The early method of producing neutrons with a natural alpha emitter, by means of the (α,n) reaction, is still widely used as a source of neutrons which is convenient and quite constant with time. A source containing one curie of radium mixed with several grams of powdered beryllium will emit about 10^7 fast neutrons per sec. The neutron emission rate will change (*97*)‡ after the source is first made because of growth of alpha-emitting decay products of radium, but after a few months the rate of change is very low. Some change in the neutron emission rate may result from shifting caused by handling of the powder in the source. The source must be sealed tightly enough to prevent escape of the gaseous decay products which would also cause changes in the emission rate. A source containing radium surrounded by, but not in contact with, a shell of beryllium, has recently been prepared by the National Bureau of Standards (*98*) as a standard source. Such a Ra-γ-Be source has only about one-tenth the neutron emmision of a Ra-α-Be source but is expected to be much more constant in value.

Both Ra-α-Be and Ra-γ-Be sources emit neutrons having a wide energy spread; they are not convenient sources for fast neutrons. However, when surrounded by enough paraffin or graphite to thermalize the neutrons, a very convenient, reproducible and constant

* Prepared under the auspices of the Committee on Nuclear Science of the National Research Council as a preliminary report of the Subcommittee on Instruments and Techniques.
† Part of this paper was written while the author was at Argonne National Laboratory, Chicago, Illinois.
§ Part I, NU, Feb. '50, p. 5; Part II, NU, May '50, p. 38.

‡ References *1–33* appeared in Part I; references *34–96* appeared in Part II. Reference numbers in Part III, the last article in this series, begin with *97*.

thermal-neutron source is obtained. The thermal-neutron flux in such an arrangement can be calculated in terms of the Q value (number of neutrons emitted per sec) of the source. Hence a standardization of Q will give the value of the thermal flux.

The availability of high specific activity gamma-emitters from the pile has made it possible to construct γ-Be and γ-D_2O "photo-neutron sources" of a wide variety (*99*) with Q's ranging up to 10^7. Because the gamma emitters usually have only a single energy gamma above the photo-disintegration threshold, the emitted neutrons are more monoenergetic than the Ra-γ-Be neutrons. Actually, the neutrons as emitted have an energy range less than 1% in general, but their energy is reduced and spread by about 15% (*100*) in passing through the beryllium in which they are produced. The photo-neutron sources have been used for fast neutron measurements (*101*) because of the reasonably small energy spread; in this work it is important to know the Q values.

At the present time absolute Q values exist for a few sources which have been measured at Argonne and Los Alamos. A number of other sources have been calibrated relative to these standards. The Argonne standard source was measured by Seidl and Harris (*102*) by determining the amount of He produced when the neutrons were stopped in boron by means of the (n,α) reaction. As the amount of He produced by the source itself would be too small to detect, the neutron flux from the source was compared to the flux in the pile by means of activation of manganese, and then the helium produced (about 10^{-4} cm^3) by the pile flux in a known amount of boron was measured. The result of the measurement was that Argonne source 38, containing 504 mg of Ra mixed with 3 gm of Be, has a Q of $(5.5 \pm 0.4) \times 10^6$ per sec. This result was quoted as a preliminary value; it is certain that the error could be reduced. However, no further work on this method has been done.

The Los Alamos standard source 44, also a Ra-α-Be mixed source (500 mg Ra), was calibrated by Walker (*103*) by measuring the number of neutrons absorbed in a boric-acid solution in which the source was placed. If all the neutrons are absorbed in the solution, the integral of the absorption rate is, of course, equal to the Q value. The difficulty occurs in finding a means to measure accurately all the absorptions which take place in the solution. The measurement was made by placing a BF_3 proportional counter in a thermal neutron flux produced by another Ra-Be source surrounded by paraffin. The neutron absorption rate of the boron in the counter, for the particular flux in the counter itself, was then given by the counting rate.

The flux in the counter was compared to the flux in the boric-acid solution surrounding the standard source by means of very thin (so as not to perturb either flux) indium or manganese foils. In this indirect way the neutron absorption rate in the solution could be determined without perturbing the flux. The integral of the absorption rate throughout the solution was obtained by moving the thin foil through the solution in such a way that its activation would be proportional to the average flux in the solution. The final source strength was $Q = (5.9 \pm 0.3) \times 10^6$ per sec. Recently the Argonne and Los Alamos sources have been compared at Argonne, by a relative method of great accuracy to be described in following paragraphs, with the result that the measured ratio of the Q values is 5% different from that expected from the figures quoted, indicating that the two sources are consistent within the quoted errors.

Once a standard neutron source is

available, it is relatively easy to calibrate others in terms of the standard. If the unknown source is of the same type (Ra-α-Be) and construction (relative amounts of Ra and Be, type of container), they can be compared with any type of neutron detector. If, however, the neutron energy distributions are different (amount of Be present, or more serious, type of source such as Na-γ-D_2O, etc.), the detector must be energy independent. The comparison can be made by placing the sources in a large tank containing an absorbing solution and measuring the integrated activity with foils. This method is somewhat cumbersome. A rapid, accurate method involving a subcritical ($k < 1$) chain-reacting pile, has been used at Argonne for comparing many sources, including the Los Alamos standard, with the Argonne standard source.

When the control rod of a pile is set so that k is slightly less than one, say 0.995, the neutron flux in the pile will be $1/(1 - k)$ times greater than it would be from the natural production rate of neutrons (from cosmic rays, *etc.*) in the pile. The multiplication results from the fact that, per neutron produced per lifetime ($\sim 10^{-3}$ sec) there will be $k + k^2 + k^3 + \cdots k^n$ neutrons produced by multiplication from preceding generations, or a total of $1/(1 - k)$. Thus a neutron source placed in the pile with $k = 0.995$ will produce a flux 200 times greater than it would if there were no multiplication. Furthermore, if this flux is detected by a counter placed in or near the lattice, the counting rate will be closely proportional to the Q of the source and independent of energy distribution, because the effect of a neutron in the pile depends only slightly on its energy. Calibrating a source in terms of the Argonne standard thus consists simply of measuring the counting rates produced by both. A number of sources have been calibrated with a relative accuracy of about 1% by this method.

Flux

The absolute measurement of neutron flux is closely related to source calibration because it is possible to produce a flux with a standard source which is known almost as accurately as the Q of the source. A source placed inside a large block of graphite will produce a certain spatial distribution of slow neutrons which can be measured quite accurately with thin foils, such as indium. The indium-foil activation is proportional to the thermal flux (the effect of resonance neutrons is eliminated by a cadmium difference), and the proportionality factor is calculated from the fact that the flux is known in terms of Q and the spatial distribution. The flux is known because the integral of the flux in the block is simply equal to Q times the distance a thermal neutron moves on the average before absorption; this distance (the "mean free path for absorption") is the reciprocal of the absorption cross section of graphite. A knowledge of the integral of the flux and its spatial distribution thus gives the absolute flux at each point in the graphite.

It is important to note that the calculated flux is proportional to the thermal velocity assumed (measurement of the velocity will be described later) but that the neutron density (n rather than nv) is independent of velocity. If the neutron velocity in the graphite should change, as it would with graphite temperature, then the activation of a $1/v$ foil placed in the graphite would not change, of course, because the v's cancel. The activation of such a foil is actually a measure of neutron density, n, rather than flux, but it is convenient to deal with flux. The velocity usually used in the calculation of the flux in the graphite is 2,200 m/sec.

As there is little error in the calculations of the flux compared to the error in Q, the "standard pile" of graphite just described produces a constant, convenient flux of neutrons known to 5%. The flux is quite low, however, and reasonable activations can be obtained only with foils that are thick enough to cause appreciable perturbations in the flux distribution. The flux perturbation has no effect in determining unknown fluxes relative to the standard pile if the unknown fluxes are also in graphite and the foil geometry is identical. However, a correction for the perturbation must be made when fluxes in open beams are to be measured, for instance, and the correction introduces a further error of several percent. In addition, the neutron velocity in the beam may not be the same as in the standard pile, and as the foil activation gives the neutron density, the difference in velocity must be considered in obtaining the flux value for the beam.

A second method of measuring a neutron flux is by means of the reaction rate of an element whose cross section is known. As already discussed, the reaction cross section for boron [essentially the (n,α), for the (n,p) and (n,γ) are negligible] can be determined from the total cross section, obtained from transmission results, by subtraction of the scattering cross section. The "best value" of the boron reaction cross section, given in the summary of Way and Haines (*104*) is 715 barns at 2,200 m/sec, accurate to about 1.5%. If the number of (n,α) reactions taking place in a certain amount of boron in a neutron flux can be measured, the flux can be obtained as well. Again, as for the standard pile, the rate of (n,α) ractions depends on the neutron density, independent of the velocity, because boron is strictly $1/v$. In stating the flux, the velocity can be taken as 2,200 m/sec; other $1/v$ cross sections measured in the flux will turn out to be the correct 2,200 m/sec values even if the true neutron velocity differs from this assumed value.

The reaction rate in a known amount of boron located in a neutron flux could be measured by a BF_3 counter or pulse-counting ion chamber if one could be sure of a one-to-one correspondence between disintegrations and counts Of course, just this question appears in the absolute source calibration done at Los Alamos—in that work the disintegration rate was measured to about 5%. The absolute disintegration rate in boron, however, has not been used in any recent determination of neutron flux. Wattenberg and Jankowski (*105*) are now carrying out an absolute flux measurement at Argonne, in which the disintegration rate of gold is measured by activation. The gold cross section, like that of boron, is known from transmission and scattering measurements to about 1.5%. The reaction rate in gold is measured by irradiating a sample to saturation in the beam and then measuring its absolute disintegration rate. The latter measurement is carried out by measuring beta, gamma, and beta-gamma coincidences from which the absolute rate can be calculated (*106*). A number of corrections must be made: for the change in the neutron velocity distribution caused by the gold foil, and for the effect of the finite thickness (departure from $1/v$ behavior) of the counter used in the transmission measurements. The work is still in progress; at the present time an accuracy of about 4% has been obtained.

It is of interest that comparison of the flux calibrated by Wattenberg and Jankowski (a thermal-column beam) with that in the Argonne standard pile shows agreement within the accuracy of the two flux measurements. It is very simple of course to compare fluxes in other neutron beams with the standard beam flux by means of any

foil of convenient half-life. Such a comparison actually is in terms of neutron density, but can be quoted as flux for $v = 2{,}200$ m/sec if cross sections at that velocity are consistently used. The comparison foil should be thin because any self-protection correction will be different for beams of different velocity and hence will not cancel out in the comparison.

Neutron Temperature

The Maxwell velocity distribution of thermal neutrons has been discussed in the first part of this article. The temperature, T, in the theoretical distribution, which is related to the most probable velocity v_0, by $\frac{1}{2}mv_0^2 = kT$, is called the "temperature" of the neutrons. Neutrons in eqilibrium with a material such as graphite, at room temperature ($T = 293°$) have the corresponding v_0 of 2,200 m/sec. The methods already described for absolute and relative determinations of neutron flux do not depend, in general, on neutron velocity because they are actually measurements of neutron density. Furthermore, if only $1/v$ materials are used, cross sections can be measured with the standardized fluxes even if the velocity distribution is unknown.

In the present section, methods of measuring the neutron temperature of a beam will be described, but it should always be remembered that such information is not necessary for the usual flux standardization. A clear distinction between flux (really density) and neutron temperature measurements will help one realize how fluxes at different parts of a pile, or even at different laboratories, have been correlated quite well, even when the neutron temperature values are still inconsistent. This state of affairs is illustrative of the difficulty of neutron temperature measurements.

A direct approach to the problem of measurement of the velocity distribution in a neutron beam would involve a crystal monochrometer or mechanical chopper as a means of getting the relative number of neutrons as a function of velocity. However, both the crystal and the chopper have an efficiency (fraction of the incident neutrons of a given velocity which get to the detector), as well as a resolution (range of velocity detected at a given velocity setting), which vary with velocity. In addition, the intensity is so low with each instrument that a detector thicker than $1/v$ must be used (it is only for a $1/v$ detector that the Maxwell distribution will hold). These facts make an accurate velocity distribution exceedingly difficult to obtain None has been measured by this direct method with even the limited accuracy of the indirect absorption methods considered next.

Because the cross section of boron has been carefully measured as a function of velocity, it can be used to determine the temperature of a Maxwell neutron distribution. The boron cross section is measured by transmission (the method is applicable mainly to beams) using a thin detector such as BF_3 counter of small diameter and a boron absorber of small transmission so as not to modify the distribution by the $1/v$ absorption. The boron cross section observed is that corresponding to the average velocity. The most probable velocity is obtained by multiplication of the cross section by $2/\sqrt{\pi} = 1.13$. In practice, boron of a finite thickness is used so that the transmission may be obtained accurately, and it is necessary to correct for the "hardening" of the beam (by means of the Bethe (*67*) correction, which has been discussed, for instance).

Temperature values which have been obtained for neutron beams from thermal columns, by absorption in boron or similar $1/v$ absorbers, have varied over a range of about 100° C in

spite of the seeming simplicity of the method. However, it must be remembered that a Maxwell distribution is assumed in the method, an assumption which will be true only if complete equilibrium in the column is reached and if a thin $1/v$ detector is used. Actually, there may be fast neutrons present in the beam, or an excess of very slow neutrons below the graphite cut-off, if the neutrons pass through enough material for filtering action (*107*). The actual temperature of the thermal column may be above room temperature; the detector may be somewhere between a $1/v$ and a thick "black" detector; and there may be uncertainty in the amount of boron in the thin absorber. Wattenberg and Jankowski (*105*) obtained 330° for a beam from the thermal column of the Argonne deuterium pile; Hughes, Wallace and Holtzmann (*83*) measured the same flux, but with a slightly different graphite geometry, as 287°. Fermi, Marshall, and Marshall (*107*) obtained 293° and 255° for beams emerging from a deep and a shallow hole in the thermal column of the Argonne graphite pile at Chicago.

The temperature of the Cd-absorbable neutrons (*i.e.*, those detected by a Cd-difference measurement) inside the pile itself can be measured by beam techniques (absorption in boron) using a hole extending into the lattice. The boron absorption technique can also be applied by irradiating thin $1/v$ foils between thin boron sheets inside the pile (the "sandwich" technique), but the results are difficult to interpret because of obliquity corrections.

The measurements which have been made show the usual discrepancy of temperature measurements but indicate a neutron temperature of the order of 100° C above the actual temperature of the moderator. Anderson *et al* (*44*), comparing the effect on pile reactivity (danger coefficient method) of a $1/v$ absorber (boron) with a black absorber (Cd), found a neutron temperature 93° C above the graphite value. Branch (*108*) measured the neutron temperature inside the Oak Ridge graphite pile, using the boron sandwich method, with a result 140° above the graphite.

Analyzing a pile neutron beam with a crystal, Zinn (*109*) obtained a temperature about 90° C above the moderator (and about the same value for the thermal column, however). Sturm (*110*), using the same apparatus as Zinn, found the same temperature value for pile neutrons, and Bernstein *et al* (*111*), a temperature of 155° C above the graphite temperature of the Oak Ridge pile. The neutron temperature inside the pile is of some importance to pile design but is not as important for research as the temperature of the thermal column neutrons—the slow neutrons of main value for research.

BIBLIOGRAPHY

97. H. L. Anderson, B. T. Feld, *Rev. Sci. Instr.*, **18**, 186 (1947); **18**, 331 (1947)
98. L. F. Curtiss, A. Carson, *Phys. Rev.* **76**, 1412 (1949)
99. A. Wattenberg, *Phys. Rev.* **71**, 497 (1947); Preliminary Report No. 6, Nuclear Science Series, National Research Council (July, 1949)
100. D. J. Hughes, C. Eggler, *Phys. Rev.* **72**, 902 (1947)
101. R. Fields, B. Russell, D. Sachs, A. Wattenberg, *Phys. Rev.* **71**, 508 (1947)
102. F. G. P. Seidl, S. P. Harris, *Rev. Sci. Instr.* **18**, 897 (1947)
103. R. Walker, MDDC 414 (1946)
104. K. Way, G. Haines, AECD 2138 (1948)
105. A. Wattenberg, F. Jankowski, private communication
106. J. V. Dunworth, *Rev. Sci. Instr.* **11**, 167 (1940)
107. E. Fermi, J. Marshall, L. Marshall, *Phys. Rev.* **72**, 193 (1947)
108. G. M. Branch, MDDC 747 (1946)
109. W. H. Zinn, *Phys. Rev.* **71**, 752 (1947)
110. W. J. Sturm, *Phys. Rev.* **71**, 757 ,(1947)
111. S. Bernstein, R. Sawyer, E. Wollan, unpublished data

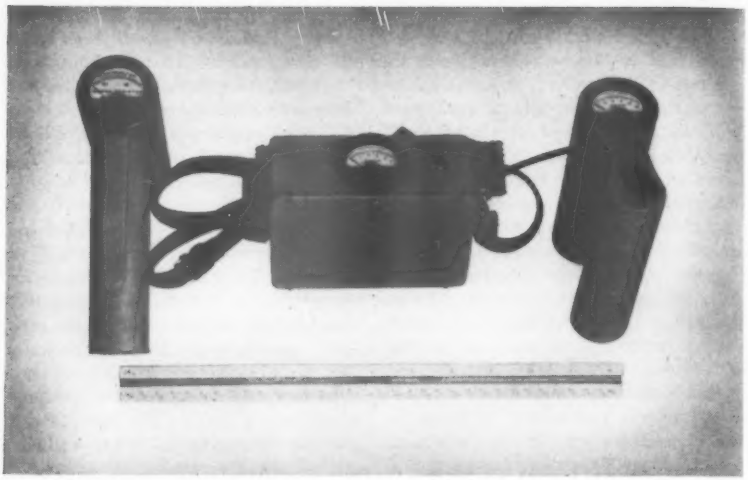

Three versions of the AEC's design for a simplified, single-scale survey meter which will cost about $15.00. Device is powered by two flashlight cells

Geiger Counter for Civilian Defense Use

By H. D. LeVINE, H. J. DiGIOVANNI, and M. R. COE

Instruments Branch, Health and Safety Division, New York Operations Office
United States Atomic Energy Commission
New York, New York

AN INSTRUMENT to be used by relatively untrained civilians for the detection of radiation in the event of atomic warfare should differ considerably from standard instruments now available. It should be of a simple type, easily carried and used under disaster conditions, and should have a minimum of controls and adjustments.

Further, the instrument should read relatively high radiation levels. The accuracy need not be great, since readings within ±20–30% should be satisfactory. One scale should cover the entire range of intensities. The instrument should be of a type that will not block and give an erroneous, low intensity indication when in high-intensity fields.

The requirements of a single scale and the extended range of the instrument dictate the use of a logarithmic or similar type of compressed nonlinear scale. Since the 0.1 r/hr and the 1 r/hr readings are of major interest in the initial phase of a disaster, the readable range of the instrument should be chosen to indicate 50 to 3,000 mr/hr.

The conditions under which this instrument might be used require light, rugged, moisture-proof and tamper-proof construction. One set of bat-

teries should operate at least 48 hours at 50% operating cycle. These batteries should be obtainable without difficulty during disaster periods. Because of the large number of units required, the instrument must be designed for mass production at a low cost. All components should have a reasonably long shelf life.

The Geiger Counter

Various means of detecting and measuring gamma radiation were reviewed. The Geiger counter was selected as the most promising device for the desired instrument, because it has the greatest inherent amplification, permitting operation without amplifying devices. It has the further advantage of a simple construction applicable to low-cost mass production, and would require a minimum of industrial tooling.

Based on this reasoning, several commercially available organic-quench type Geiger tubes were tested in the simple series circuit of Fig. 1. The tubes tested were unsuited to this application for several reasons. First, the organic-quenched type of tube changed operating characteristics in high intensity fields because of rapid exhaustion of the quenching agent. Second, the maximum values of direct current obtainable were of the order of 1–3 μa. This current was too small to operate standard panel-type instruments. Third, the saturation, or leveling off, of the current occurred at very low gamma intensities.

The halogen-quenched counter offered a solution to the first two problems. In this type of tube, the quenching agent is not decomposed, and the charge per pulse during operation may be 50 times greater than in organic-quench tubes. A halogen tube which has been properly constructed, filled and seasoned will maintain its characteristics over long periods of time in high-intensity fields.

Effort was therefore concentrated on the commercial development of a suitable halogen-quenched tube to operate in the required range. Several manufacturers have submitted satisfactory samples; some are shown in Fig. 2. The various tubes vary in dimension from ¼–⅜ in. in diameter and from 1½–2½ in. in length. Of simplified design, they can be produced economically in large quantities on automatic equipment.

Operating characteristics of these tubes offer the advantages of approximately logarithmic response to radiation over a considerable range and freedom from blocking at high intensities. Figure 3 shows the actual characteristics of a typical tube operating

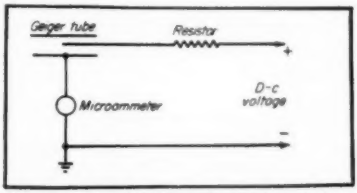

FIG. 1. Circuit for testing Geiger tubes. D-C voltage is high enough to permit operation of tube above Geiger threshold

FIG. 2. Halogen-quenched 700-volt Geiger tubes developed commercially and tested by the AEC for use in the instrument described here

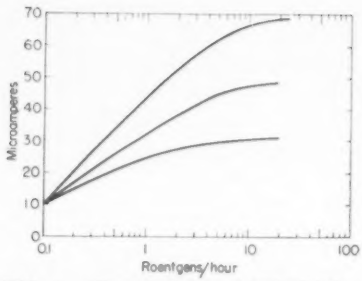

FIG. 3. Characteristics of typical halogen-quenched Geiger tube operating from 700-volt source

from a 700-volt source. It is of interest to note that in the circuit of Fig. 4, the slope of the curves can be changed within reasonable limits by varying the value of the series resistor, R_2, from ½ to 5 megohms. Thus, a simple noncritical means of calibration can be provided.

Indicator Circuit

In designing the circuit, since a halogen-quenched Geiger tube can develop currents over 250 μa at the radiation levels of interest here, it was possible to choose between a low sensitivity meter coupled with a high current supply or a high sensitivity meter used with a relatively low current supply. Since low battery drain was desired, and since microammeters having a range of 20 to 50 μa are available at reasonable cost in large quantities, the initial instrument models were constructed using such meters.

Investigations are being made to determine the feasibility of using other types of indicators.

Power Supply

The Geiger tubes require a power supply stabilized at 700 volts. The 1½-volt type D flashlight cell can be obtained without difficulty in an emergency, since it is normally stocked by a large variety of stores in all localities. Consequently, a suitable vibrator type of power supply was designed to operate from two of these cells.

Figure 4 is a schematic diagram of the complete instrument. The vibrator, V_1, is designed with a single-pole double-throw contact arrangement. The normally-closed contact is used to interrupt the reed driving coil circuit to maintain it in oscillation. The normally-open contact is used to energize the primary circuit of the high-voltage transformer, T_1.

Although a single contact can be used to interrupt both circuits either by a series or parallel arrangement of the coils, an accurate balance of the characteristics of the transformer and vibrator is then essential. The separate contact arrangement allows optimizing of the vibrator and transformer designs independently.

The voltage induced in the secondary of the transformer is rectified by a cold-cathode rectifier, T_3, and is smoothed by capacitor C_1. The inverse voltage on the transformer is only about 10% of the forward voltage. This reduces the inverse voltage requirement for the rectifier to one-half that of a conventional circuit.

Since a power supply of this type has poor voltage regulation, the corona voltage regulator tube, T_2, is used in conjunction with resistor R_3 to stabilize the voltage. Voltage regulator tubes are available with less than 1% total voltage variation from 2 to 100 μa through the regulator. The resulting voltage appearing across the voltage regulating tube is then applied to the Geiger counter and indicator circuit.

The small neon light in series with the regulator tube serves as an indicator of the condition of the batteries. The length of the illuminated tube wire indicates the amount of current through the neon tube. When the secondary voltage produced is less than the regu-

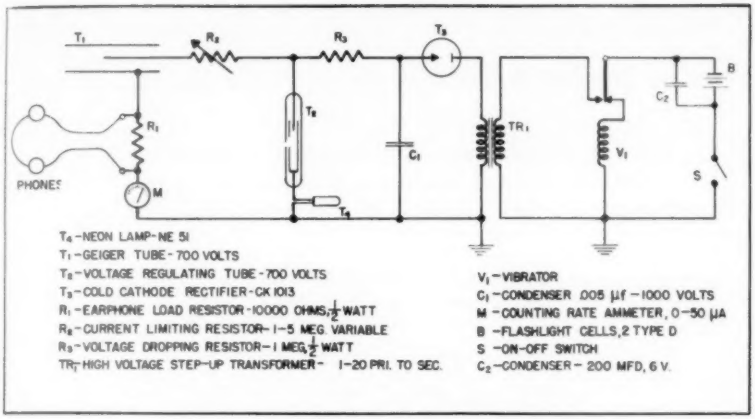
T1
R2
R3
T3
B
C2
T2
R1
C1
TR1
V1
S
PHONES
M
T4
T4 – NEON LAMP – NE 51
T1 – GEIGER TUBE – 700 VOLTS
T2 – VOLTAGE REGULATING TUBE – 700 VOLTS
T3 – COLD CATHODE RECTIFIER – CK 1013
R1 – EARPHONE LOAD RESISTOR – 10000 OHMS, 1/2 WATT
R2 – CURRENT LIMITING RESISTOR – 1-5 MEG. VARIABLE
R3 – VOLTAGE DROPPING RESISTOR – 1 MEG, 1/2 WATT
TR1 – HIGH VOLTAGE STEP-UP TRANSFORMER – 1-20 PRI. TO SEC.
V1 – VIBRATOR
C1 – CONDENSER .005 µf – 1000 VOLTS
M – COUNTING RATE AMMETER, 0-50 µA
B – FLASHLIGHT CELLS, 2 TYPE D
S – ON-OFF SWITCH
C2 – CONDENSER – 200 MFD, 6 V.

FIG. 4. Circuit diagram of complete instrument

lator-tube conduction voltage, the neon light will extinguish.

This power supply will furnish the necessary output current to the meter (50 µa minimum) at 700 volts from two 1½-volt type D flashlight cells in series. Useful battery life is 48 hours at 50% duty cycle. Efficiency of the supply is 33%. Shunting the battery with a large low-voltage capacitor extends the range of usable operation to 1.1 volts per cell. If it is necessary to use this device in relatively low-intensity gamma fields, high-impedance earphones can be connected across resistor R_2, and pulses counted as in conventional units.

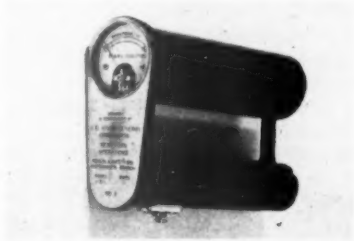

FIG. 5. Three-cell counter reported to Congress

The variety of shapes into which this instrument has been built is shown by the photograph on p. 56. The two-cylinder version on the right is similar to a three-cell model (Fig. 5) reported by the AEC at recent meetings of the Joint Congressional Committee. Batteries are housed in a tube 1½ in. in diameter and 5¼ in. long; the larger tube, 2 in. in diameter and 5½ in. long, houses the balance of the circuit. The "T" type model on the left uses the same size tubes. A "camera" version, 5 × 3¾ × 2 in., is shown in the center of the illustration. Weight of each of these instruments, including batteries, does not exceed 1¾ pounds.

The scales of the instruments are calibrated at 0.1 r/hr and at 1 r/hr. Below 0.1 r/hr, the scale is blue; between 0.1 and 1 r/hr, the scale is yellow, and above 1 r/hr, it is red. There are no controls or adjustments for the operator to manipulate, except for the push-button battery switch which is depressed only when a reading is to be taken.

It is estimated that the cost of producing this type of instrument in large quantities will not exceed $15.00. END

RANDOM SAMPLING (Monte Carlo) TECHNIQUES in Neutron Attenuation Problems—II*

Statistical analysis can reduce the work necessary to solve complex problems. The author adds two more methods to those given last month, and discusses their reliability.

By HERMAN KAHN

The Rand Corporation
Santa Monica, California

RANDOM SAMPLING, used as an analog device, can be applied to neutron attenuation problems. This allows deduction of the behavior of many neutrons from a study of relatively few. But, with the straight analog, 10^9 to 10^{12} histories are still required to obtain any accuracy.

Four special techniques, however, make reduction to as few as 10^3 histories possible with a probable percent error of 10%. Two of these—integration by random sampling, and the exponential transformation—were described in Part I of this article (NU, May '50, p. 27). The remaining methods—quota sampling† and statistical estimation—are discussed in this second and concluding part of the article.

Quota Sampling

Quota sampling is possibly the most versatile and important technique available, because it can often be used to reduce the error by taking advantage of what knowledge or physical intuition is possessed about the problem. It is clear, for example, that the most energetic neutrons and those with small angular deviations from the normal are more important than the others and should be studied more intensively. Though some work has been done in this field (by S. W. W. Shor, H. Kahn, T. E. Harris, and possibly others), this type of quota sampling will not be discussed here because of the lack of space. Instead, the discussion will be restricted to the sampling of the spatial part of the history.

In its simplest form, an example of quota sampling is as follows. A plane slab is divided into n subslabs. The probability that a neutron has its first collision in the ith subslab is q_i. If a straightforward system of tracing neutrons is followed, there will be a probability Q_i that a neutron which had its first collision in the ith subslab will pierce the shield. In the more general methods of calculating histories, there is a function $f_i(w)\Delta w$ which gives the probability that a neutron will pierce the slab with a weight between w and $w + \Delta w$. The standard deviation σ_i of the histories with first collisions in the ith subslab is defined by $\sigma_i^2 = Q_i(1 - Q_i)$ or by

$$\sigma_i^2 = \int w^2 f_i(w)dw = [\int w f_i(w)dw]^2 = \int w^2 f_i(w)dw - Q_i^2 \quad (15)$$

whichever applies.

If N histories are followed, it can be

---

* Copyright 1949. The Rand Corporation, Santa Monica, California.

† In this report, "quota sampling" is used to describe somewhat more general techniques than would ordinarily be considered under this classification. As used here, it is sometimes called "importance sampling."

shown that it is best to let n_i have their first collisions in the ith subslab where

$$n_i = \frac{N q_i \sigma_i}{\bar{\sigma}}$$

$$\bar{\sigma} = \Sigma q_i \sigma_i \qquad (16)^*$$

If a straightforward nonquota type of sampling is used, the probable error is $0.6745\sigma/\sqrt{N}$ where

$$\sigma^2 = \sum_{i=1}^{N} \sigma_i^2 q_i + \sum_{i=1}^{N} Q_i^2 q_i - \left(\sum Q_i q_i\right)^2 \qquad (17)^*$$

Where quota sampling is used, the probable error becomes $0.6745\bar{\sigma}/\sqrt{N}$. $\bar{\sigma}$ is less than or equal to σ, and, in many problems of importance, it is decidedly less. It is usually necessary to work a small sample problem to estimate σ_i, though sometimes a fair guess of this quantity (or at least of relative values) can be made with the use of physical intuition.

A variation of quota sampling as described previously is to take the points of first collisions randomly but proportionate to the probabilities $q_i\sigma_i/\bar{\sigma}$. Since the points of first collision should have been taken according to the probability q_i, each pick must be weighted with the factor $\bar{\sigma}/\sigma_i$ (see Eq. 7*a*, Part I).

The continuous analog of this type of quota sampling is to pick a random variable from a probability density $f^*(u) = f(u)g(u)/\bar{g}$ instead of $f(u)$, where $f(u)$ is the given probability density, $g(u)$ is a function which measures the importance of u (it corresponds roughly to the σ_i of the preceding paragraphs) and $\bar{g} = \int_{-\infty}^{\infty} f(u)g(u)du$. In the neutron problem the importance of a region is defined as the probability that a neutron would get through a shield if it started from that region. More generally, if we have a two dimensional integral over a region in the u,v plane and wish to do quota sampling only for the u dimension, then the optimum $g(u)$ is defined by

$$g(u) = \sqrt{\int_{-\infty}^{\infty} G^2(u,v)\, f_u(v)dv}$$

where $G(u,v)$ is the importance (relative contribution to the answer) of the point (u,v) and $f_u(v)$ is the conditional probability density of v given u. This formula is proved by considering what $f^*(u)$ makes the probable error a minimum (see Eq. 7*a*, Part I).

As before, we must correct for picking the random variable from the wrong probability density by carrying along the weighing factor $w_i = f(u_i)/f^*(u_i) = \bar{g}/g(u_i)$. An approximate $g(u)$ function is obtained by the use of approximate analytic techniques, physical intuition, experiments, or previous computations.

The weight w_i can be viewed in two ways. The first is to treat the history not as representing one neutron at that point, but as representing w_i neutrons, where all of these w_i neutrons are treated as a unit and held together. The other is to specify an arbitrary set of $r + 1$ probabilities p_j, where the p_j are subject to the condition

$$w_i = \sum_{j=0}^{p} j p_j \qquad (18)$$

Each p_j represents the probability that there are actually j independent neutrons present at that point of the history, and w_i is simply the expected or average number of neutrons. A game of chance, specified by the p_j, is played to decide how many neutrons are actually present.

It is also possible to combine the two viewpoints by letting a neutron split into a number of weighted neutrons, either in a deterministic manner or by a game of chance. Which of these three processes actually should be carried through is dependent on many

* S. S. Wilks, "Mathematical Statistics," p. 89 (Princeton University Press, Princeton, N. J., 1943)

factors. In many cases, it is still an open question. If a good f^* has been picked, then it is generally not necessary to split.

It is interesting to note that the exponential transformation is a form of quota sampling. For example, if $\cos \lambda_{i-1}$ is positive, the correct distribution function for the i point of collision given that the $i-1$ was at x_{i-1} is

$$f(x) = \frac{\mu_{i-1}}{\cos \lambda_{i-1}} e^{-\frac{\mu_{i-1}(x_i - x_{i-1})}{\cos \lambda_{i-1}}} \quad (19)$$

If, instead, an $f^*(x)$ is chosen of the form

$$f^*(x) = \frac{\mu_{i-1} - c \cos \lambda_{i-1}}{\cos \lambda_{i-1}} \times e^{-\frac{(\mu_{i-1} - c \cos \lambda_{i-1})(x_i - x_{i-1})}{\cos \lambda_{i-1}}} \quad \text{for} \quad x_i < a \quad (20a)$$

and with a discrete probability

$$f^*(a) = 1 - e^{-\frac{(\mu_{i-1} - c \cos \lambda_{i-1})(a - x_{i-1})}{\cos \lambda_{i-1}}} \quad (20b)$$

for going through the slab, then, if the analogous process is carried out for negative $\cos \lambda_{i-1}$, it can be shown that this particular type of sampling is identical with the exponential transformation. Equations 20*a* and 20*b* are derived from the rule $f^*(x) = f(x)g(x)/\bar{g}$ where the approximate importance function $g(x)$ is assumed to be of the form $e^{-c(a-x)}$.

Parametric studies. The f^* process often can be used very advantageously in conducting parametric studies. In such studies, it is usual to specify n different problems with n slightly different probability distributions $f_1(x), \ldots, f_n(x)$. If the study is done by random sampling, it is not necessary to do these n different problems. It is sufficient to pick one of the probability functions, say $f_1(x)$, and use it in calculating the life histories. Then, instead of working the other problems, the weighting factors given by $f_i(x)/f_1(x)$ are simply carried along in the first problem.

Splitting. There is another process which is quite analogous to the exponential transformation. In one of the simplest forms of this process, $n-1$ planes are passed through the slab at points $a_1, a_2, \ldots, a_{n-1}$. These points are so chosen that the probability of a neutron reaching the point a_i should be approximately 2^{-i}. Neutrons are traced in the manner described previously, with one difference. Every time a neutron passes one of these planes from left to right, it is split into two independent neutrons, each of one-half the original weight. When it passes a plane from right to left, its weight is doubled, but a game is played with a coin or any other equiprobable gambling device to decide if it is absorbed or not. It is easy to see that this process focuses more attention on those neutrons which penetrate deep into the slab than those which do not, and therefore is a form of quota sampling. This splitting technique, which is due to J. von Neumann, can easily be generalized to problems which are not symmetrical and is thus a very valuable tool. In the case of plane slabs, it can be shown that if a suitable limiting process is carried through, in which the number of subslabs is made infinite, a variation of the exponential transformation is obtained. In actual practice it is necessary to consider $n-1$ surfaces defined in the three-dimensional space of α, λ, and x, rather than $n-1$ planes located at $x = a, \ldots, a_{n-1}$, if the splitting is to be optimized.

In addition to the various forms of quota sampling, it is often useful to use stratified sampling, systematic sampling, or other tricks of the statistician. For a discussion of advantages gained, refer to the statistical journals.

Statistical Estimation

The fourth technique will be discussed only briefly. It consists of taking the data obtained in calculating

a history and seeing how much information can be extracted from it. For example, every separate neutron life history is in a sense an estimate of the function $\psi(x,\alpha,\lambda)$, defined in the discussion of the exponential transformation. It is well known that any approximate solution of an integral equation (such as an estimate of $\psi(x,\alpha,\lambda)$ by a single neutron history) can be improved by iterating it against the kernel of the integral equation. Thus, if φ is an approximation to ψ, then an approximation to P corresponding to a single iteration of the transport equation is

$$P = P_0 + \int\int\int\int\int \varphi(x,\alpha,\lambda)\sigma(\alpha)v(\alpha) k(\alpha,\lambda,\alpha',\lambda') e^{-\mu(\alpha')(a-x)\cos\lambda} \times \sin\lambda' \sin\lambda \, dx d\alpha d\lambda d\alpha' d\lambda' \quad (21)$$

Corresponding to Eq. 21 is an estimate of P for the nth history

$$H_n = P_0 + \sum_{i=1}^{k} w_i H(\alpha_i,\lambda_i,x_i) \quad (22)$$

where k = the number of collisions in the slab, w_i = weight of neutron, i = number of the collision, and P_0 = exp $[-\mu(\alpha_0)a/\gamma_0]$ = problem of getting through with zero collisions.

$$H(\alpha,\lambda,x) = \int\int e^{-\frac{\mu(\alpha')(a-x)}{\cos\lambda'}} k(\alpha,\lambda,\alpha',\lambda') \sin\lambda' d\alpha' d\lambda' \quad (23)$$

Equation 21 states that the probability of getting through the slab is equal to the probability (P_0) of getting through with no collisions, plus the probability ($\sigma v k \sin\lambda'$) that a neutron at the point x, α, and λ has a collision, which changes its energy to α' and its angle to λ', times the probability exp $[-\mu(a-x)/\cos\lambda]$ sin λ that the neutron gets out with no further collision. This last set of probabilities is integrated over all possible $(x,\alpha,\lambda,\alpha',\lambda')$. Instead of evaluating Eq. 21 numerically, part of the integration is done by sampling as described by Eq. 22, using the x_i, α_i, λ_i picked out of $\psi(x,\alpha,\lambda)$. The integrations on α' and λ' are still done exactly as in Eq. 23. As usual, the estimate of P for N histories would be

$$P = \frac{1}{N}\sum_{n=1}^{N} H_n \quad (24)$$

and the estimate of the probable error,

$$\text{p.e.} = 0.6745\sqrt{\frac{1}{N^2}\sum_{n=1}^{N} H_n^2 - \frac{\bar{H}^2}{N}} \quad (25)$$

Equation 22 is probably a very efficient type of estimate. Unfortunately, however, the function $H(\alpha,\lambda,x)$ is usually too complicated to use. Therefore, other estimates are used. The one corresponding to the Monte Carlo integration of Eq. 23 is especially simple:

$$I_n = e^{-\frac{\mu(\alpha_0)a}{\cos\lambda_0}} + \sum_{i=1}^{k} w_i e^{-\frac{\mu_i(a-x_i)}{\cos\lambda_i}} \quad (26)$$

This equation can be derived directly by considering that a neutron which collides at x_i and scatters to energy α_i and angle λ_i has the probability exp $[-\mu(\alpha_i)(a-x_i)/\cos\lambda_i]$ of getting out with no further collisions if cos λ_i is positive, and the probability zero if the cosine is negative. Then the probability I_n that the nth neutron sampled penetrated the slab is just the probability that it passed through on some collision or without any at all. Since these events are mutually exclusive, the probability I_n is given by the sum of the individual probabilities as shown in Eq. 26, where the summation is over positive cos λ_i. Many other estimates of this general type are possible. Some of them will be found discussed in detail in a forthcoming Rand report.*

A particularly valuable estimate of this type can be obtained by taking a

* T. E. Harris and H. Kahn. Preliminary estimation of particle transmission by random sampling. *Report R-148* (Project RAND. The Rand Corporation, not yet published).

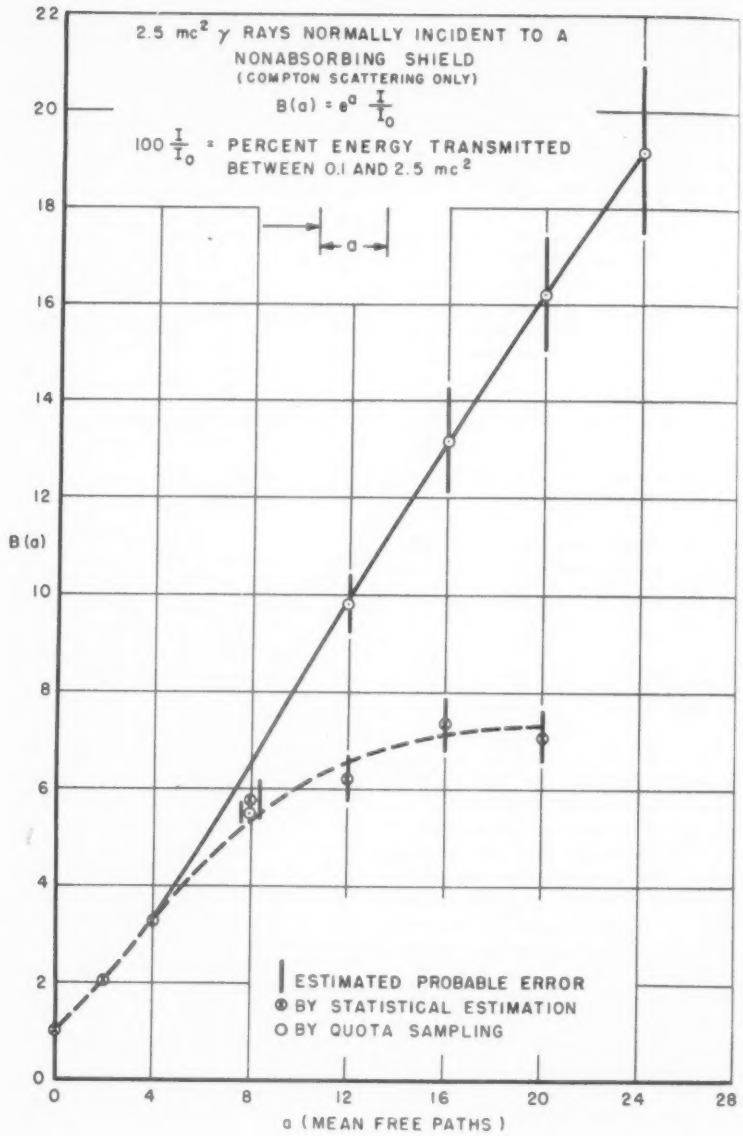
2.5 mc² γ RAYS NORMALLY INCIDENT TO A NONABSORBING SHIELD
(COMPTON SCATTERING ONLY)
B(a) = e^a I/I0
100 I/I0 = PERCENT ENERGY TRANSMITTED BETWEEN 0.1 AND 2.5 mc²
a
B(a)
ESTIMATED PROBABLE ERROR
BY STATISTICAL ESTIMATION
BY QUOTA SAMPLING
a (MEAN FREE PATHS)
0
2
4
6
8
10
12
14
16
18
20
22
0
4
8
12
16
20
24
28

FIG. 4

history and weighting it in a fashion given by Eq. 26 and, at the same time, also weighting the history by considering all possible points of first collision. This is done by integrating an equation similar to Eq. 26 over the possible points of first collision. The corresponding estimate is given explicitly as

$$T_a = e^{-\frac{\mu(\alpha_0)a}{\cos\lambda_0}} + \sum_{i=1}^{h} w_i e^{-\frac{\mu(\alpha_i)}{\cos\lambda_i}(a-x_i)} \int_{A_i}^{a-B_i} \frac{\mu(\alpha_0)}{\cos\lambda_0} e^{-\left[\frac{\mu(\alpha_0)}{\cos\lambda_0} - \frac{\mu(\alpha_i)}{\cos\lambda_i}\right]x} dx \tag{27}$$

where

$A_i = -\min [0, x_2 - x_1, \ldots, x_i - x_1]$

$B_i = \max [0, x_2 - x_1, \ldots, x_1 - x_1]$

and h is the number of collisions in the slab, and the summation is over those terms for which the $\cos\lambda_i$ is positive and for which $A_i + B_i < a$.

Reliability of Monte Carlo Calulations

Before closing this report, it should be mentioned that some of the techniques described give rise to distributions with very large tails. This occurs when the system of quota sampling is faulty, so that certain regions of the phase space are not sampled very often, though their contribution to the answer may be quite large (See Fig. 3 and discussion in Part I.) If the sample is small, the region in question may be missed completely, and not only will the sample mean (computed answer) be a poor estimate of the population mean (actual answer), but the estimate of the probable error may be small, so that the computer will have no indication that things have gone wrong. For this reason it is essential, in any case where the system of quota sampling is not fairly close to optimum, to take the size of the sample large enough to allow any possibly important but neglected regions of phase space to influence the result. It is also possible that, in certain cases, more refined techniques of estimating the mean than just taking the average of the sample values may eliminate the difficulty. This question is under investigation.

This last difficulty is not an academic one, but can actually arise in practice. For example, two calculations were made to determine the energy transmitted by gamma rays through plane slabs. The results of the first one (shown by the dotted line in Fig. 4) were obtained by using Eq. 27 and histories originally calculated by the Institute for Numerical Analysis at Los Angeles to obtain the albedo (reflection) from plane slabs. There was a danger in doing this, for as the slab thickness increases, those gamma rays which have small-angle and high-energy collisions become relatively more and more important. For this reason (and also because there was a sharp disagreement between the dotted curve and some approximate calculations made by T. A. Welton) a small hand calculation, especially designed to test the region in interest, was carried through. This calculation showed that the original sampling technique probably could not be trusted for a greater than 8, so a new calculation (using only quota sampling) designed for a around 16 was done. The results of this new calculation are shown in the solid line. It is believed that these latter results are quite accurate (within the limits set by the probable error) for a = 12, 16, 20, and probably 24. It should be noticed that typically we get a significant underestimate at a = 8 (it is even worse than the old estimate). This is not surprising; a method designed for a = 16 would not be expected to work at a = 8. The unreliability of the probable-error estimate when the sampling is inefficient should also be noted. In any problems in which the probable-error estimate is not trusted, additional investigations should be made. These are usually comparatively easy calculations investigating a small region. END

CROSS SECTIONS

Colorimetric Dosimeter for Penetrating Radiation*

A simple, inexpensive device for measuring high intensities of penetrating radiation would be a necessity in emergencies where large amounts of radioactivity were released. George V. Taplin and Clayton H. Douglas, of the University of California at Los Angeles, have developed a chemical dosimeter for measuring dosages in the range from 20–1,000 r. Based on the linear relationship between acid evolution from chloroform and the amount of radiation, the device utilizes the change in color of an aqueous dye solution caused by the acid produced by the radiation.

Although not fully developed, the new device apparently fulfills both medical and instrumentation requirements for a personnel monitoring device for use in atomic explosions. It can measure gamma radiation with high energy values—0.25 to 10 Mev—in three dosage ranges, from 0–200, 200–400, and 400–600 r. It can be protected from reacting to low-energy radiations of less than 0.25 Mev. In production form, it can be made small, light, cheap and rugged. The three exposure levels can be read immediately after radiation, with an accuracy of ±50 r. Furthermore, no calculations, complicated instrumentation, or specialized training is necessary since the instrument is readable directly.

Medical Considerations

The three ranges indicated coincide with estimates of radiation intensities which would affect the human body. Based on results of animal experimentation, effects of the atomic bomb on the Japanese, and on study of patients receiving total-body radiation therapy, these estimates may later be revised. At present, nearly all persons who receive 0–200 r of penetrating radiation are expected to recover completely. Exposure to 200–400 r is expected to be fatal to only a small fraction of persons receiving this dose, although late effects have not been determined.

It is estimated that at least 50% of a group of individuals receiving 400–600 r would eventually die. This group would require the major part of medical attention. Based on present information, few persons exposed to more than 600 r would be likely to survive even if provided with the best medical care.

No rapid clinical methods of diagnosis have been discovered by which a medical classification according to the amount of radiation received could be made. Nearly all persons receiving more than 200 r would exhibit the same symptoms. The colorimetric dosimeter provides a method of differentiation which would enable medical personnel to concentrate their treatment on those casualties that treatment would help.

Available Detectors

No monitoring device, including the one reported here, will measure accurately X- or gamma radiation with a broad energy range, say 0.1 to 10 Mev. All radiation measuring equipment

* From AEC document UCLA-58, available at $0.20 from the Technical Information Division, U. S. AEC, Oak Ridge, Tenn.

must be standardized against standard sources because of wavelength dependence and other factors.

Even when calibrated, available radiation detectors are not satisfactory with regard to medical requirements. Electronic instruments are highly susceptible to the effects of flash, blast and short circuits. Sensitivity of the pocket electroscope is far too high (0–200 mr), and film badges, while they may be altered to measure the required range, have to be developed and then read with an expensive densitometer.

Available instruments, however, still find their place in protecting disaster relief personnel and delineating safe areas.

Preliminary Experiments

Since the discovery of radioactivity, various experimenters have used chemical changes caused by radiation as a measurement of radiation dosage. In developing the dosimeter, solutions of ferrous sulfate and potassium thiocyanate, potassium iodide and starch, iodoform and starch, mercury compounds, and many previously known reactions were studied. All were found to be far too insensitive to X-radiation to have any practical applicability as personnel dosimeters.

Solutions of chloroform and carbon tetrachloride mixed with 95% alcohol in a 1:1 ratio were studied with regard to the quantity of acid evolved following X-irradiation. Both compounds were found to be relatively sensitive to X- and gamma radiation.

To measure acid evolution colorimetrically in a single-phase system, it was necessary to add a dye in alcohol to either compound because aqueous dye is immiscible. Brom cresol green was found to be a suitable indicator.

Chemical instability was present, however, at temperatures above 37° C. An investigation of factors causing this revealed that the presence of alcohol or inorganic alkali increases the instability at high temperatures. Dye dissolved in acetone, with piperazine added to raise the *p*H value of chloroform above the end point of the dye, provides a stable and relatively sensitive indicator, but the color reaction fades after 20 hours exposure at temperatures between 56–58° C, and the dye tends to precipitate out of solution.

Two-Phase Systems

Because *p*H indicator dyes are relatively heat stable in aqueous solution and commercial chloroform and carbon tetrachloride also have this property, it was decided to use chloroform overlayered with a *p*H indicator dye in pure water. The *p*H of distilled water separated from chloroform following shaking was neutral or only slightly alkaline, ranging between *p*H 7.2 and 7.4. This observation made it possible to use *p*H indicator dyes which react near neutrality.

It is well known that extremely small amounts of acid added to neutral water cause large reductions in *p*H. Also, the affinity of hydrochloric acid for water is far greater than it is for chloroform. Thus, slight shaking washes the greatest fraction of HCl present in chloroform into the aqueous layer of a two-phase system (chloroform overlayered with water).

Preliminary X-irradiation experiments using the two-phase chloroform-aqueous dye systems indicated that the radiation sensitivity was well within the range required for the purposes intended (200–600 r). Heat stability tests demonstrated the superiority of the two-phase system over chloroform-alcohol-dye mixtures. Of the three *p*H indicator dyes available, reacting in the proper range (pH 6.8–5.2)—namely, brom cresol purple, brom thymol blue and chlorophenol red—brom cresol purple was selected for showing a distinctly visible color reaction (purple–yellow).

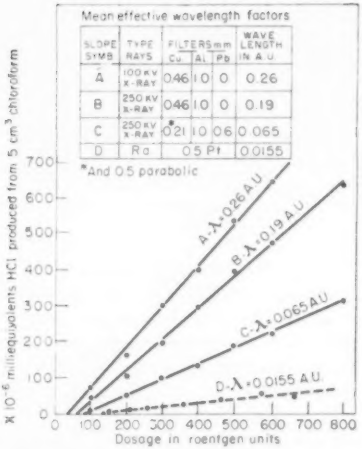

FIG. 1. Acid production from chloroform following exposure to radium and X-rays

Chloroform overlayered with aqueous solutions of any one of the three dyes is stable at 56–58° C for at least twelve weeks. The same systems are resistant to near freezing temperatures (3° C) and to frequent shaking before and after exposure to X- and gamma irradiation. Also, the three dyes in aqueous solution are not affected by either X- or gamma irradiation with doses as high as 3,000 r.

Experimental Methods

A series of experiments was carried out to determine characteristics of the two-phase system. The results showed both merits and limits of the process. Figure 1 shows the linear relationship between acid production from chloroform and radiation dosage. The effect of wavelength is apparent.

Soft glass sample containers gradually liberated small quantities of alkali into the chloroform. This was initially a factor producing an apparent difference in radiation sensitivity between X- and gamma rays, because gamma radiation was administered at a slower rate.

Wide variations in rate of exposure to X-radiation, however, produces no significant difference in the quantity of acid liberated.

As the temperature of chloroform is increased from 5 to 37° C, more acid is produced by X-radiation. Differences observed between values obtained at 23 and 37° C, however, are less than those induced by wavelength dependence.

The system is relatively insensitive to artificial light, but definite chemical changes are induced in chloroform samples in quartz containers following 40–60 minute exposure to a standard mercury-arc ultraviolet lamp. Studies with beta radiation and neutrons have been made, but the sources and techniques have been inadequate.

Adjusting the Range

Because of the linear proportionality between acid evolution from chloroform and the amount of radiation in roentgen units absorbed, it is possible to alter the sensitivity of the systems by three methods. First, as the ratio between the quantities of chloroform and water is increased, the sensitivity is made greater. Secondly, the sensitivity to radiation is decreased in almost direct proportion to an increase in concentration of the dye in the aqueous phase layered over the chloroform. The latter method is preferred for practical reasons. By increasing the dye concentrations, the end point of the color reaction is made more easily distinguishable. Thirdly, adjusting the *p*H of the aqueous dye to a value near the lower end point of the indicator increases the sensitivity of the system.

By using relatively high ratios of chloroform to water, such as 15:1, and rather weak concentrations of dye, the system may be adjusted to sensitivity ranges wherein as little as 5 r units of X-irradiation may be measured. However, for purposes of personnel casualty monitoring it is advantageous to use

strong concentrations of dye with a high ratio of chloroform to aqueous dye phase. Figure 2 shows the variations in radiation sensitivity to X- and gamma rays when the ratio between chloroform and water is changed and when the ratio is kept constant, but the dye concentrations are altered. The points A and A′ and B and B′ represent the minimum amounts of radiation required to cause a color change in the aqueous dye phase.

Specifications

Because of wavelength dependence, the amount of acid produced in chloroform after exposure to gamma radiation from an atomic bomb air burst emitting gamma rays with an energy ranging between 0.25 and 10 Mev, with a mean energy of approximately 3 Mev, about half as much acid might be evolved as that produced by radiation from a radium source. However, it is possible that a small amount of neutron and soft gamma radiation might penetrate beyond the 1,000 meter radius; therefore, tentatively, the system has been adjusted to measure gamma rays with a mean energy similar to that from radium (0.7 Mev). Additional investigation may require revision of this estimate and adjustment for measuring the three ranges of gamma dosage specified for atomic bomb casualty and area monitoring.

General specifications. The chemical reagents, chloroform, pure water and aqueous brom cresol purple (acid form) should all be of the highest chemical purity. The containers for the mixture should not react to the reagents in any way and should not contain acid or alkaline material. Pyrex glass, 2 cc volumetric tubes with ground glass stoppers, sealed with silicone around the stopper and protected on the outside with plastic tape or sealing wax, make satisfactory primary containers for an area monitoring device. Soft glass

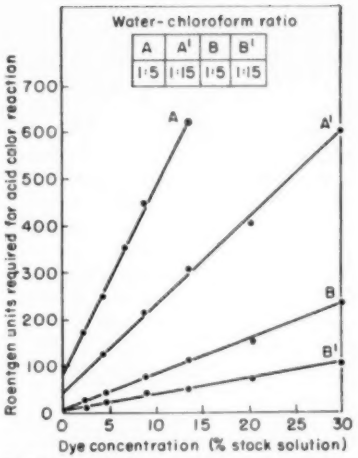

FIG. 2. Effect of varying water-chloroform ratios and dye concentrations on sensitivity of color reaction. *A* and *A′* for radium gamma rays, *B* and *B′* for 85-kv X-rays

should not be used because it liberates alkali. A few polyethylene-type plastics may be suitable. Thick-walled pyrex glass capillary tubes may be cut and sealed in proper sizes for use as sample containers in small personnel casualty badges. The sample container must be protected from ultraviolet light and from soft rays by suitable shielding.

Recommended reagents. Forty mg of the acid form of brom cresol purple are dissolved in 75 cm³ of distilled water, using sufficient 10^{-2}-*N* NaOH to bring the *p*H to 7.25. Volume is then adjusted to 100 cm³ and the *p*H readjusted to 7.25. This was the standard dye solution used in all experiments, from which various dilutions were prepared to give the desired color changes following radiation exposure. The various dye concentrations mentioned below refer to *v*/*v* dilutions of this stock supply as 100%.

A 15:1 ratio of chloroform to aqueous dye has been found satisfactory to meas-

ure radiation throughout the range between 200 and 600 r of gamma radiation. 1.5 cc of chloroform, plus 0.1 cc of a 9.0% aqueous brom cresol purple dye solution is added to a 2 cc volumetric glass-stoppered tube. This ratio and dye concentration reacts at approximately 200 r of gamma radiation (radium source) changing color from purple to yellow. To measure radiation at values of approximately 400 r, the same ratio plus 20.0% aqueous dye is used; for the measurement of 600 r, 30.0% dye and the same ratio are satisfactory.

By preparing three tubes, each containing 1.5 cc of chloroform and 0.1 cc of aqueous brom cresol purple in the concentrations specified, it is possible to measure the dosage ranges of gamma radiation which correspond to the three specified groups of individuals.

The colorimetric dosimeter containing three tubes of the above mixture plus color standards of the dye, worn on a person exposed to 200 r of 0.7 Mev gamma radiation, would cause the first tube to change from purple to yellow but the second and third tubes would remain purple. After exposure to more than 600 r all tubes would turn yellow or colorless. With intermediate dosage, for example, 350 r, the first tube would be yellow, the second tube a faint violet or light gray, and the third tube purple. If the instrument were radiated with approximately 150 r, the first tube would be light gray or violet and the second and third tubes purple.

Further Study

If somewhat higher energy gamma radiation (3 Mev average) plus a small amount of neutron and soft gamma radiation (0.25–0.5 Mev) produce effects in chloroform similar to gamma rays from radium, this method of measurement may be sufficiently accurate to be of distinct value in classifying casualties with radiation injury into three groups. Further investigation is needed with this method of measurement to discover factors which may alter its accuracy.

*Ionizing Radiation Material as an Air Pollutant**

In the laboratory and production operations of the United States atomic energy program potentially harmful waste materials result. Some of these may be chemically toxic, while others are radioactive. For operations directly under AEC supervision, discharges into the atmosphere of toxic and radioactive materials have produced varied particle sizes up to 30–40 microns but were frequently as low as 1 to 2 microns. The average activity of smaller particles was of the order of 1.0 micromicrocurie. Gaseous contaminants were predominantly radioactive, I^{131}, A^{40}, Xe^{133} and Kr^{85} with the half-life of 8.3 days, 110 minutes, 5.4 days and 4.0 hours respectively. The total quantity of radiation in the atmosphere was small.

On the other hand, absorption of I^{131} by vegetation, and in some instances to concentration in parts of plants, raised the question of exceeding permissible tolerances of I^{131} in vegetation which might limit its grazing potential. Removal of I^{131} by chemical scrubbing was instituted to resolve this question.

The Commission's studies have disclosed the necessity for greater uniformity in sampling procedures, for simpler identification of particle sizes of less than 5 microns, for more uniform tests for measuring purification efficiency, for improved equipment for the removal of small particles and mists and for the testing of the performance

*From an address by Abel Wolman, delivered at the United States Technical Conference on Air Pollution, Washington, D.C., May 3, 1950.

potential of commercial equipment now available for dust collection.

Some general agreement is still desirable with respect to permissible limits for human and lower animal exposure to radioactive contamination of the atmosphere. The search for alternative basic chemical processing methods is also being pressed in order to reduce radioactive materials at the source. At the same time, incineration studies have been contracted for in order to determine whether a practicable unit may be designed and built which would "bottle-up" the radioactive products of combustion.

For the moment, the best estimate of maximum permissible doses in inspired air for the general population is:

Element	*Best estimate of safe body accumulation*	*Max. concentration—24 hour continuous exposure*
Argon^{41}	.....	10^{-8} μc/cc
Iodine^{131}	0.001 μc	10^{-11} μc/cc
Carbon^{14}	0.3 μc	10^{-8} μc/cc
Xenon^{133}	.....	10^{-7} μc/cc

AEC Releases Patents for Industrial Use

A new group of 18 patents raises the total number of patents released by the Atomic Energy Commission for licensing to 122. Nonexclusive, royalty-free licenses on the patents listed here will be granted by the AEC as part of its program of making nonsecret information available for use by industry.

Air Proportional Counter (2,499,830), E. W. Molloy. An alpha-sensitive counter operates at atmospheric pressure with air as the ionizing medium.

Method of Making Fluorinated Organic Compounds (2,499,833), M. A. Perkins. Undecachloro-octene and its dehydrochlorination products are used to obtain such products as C_8F_{16} and C_8ClF_{15}.

Preparation of Higher Chlorides of Uranium (2,499,836), H. G. Reiber. Uranium hexachloride is formed by chlorinating uranium oxides.

High Speed Mercury Diffusion Pump (2,499,839), G. R. Stoltenberg.

Apparatus for Handling Materials (2,500,492), F. C. Henriques, Jr. Remote control apparatus for handling radioactive samples for assay.

Rectangular Pulse Amplifier (2,500,756), Q. A. Kerns.

Valve (2,501,461), H. E. Wirth. For single direction flow of fluids.

Perhalogenated Ethylcyclopentane (2,503,077), F. B. Stilmer, W. S. Struve, R. N. Lulek.

Cyclic Compounds and Method of Making (2,503,078), F. B. Stilmer, W. S. Struve, R. N. Lulek. New compounds formed by fluorination and cyclization.

Vacuum Leak Detector Method (2,504,530), R. B. Jacobs. A mass spectrometer system utilizing a flow proportioning valve.

Cyclotron Target (2,504,585), A. F. Reid. Improved target has heat-conductive base coated with thin layer of thallium tellurite.

Vapor Phase Fluorination Process (2,505,877), A. F. Benning.

Proportional Counter (2,505,919), J. A. Simpson, Jr. Adaptable to probing small containers, this counter is sensitive to alpha particles.

Method and Apparatus for Detecting Ionizing Particles (2,506,419), E. R. Graves. A counting device and electrode assembly for detecting fission fragments in the presence of other ionizing particles.

Condensation Product and Process (2,506,428), E. T. McBee, J. S. Newcomer. A new compound, C_5HCl_{11}, is obtained.

Pressure Measuring Device (2,506,431), W. R. Perret, T. Davis. Phillips-type gage operating on full-wave current.

Magnetic Flux Measuring Apparatus (2,506,433), E. H. Plesset.

Radiation Measurement (2,506,435),

B. B. Rossi, J. S. Allen. High amplitude voltage pulses from a radiation counter are produced by periodically impressing a potential upon the electrodes greater than the sparking potential of the tube.

Copies of these patents can be obtained from the U. S. Patent Office, Washington, D. C. For licenses, apply to the Chief, Patent Branch, Office of the General Counsel, U. S. Atomic Energy Commission, Washington, D. C.

REFLECTIONS

Reactor Engineering

DEAR SIR:

I enjoyed reading L. A. Ohlinger's discussion of "Engineering Aspects of Nuclear Reactors."

In the second installment (NU, Jan. '50), however, on page 25, he states, "As long as oxygen is kept out of the system, hydrogen is inert to most materials even at high temperatures." We have had several somewhat unfortunate experiences, which lead me to doubt the accuracy of this statement.

We have had several failures of steam generating tubes in large units where our analysis has led us to conclude that the failure was the result of the penetration of atomic hydrogen into the steel structure of the tubes. Apparently, the hydrogen travels rather freely along the grain boundaries and then combines with carbon from the cementite to form methane. The result is doubly disastrous. The destruction of the cementite weakens the metal along the grain boundaries, while the considerable increase in volume that results from the formation of the methane results in high internal gas pressures which create significant internal stresses.

The reaction takes place at relatively moderate temperatures, that is, in the range 700°–1000° F. It has been discussed at some length in several papers by Hall, Partridge, and others, mostly before the ASME.

Of course, I shall first have to account for the presence of atomic hydrogen in a reactor but this seems to be a relatively easy thing to do, for the neutron-gamma reaction to form deuterium would take place in only one of the atoms of a hydrogen molecule, leaving a free atom of hydrogen quite active and ready to attack the steel.

WARD F. DAVIDSON
Research Engineer
Consolidated Edison Co. of New York, Inc.
New York

• *To which the author replied:* Please extend my sincere thanks for the information Mr. Davidson has offered. Apparently I have not kept current on this particular phase of the broad subject, and my information was based on earlier and less complete data than his letter submits. I offer no apologies for my having missed this point since the subject of nuclear power covers such a wide variety of fields that it is impossible for one poor engineering scientist to keep fully abreast of all the developments in all phases of this field.

L. A. OHLINGER
Chief, Computing Department
Northrop Aircraft, Inc.
Hawthorne, California

DEAR SIR:

The series of articles on "Engineering Aspects of Nuclear Reactors" have given a much broader idea of the possible arrangements of atomic piles and possible methods of control than have appeared anywhere else in the literature.

However, a statement in the first

article (NU, Dec. '49), which appears again in the subsequent articles, is not entirely clear. This is on page 45 in the box entitled "Pile Energy Release Paradox." The author says that "the amount of energy that may be released within a reactor and, hence, the amount of power that may be produced thereby, does not depend upon the size of the reactor as determined by nuclear considerations." Why does he include the words "as determined by nuclear considerations"?

I can understand clearly that unlike a boiler or other common form of energy converter, where the physical size of the unit must be larger in order to handle more power, and where the possible power output from a unit of any given physical size is definitely limited, the same thing does not hold true for the nuclear reactor.

In the reactor, the potential possible power development far exceeds any known method of power removal or dissipation, and hence if the power production of the reactor were allowed to rise naturally, the power would rise to a point where its concentration per pound of material or per cubic foot of space, would be so great that the reactor would destroy itself.

Then why doesn't his sentence merely read ". . . the amount of energy that may be released within a reactor does not depend upon the size of the reactor"? Was it the author's intention to point out that "nuclear considerations" require the reactor to be of a certain size in order to make the chain reaction possible, but that this size is entirely independent of the possible power production?

R. J. KRYTER
The Esterline-Angus Company, Inc.
Indianapolis, Indiana

• *To which the author replied:* In designing a nuclear reactor from an engineering standpoint, the problem is essentially one of designing a suitable heat exchanger with the proper transfer rates and coefficients, transfer surfaces, etc. When designing the same reactor from a nuclear standpoint, the size is determined by the kind and amount of fissionable material, the kind and amount of engineering materials in the reactor, the kind of moderator, the shape of the reactor, and the geometrical arrangement of these components.

The pile that has been designed to the right size from a nuclear standpoint may be too small to permit the removal of large amounts of heat. Hence, this pile would have limitations on the amount of power that could be produced from an engineering standpoint. Similarly, there is no guarantee that the reactor designed correctly from engineering considerations will ever be capable of sustaining a nuclear chain reaction at all.

The critical factor to my mind has always been the reactor size "as determined by nuclear considerations," and hence the use of this expression in the article. Mr. Kryter's revision of my statement in the last paragraph of his letter reads perfectly correctly. My qualifying phrase was simply an expression of recognition of the relative importance of the factors that determine the size of the reactor.

L. A. OHLINGER

Correction

DEAR SIR:

In the italicized note on page 86 of the May NUCLEONICS, mention is made of " . . . Lt. Col. Clinton Maupin of the Marine Corps . . . "

I am not a member of the Marine Corps but am a member of the *Medical* Corps, United States Army.

CLINTON S. MAUPIN, Lt. Col., MC, USA
Army Industrial Hygiene Laboratory
Army Chemical Center, Maryland

NUCLEONIC EVENTS

U. OF ROCHESTER OPENS MEDICAL ATOMIC CENTER

The University of Rochester last month opened a new million-dollar center, financed by the Atomic Energy Commission, for research and training of physicians and technicians in medical problems relative to atomic energy development.

Attached to the University of Rochester School of Medicine and Dentistry, the center will be used to train medical and staff personnel of the armed forces for atomic warfare defense, build up a nucleus of civilian medical personnel having a knowledge of the various aspects of atomic energy, and supply a source of trained research scientists in the branches of medicine, biology, physics, biophysics, physiology, chemistry, biochemistry, etc., in which the new nuclear techniques may be used.

Dr. Henry A. Blair, physiologist and biophysicist, is director of the AEC project at Rochester.

TRUMAN SIGNS NATIONAL SCIENCE FOUNDATION BILL

On May 10, 1950, President Harry S. Truman signed S.247, an act creating the National Science Foundation.

As established, the foundation will be an independent agency in the Executive branch of the Government, headed by a 24-man national science board and a $15,000-a-year director. The foundation's function will be to develop a national policy for the promotion of basic research and education in the sciences, initiate and support basic research in the physical, biological, engineering, and other sciences, grant scholarships and graduate fellowships, and in other ways encourage scientific progress in this country.

Recommendation for creation of such an agency was first made in 1945 in a report to President Truman from Vannevar Bush and his colleagues.

The act, as finally passed, was a compromise between the House version and an earlier Senate version (NU, Apr. '50, p. 79). Two points resolved in compromise provide for authorization of $500,000 for the fiscal year 1951, and up to $15,000,000 a year thereafter for operation of the agency, and for a FBI check on all employes who handle restricted information. In connection with the latter, the foundation will evaluate the FBI data and give the actual security clearance.

CHICAGO'S 100-MEV BETATRON PUT INTO OPERATION

The University of Chicago's 100-Mev betatron—second most powerful electron accelerator in the world—made some trial runs last month.

Built by the General Electric Company, the 200-ton machine has an electromagnet of laminated silicon steel weighing 160 tons. This magnet is 10½ feet high, 6 feet wide, and 17 feet long, and is excited at 24,000 volts.

Operation of the betatron marks an important stage of progress in the university's $12,500,000 post-war investment in basic research on nuclear energy and metals. A $2,200,000 synchrocyclotron, producing 450 Mev, is also approaching completion, as are the huge laboratories for the three institutes for nuclear studies, radiobiology and biophysics, and metals.

U. OF NORTH CAROLINA OFFERS NUCLEAR ENGINEERING STUDY

A curriculum in nuclear engineering, including a full undergraduate course of study and a master's degree program, has been devised by the Physics Department of North Carolina State College of Agriculture and Engineering. It will be opened to students this Fall.

Of the prescribed 128 quarter hours in the undergraduate curriculum, 45 quarter hours will be devoted to nuclear technology.

As presently planned, the courses in the nuclear technology sequence of the whole engineering curriculum will begin at the junior year and extend to the end of the fifth year (master's program) and include:

Required

Modern Physics
Nuclear Engineering
Nuclear Instrumentation
Nuclear Physics
Health Physics
Radioactive Tracer Technology
Elementary Reactor Theory
Advanced Health Physics
Advanced Nuclear Physics

Optional

Medical and Biological Applications of Tracers
Micro- and Trace-Chemistry
Radiochemical Technology
Chemical Processing of Radioactive Materials
Biological and Chemical Effect of Radiation

Plans for significant experimental work in this field are also in progress.

EDITORS' GROUP CONDUCTS FILE SEARCH AT Y-12

Seeking out publishable information for industry, the working party (of AEC's Ad Hoc Committee on Technological Information), representing technical and engineering societies and the business press, recently visited the Y-12 (electromagnetic separation) plant at Oak Ridge. The trip was arranged when the group concluded from a search through the Atomic Energy Commission's patent abstracts files in Washington, earlier in the year, that a study of the complete technology of a major atomic energy process, such as is carried on at Y-12, seemed warranted.

At Oak Ridge, the working party had an opportunity to evaluate technology developed in connection with the electromagnetic separation process by scrutinizing applicable individual technical reports on processing and operations of the Y-12 plant, inspecting the plant operations, and examining plant

ABOUT THE COVER

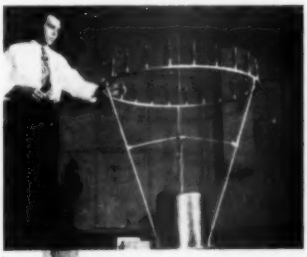

CHECKING the calibration of health monitoring instruments is a continuing process at the AEC's New York Operations office. This month's cover picture was taken in the calibration room as M. R. Coe was preparing to check pocket electrometers against a standard source. Five standard radioactive sources of different strengths —four radium and one Co^{60}—are stored inside the lead shield (looks like an inverted pot at bottom of photo). The tube projecting from its top is hollow; compressed air is used to force the desired source up into the tube and hold it at a specified position. The rack fixes the position of the electrometers so that reproducible measurements can be made. A different rack for calibrating film badges or a movable pedestal for calibrating survey meters can be substituted. All controls are at the opposite end of the room—about 40 feet away. Photo by Mosbacher.

technology with the aid of engineering and technical personnel.

This is part of the AEC's trial program to make atomic energy information more readily available to industry (NU, Sept. '49, p. 80). Members of the party include: Keith Henney, S. A. Tucker, F. J. Van Antwerpen, Sidney Kirkpatrick, and E. E. Thum (NU, Feb. '50, p. 92).

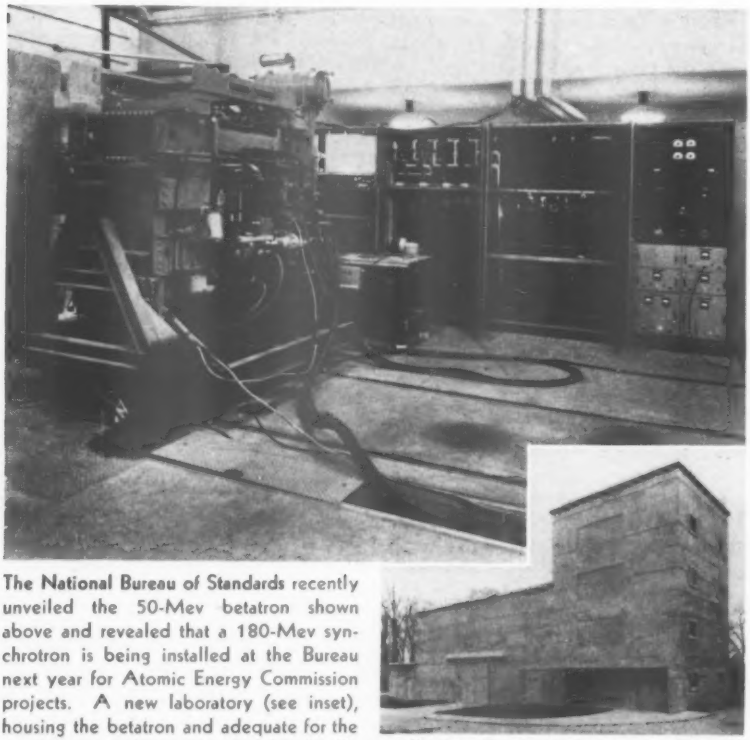

The National Bureau of Standards recently unveiled the 50-Mev betatron shown above and revealed that a 180-Mev synchrotron is being installed at the Bureau next year for Atomic Energy Commission projects. A new laboratory (see inset), housing the betatron and adequate for the synchrotron under construction by the General Electric Company, has been especially designed for high-energy research work. It is a three-story building with reinforced concrete walls varying in thickness between 2 and 8 feet.

Besides the principal bay for the accelerator installations, there is a radiation room that provides complete instrument shielding. Beams can be passed into this room through any type of shield up to 10 feet in thickness—for studies of protective barriers and walls. The beam can also be taken out-of-doors for a distance of about 500 yards.

The combined facilities make the betatron laboratory unique in that NBS scientists will be able to cover the range from 5,000 to 180,000,000 volts with more versatility and high-beam intensities than any other group in the country.

Their research program includes investigations of the basic properties of, and shielding against, high-energy X-rays, and medical and industrial applications of these radiations.

MIT SCHEDULES SUMMER MODERN PHYSICS LECTURES

Five series of lectures in modern physics will be a feature of the 1950 summer session at the Massachusetts Institute of Technology from July 10 to August 18.

Prof. P. Scherrer of the Eidgenossische Technische Hochschule, Zurich, will lecture on "Experimental Atomic Physics," and Prof. E. Amaldi of the University of Rome will talk on "Nuclear Physics."

MIT faculty members who will participate include Victor F. Weisskopf, professor of physics, lecturing on "The Theory of Nuclear Reactions;" Philip M. Morse, professor of physics, on "Special Relativity;" and Jerrold R. Zacharias, director of the Laboratory for Nuclear Science and Engineering, together with other members of the laboratory, on "Radio-frequency Spectroscopy of Atoms and Molecules."

The program is intended for graduate students or teachers of physics who wish to follow recent aspects of physics.

MINERALOGISTS MEET TO DISCUSS URANIUM RESEARCH

A symposium on current progress and problems in research being conducted on uranium mineralogy in a number of institutions in Canada and the United States was held in the New York office of the Atomic Energy Commission on April 24 and 25, 1950.

The meeting was attended by five mineralogists from the Department of Mines and Technical Surveys of the Canadian Government and by fourteen mineralogists and chemists representing Columbia University, Harvard University, the University of Minnesota, the U. S. National Museum, the U. S. Geological Survey and the U. S. AEC.

Papers were presented by various members of the groups on problems relating to the general mineralogy of the radioactive minerals and techniques by which these problems are being attacked. In addition, specific mineralogic studies of uraninite and pitchblende deposits were reviewed.

U. OF MICHIGAN SIGNS TWO NEW AEC CONTRACTS

Two one-year contracts totaling $38,637 have recently been signed by the University of Michigan under a new three-year cooperative agreement with the Atomic Energy Commission.

The contracts provide funds for the first year of contemplated two-year projects. $33,480 will be used to remodel the university's 42-inch cyclotron and conduct research on atomic reactions. $5,157 will be used by the Department of Chemistry to study the behavior of three-component systems involving water, salts and organic liquids (compounds containing carbon).

OAK RIDGE, U. OF TEXAS TO BUILD COBALT IRRADIATOR

The Atomic Energy Commission announced last month approval of a new cancer research project which will pioneer the use of radiocobalt in a therapy unit comparable to an X-ray unit operating in the 1 to 2-Mev range. It will be a joint endeavor of the Oak Ridge Institute of Nuclear Studies and the University of Texas' M. D. Anderson Hospital at Houston, under a contract calling for the construction, testing and ultimate use of the radiocobalt irradiator for cancer treatment.

The Oak Ridge Institute will supply the facilities of its Medical Division's new Cancer Research Hospital and the Texas Hospital will design and fabricate the irradiator. The latter will consist of a spherical shield of some heavy metal such as lead with the radioactive cobalt enclosed in the middle. The shield will be approximately a foot in diameter and will have a slit in it through which the radiation from the

radiocobalt will pass. With the irradiator, it will be possible for investigators to direct a small but very intense beam of penetrating gamma radiation to the tissue to be irradiated.

U. OF DELAWARE SCHEDULES RADIATION PHYSICS COURSE

A course in radiation physics—one of the first of its kind to be offered by any American college—will be given this summer from July 24 to August 31 at the University of Delaware. Vincent E. Parker, professor of physics and chairman of the department at the university, who recently represented the state of Delaware in a five-week training course in radiation physics at Brookhaven National Laboratory, will be the instructor.

The purpose of the course will be to familiarize and train a select group of Delawareans in the basic principles of radioactivity and the hazards of handling radioactive materials. It is designed principally for science teachers, hospital laboratory technicians, industrial research personnel, and science students at the university.

FORUM WILL COMMEMORATE RADIUM'S 50TH ANNIVERSARY

In commemoration of the 50th anniversary of the discovery of radium by Pierre and Marie Curie, a series of meetings and forums will be held at l'Ecole Supérieure de Physique et de Chimie in Paris from July 17–19. Subjects relating to radiophysics will be discussed on July 17, radiochemistry on July 18, and radiobiology on July 19.

Each meeting will be dedicated to presentation and discussion of communications (limited to 15 minutes each) on either experimental facts or original theories. Arrangements and communications for the meeting are being handled by M. Georges Champetier, Ecole Supérieure de Physique et de Chimie, Paris 5, France.

RADIATION EFFECTS DATA MADE AVAILABLE TO M.D.'S

The Navy's experimental research data concerning certain effects of atomic radiation upon living tissue are being made available to civilian physicians and medical officers of the armed services and Federal agencies under a program announced recently by Rear Admiral Clifford A. Swanson, Chief of the Navy Bureau of Medicine and Surgery.

This particular group of study slides concerns lesions produced by total body ionizing radiation. The tissue sections were prepared from swine which had been exposed to 1 and 2-Mev X-rays. The response of the tissues of these animals to X-radiation is comparable to the response of tissues in man in atomic bomb radiation.

The commanding officer of each Naval hospital has been instructed to arrange with the local county medical society, commanding officers of Armed Forces reserve components and Federal agencies in their areas for interested physicians to join with Navy doctors in the use of this study material.

Future plans for supplying additional study material will depend upon the degree of success realized from use of the present material and the measure of interest manifested by those in a position to benefit from the offering.

AIR FORCE IS BUILDING ATOMIC POWER CENTER

A new Air Force engineering development center, named for the late Maj. Gen. H. H. Arnold, is being erected at Camp Forrest, Tennessee, for the purpose of conducting research on problems dealing with the propulsion of aircraft by atomic energy. Disclosure of this Air Force activity was made in a speech last month by Maj. Gen. F. O. Carroll, commanding general of the center.

SCREENING BEGUN FOR REACTOR SCHOOL CANDIDATES

The Oak Ridge School of Reactor Technology recently began screening applications of potential candidates for the school course that begins early in September, 1950. The school is operated at the Oak Ridge National Laboratory under sponsorship of the Atomic Energy Commission (NU, Jan. '50, p. 95). Filing of applications closed on June 1.

Fifty students will be accepted for the first formal course which will run for a year. Of these, 30 will come from industry, AEC contractors and appropriate Governmental agencies and their contractors, and will return to their sponsoring organizations on completion of the course. Twenty will come from the ranks of recent college graduates.

A preliminary course already is under way, attended by 19 representatives from industry, the Navy and Air Force.

NUCLEAR NEWSMAKERS

Fred C. Schlemmer has resigned as AEC manager of operations at the Hanford plutonium production center. He will return to private industry.

W. F. Libby, Alfred O. C. Nier, and **Bruno Rossi** were among the thirty American and three foreign scientists recently elected to membership in the National Academy of Sciences.

M. H. L. Pryce has been named chief of the theoretical physics division at the Atomic Energy Research Establishment at Harwell, England, to replace Klaus Fuchs.

Norman F. Ramsey has been promoted to full professorship of physics at Harvard University. He formerly served at MIT's Radiation Laboratory and at Los Alamos during the war.

William E. McQuiston has joined the staff of the Los Alamos Scientific Laboratory as a chemist in the GMX Division. **Lawrence Cranberg,** who also received an appointment to the laboratory staff, has joined P Division as a physicist.

Donald B. Sinclair has been appointed chief engineer of the General Radio Company to succeed Melville Eastham who retired from that post in February.

Dana W. Atchley, Jr., of Tracerlab, Inc., has been appointed its director of engineering. He had formerly been sales manager. **William A. Kerr** has been appointed general sales manager. Tracerlab's newly formed engineering division will include electronic and mechanical engineering designs.

David M. Stearns, has been named technical information adviser of the Los Alamos Scientific Laboratory. The announcement was made in connection with the recent establishment of a technical information office in the Documentary Division. Mr. Stearns will serve on the staff of **Ralph Carlisle Smith,** who is an assistant director of the Laboratory and the leader of the Documentary Division.

• • •

BOOKS

Atomic Medicine (Radioactivity in Peace and War), edited by C. F. Behrens, MD, Capt. MC, Thomas Nelson & Sons, New York, 1949, 416 pages, $7.50. *Reviewed by Richard H. Chamberlain, MD, Dept. of Radiology, University of Pennsylvania.*

This book is a collection of chapters covering subjects which might be pre-

sented in a course in radioactive isotopes and nuclear physics with a particular slant to the medical aspects and applications of these subjects. The quality of the chapters is rather uneven, although some of the best are those written by the editor. Perhaps the most unfortunate aspect of this work is the title, which is unduly presumptuous and not entirely accurate in that the emphasis is certainly not directed primarily to clinical medicine.

Nevertheless, the project is a major undertaking and does great credit to the editor and contributors in that it is the first volume to include most of the background data that should be known to radiologists, internists interested in physiological and clinical applications of isotopes, and probably to all medical men who might be called upon in our era to help with military as well as peacetime applications of atomic energy.

Particularly to be recommended is the largely successful effort to reduce the physical explanations to clear and understandable language without undue use of mathematical language.

The chapters on radiophosphorus and radioiodine, as well as the other radioisotopes of medical interest, are not sufficiently complete to furnish a guide book for the application of these agents without supplemental reading but should furnish a reasonable background for the references cited at the end of each chapter.

The format of the book is of the type of paragraphing familiar to those who have been in the Armed Services but does not interfere with the flow of reading and is useful in referring to certain portions of it.

The chapter on atomic-disaster planning is disappointingly inconclusive and non-specific, but this seems to be due to the lack of formulated plan at a higher level, rather than to deficiencies in the coverage of the authors.

I believe that no other volume is available which will furnish the coverage of information that is contained in this book and that it would be profitable, if not obligatory, reading for every medical practitioner in our land.

The Chemistry and Metallurgy of Miscellaneous Materials (Thermodynamics) (Div. IV, Vol. 19B, of National Nuclear Energy Series), edited by Laurence L. Quill, McGraw-Hill Book Co., Inc., New York, 1950, 329 pages, $3. *Reviewed by G. Derge, Metals Research Laboratory, Carnegie Institute of Technology.*

Although a part of the National Nuclear Energy Series, this book contains no specific information on fission processes or materials. It is, instead, a collection of incidental information which was required as background material for the conduct of the more spectacular phases of the Manhattan Project. As such, it is a good indication of the vast amount and range of scientific data required to reach the major objective. It can be cited as an example of the necessity of maintaining a uniformly high research productivity in all fields of science in order to provide the means for rapid success in any one field that may become vitally important.

As the title implies, the book includes such a miscellany of information that even the table of contents provides only a sketchy outline.

Those interested in the metal halides will find new and much old data collected together in convenient form for reference.

Others who are interested in high-temperature reactions and applications of materials will find that the thermodynamic tables of Leo Brewer are in a useful form. His discussions of the special methods and cycles which were used to derive estimates of thermodynamic values must be read if mis-

interpretations are to be avoided. Based on these calculations, the appraisal of the possible refractory applications of such special materials as nitrides, phosphides, carbides, silicides, sulfides, molybdenum, and wolfram will be found a helpful guide rather than the final answer to many of the perplexing problems in this field.

The editor is to be commended for his arrangement of such variety in a consistent framework of terminology and form. It is unfortunate that each of the cooperating authors cannot be recognized adequately within the limits of this review. Knowing the pressure under which the work was done and the diverting influences which might have prevented its publication, there can be little justification for any form of criticism. The reader can only be grateful to all the agencies and individuals involved for making the work generally available.

BOOKS RECEIVED

Biological Studies with Polonium, Radium, and Plutonium (Div. VI, Vol. 3, of National Nuclear Energy Series), edited by Robert M. Fink, McGraw-Hill Book Co., Inc., New York, 1950, xvi + 411 pages, $3.75.

Classical Mechanics, by Herbert Goldstein, Addison-Wesley Press, Inc., Cambridge, Mass., 1950, xii + 399 pages, $6.50.

Cosmical Electrodynamics, by H. Alfvén, Oxford University Press, New York, 1950, vii + 237 pages, $5.

The Autobiography of Robert A. Millikan, Prentice-Hall, Inc., New York, 1950, 311 pages, $4.50.

The Foundations of Arithmetic (a logico-mathematical enquiry into the concept of number), translation by J. L. Austin. The original German text by Dr. G. Frege, published in 1884, appears with the translation. Philosophical Library, New York, $4.75.

Internationaler Kongress über Kernphysik und Quantenelektrodynamik (proceedings of meeting which took place in Basel from September 5–9, 1949, edited by staff of *Helvetica Physica Acta*). The 41 papers presented at the congress are divided according to the following subjects: Instruments for producing high-energy particles and neutrons; Instruments for detecting particles and quanta, Experimental results of nuclear physics; Theory of the atomic nucleus and its experimental foundation; and Quantumelectrodynamics. The majority of papers appear in English; the remainder are in French or German. Verlag Birkhauser, Basel, Switzerland, 1950, 247 pages, Swiss fr. 16 (paper cover).

Theorie und Lösungsmethoden des Mehrteilchenproblems der Wellenmechanik, by P. Gombás, Verlag Birkhauser, Basel, Switzerland, 1950, 268 pages, Fr. 24.50 (paper cover), Fr. 29.50 (linen binding).

Nuclear Physics, by Francis Bitter, Addison-Wesley Press, Inc., Cambridge, Mass., 1950, 200 pages + 18-page nuclear data chart, $5.50.

OTHER LITERATURE

A-W Chart of Nuclear Data. Published in handy book form, this three-color chart is intended for students of physics; therefore no attempt was made to put into it data of more specific nature which are included in more elaborate charts. It is a reprint of Appendix 5 of the new book "Nuclear Physics" by Francis Bitter (see listing above). Addison-Wesley Press, Inc. Cambridge, Mass., 1950, $.50.

Infrared Radiation Therapy Sources and Their Analysis with Scanner, by Leopold Rovner, Charles C. Thomas, Springfield, Ill., 1950, 35 pages, $1.50.

PRODUCTS and MATERIALS

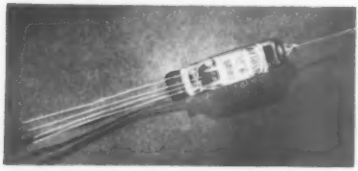

ELECTROMETER PENTODE

Raytheon Manufacturing Co., Special Tube Section, 55 Chapel St., Newton 58, Mass. A new subminiature electrometer pentode, type CK5889, has a 7.5 ma low microphonic filament. Double-ended construction separates the control grid lead at the top of the tube from the other four leads, and a permanently bonded guard ring encircling the control grid lead is said to break leakage paths between leads at top and bottom of the tube. Maximum grid current is 3×10^{-15} amp, but the nominal value is 1×10^{-15} amp. High transconductance, good emission stability, low drift, and low microphonics are claimed.

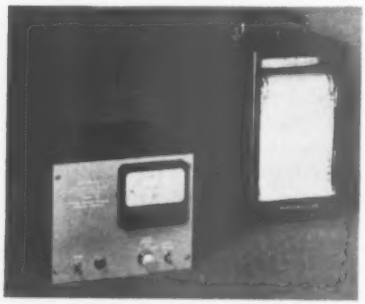

COUNTING RATE COMPUTER

Berkeley Scientific Co., 6th and Nevin Sts., Richmond, Calif. The model 1600 counting rate computer converts information from a scaler or counter into an electric impulse proportional to counting rate. Provision is made for using the computer's output to record counting rate on a standard one milliampere recorder. The output pulse from a scaler at the end of a predetermined count is fed into the computer, which calculates counting rate from the elapsed time between pulses. For a predetermined count of 100, the computer provides ranges of 4–400, 40–4,000, and 400–40,000 cpm. Changing the predetermined count changes the ranges by a corresponding factor. The computer operates from a 110-volt source.

GAMMA-RAY DETECTOR

Halross Instruments Corp. Ltd., 171 Garry St., Winnipeg, Canada. A gamma-ray spectrometer feature of the model 939 Scintillometer allows the operator to distinguish between thorium and uranium ore deposits, and will indicate the uranium concentration in an ore containing both radioactive minerals. Utilizing the scintillation principle, the portable battery-operated instrument is housed in an aluminum

alloy case measuring 3½ by 11 by 13 in. A removable probe is contained in the lower section of the case. The electronic circuit is protected against vibration, shock, temperature and humidity.

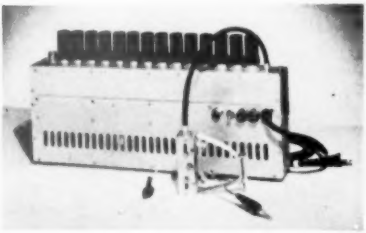

CHAIN PULSE AMPLIFIER

Spencer-Kennedy Laboratories, Inc., 186 Massachusetts Ave., Cambridge 39, Mass. The model 214 chain pulse amplifier is designed to amplify very fast pulses and transients. Employing a traveling-wave circuit, it has a bandwidth of 40 kc to 100 Mc and a gain of 30 db. Imput impedance is 180 ohms. A special termination at the end of a 15-in. cable is provided for convenient use with a cathode-ray tube for the viewing of high-speed pulses. A second output is provided for connection to high-speed counters and other associated equipment. Standard connectors are used at the input. The amplifier is housed in an aluminum chassis and can be supplied for either table or rack mounting.

COOLANT FLOW CONTROL

Electro Chemical Supply & Engineering Co., 750 Broad St., Emmaus, Pa. Designed as a safety device to protect water-cooled, electrically operated equipment, the Esto water control can be adjusted to operate at any water flow the equipment requires. The unit prevents the starting of equipment before cooling water is turned on. If water supply fails or is inadequate, the control stops the equipment.

STAINLESS TUBE CUTTER

Gilman Engineering & Mfg. Corp., Janesville, Wis. A portable cut-off machine for stainless-steel tubing uses an abrasive wheel for cutting. According to the manufacturer this eliminates the loss of stainless properties which occur when tubing is cut with a blowtorch. The unit will handle tubing from 4 to 24 in. in diameter. It is said to cut off the tube with 0.010 in. accuracy.

PROBING NEEDLE COUNTER

Radiation Counter Laboratories, Inc., 1844-50 W. 21st St., Chicago 8, Ill. The mark 1, model 101 probing needle counter, designed for neurosurgical exploration, has a 3-in. probe that is ⅛ in. in diameter. The stainless steel wall has a thickness of 100 mg/cm², permitting detection of beta radiation greater than 350 kev. With an operating voltage of 900 volts, the counter has a 50-volt plateau with a slope of 15% per 100 volts. Background is said to be 8 cpm.

WIDE-BAND D-C AMPLIFIER

Furst Electronics, 12 S. Jefferson St., Chicago 6, Ill. The model 120 wide-band d-c amplifier was designed to increase the sensitivity of cathode ray oscilloscopes with extended low-fre-

quency response. It is also suitable for use in extending the range of vacuum-tube voltmeters, frequency analyzers, and other instruments when unusually low frequencies are involved. Operating from a 115-volt a-c supply, the instrument is said to reduce long waiting times caused by coupling time-constants. Push-pull amplification is used throughout for a maximum gain of 100.

VOLTAGE STANDARD

Sorensen & Co., Inc., 375 Fairfield Ave., Stamford, Conn. Extreme stability is the most important characteristic of the model VS50-50 voltage reference standard. The unit operates from an input of 100–130 v a-c from 45 to 800 cps, and delivers 50 volts d-c regulated to ±0.5%. Ripple is less than ±0.5%. Dual output terminals are provided, either of which can carry 50 ma. Internal impedance of one output terminal is 8.5 ohms; the other has an internal impedance of 700 ohms, protecting the unit from damage caused by shorting.

LABELING TAPE

Labelon Tape Co., 100 Anderson Ave., Rochester, N. Y. Labelon, a smudge-proof, pressure-sensitive labeling tape, is said to be waterproof, oil proof, and acid resistant. It will withstand temperatures up to 150° F. Made of two sheets of acetate tape with a carbon material sealed between them, the tape is available in 500-ft rolls in either ⅝ or ¾ in. widths. Identification written on the tape cannot be erased, smudged, or rubbed off.

"NUCLEAR" CALCULATOR

Nuclear Instrument & Chemical Corp., 229 W. Erie St., Chicago 10, Ill. The "Nuclearule" calculator is a special circular slide rule with scales for use in radioactivity calculations. It can be used for computation of count rate, statistical error, coincidence loss, sample activity vs half-life, and radiation flux after passage through absorbers.

STILBENE CRYSTALS

Organic Specialties, Inc., 109 Fifth Ave., Paterson, N. J. Trans-stilbene, said to be especially pure, is available for use in the growing of crystals for scintillation counting equipment. Another crystalline hydrocarbon, tolane, is also available.

LITERATURE AVAILABLE

Megohmeter. Bulletin 465 describes the "Major Megohmer," an instrument which measures resistances in the 0–50 megohm range. *Herman H. Sticht Co., Inc., 27 Park Place, New York, N. Y.*

Resistors. Catalog 11Ax describes precision wire-wound resistors, including miniature types. *Cinema Engineering Co., 1510 W. Verdugo, Burbank, Calif.*

Now – exact laboratory measurements of RADIATION INTENSITIES

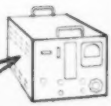

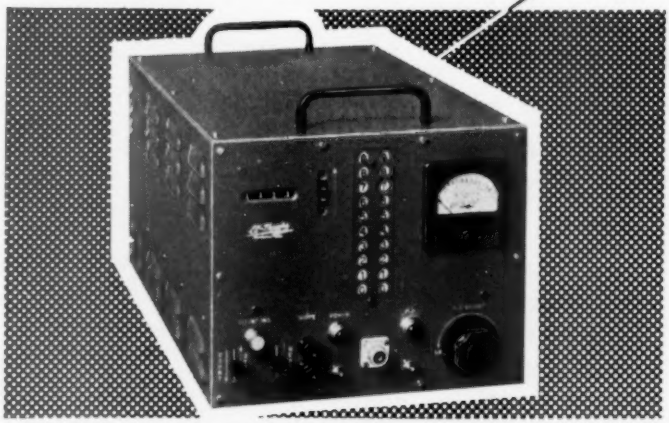

LS1000 or LS100 LABORATORY COUNTER

Decade Scaling Type

El-Tronics INC.

2647-67 N. HOWARD STREET
PHILA. 33, PA.

America's Foremost Crafters
Of Scientific Equipment

For more reliable, precise direct readings of radiation intensities the El-Tronics LS1000 or LS100 Decimal Decade Scaler is the instrument that perfectly fits every laboratory installation. Counts up to 9,999,999 before recycling. Final count is direct reading—no additional computing is necessary. A compact chassis neatly contains six circuit components in one unified assembly. 1000 Scale will count 10,000 evenly spaced pulses per second. LS100 will count 1,000 evenly spaced pulses per second. Impulse register (recording clock) is built-in. Higinbotham Scaling circuit. Hermetically sealed transformers and oil filled high voltage capacitors are just a few of the LS1000's modern features. Operates on common 115 Volt 60 cycle power source. Cabinet finished in grey Hammertone. Complete with coaxial cable for connecting G.M. counter tube.

LS100 . . . . . **$385 F.O.B.**
LS1000 . . . . . **$425 PHILA.***

**Less Geiger Muller Counter Tube*

Write for free illustrated descriptive bulletins

The FUME HOOD of the FUTURE . .

is Yours Today

Kewaunee's New LOW VELOCITY FUME HOOD for Handling RADIO-ACTIVE ISOTOPES

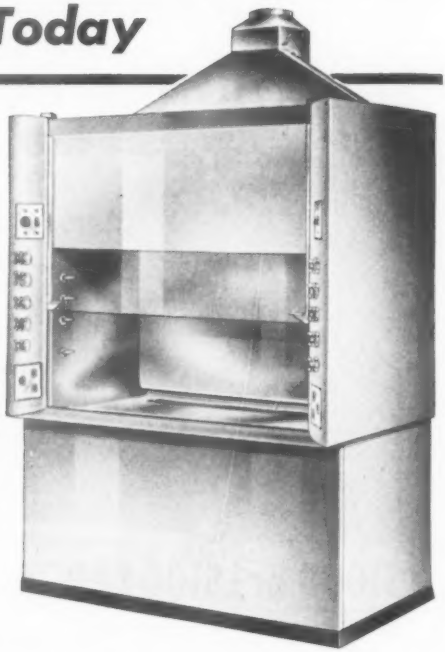

Design Approved for Use by the OAK RIDGE INSTITUTE of NUCLEAR STUDIES

No. 3600—Kewaunee's "FUME HOOD of the FUTURE"

The Hood is made with stainless steel interiors and ducts throughout and incorporates a stainless steel working surface and trough. The working surface will support a load of 4,000 pounds. The Hood incorporates a new system of airfoils, baffles and ducts which provides a uniform flow of air over the entire face of the Hood, thus assuring evacuation of gases at extremely low velocities without interference from reverse eddies or turbulence. No auxiliary duplicate duct system for incoming air is required.

Write for Descriptive Literature and Drawings available now on Kewaunee No. 3600—"The Fume Hood of the Future"

Kewaunee Mfg. Co.

C. G. Campbell, *President*

5083 S. Center Street Adrian, Michigan

Representatives in Principal Cities

Manufacturers of Wood and Metal Laboratory Equipment

NOW—

read pulse-rates *DIRECTLY!*

—with RCA's "plug-in" COUNT-RATE METER

Type EMA-6

This compact and easy-to-carry instrument indicates *directly* the average number of pulses per second. It is self-calibrating, by means of rectified pulses from the 60-cycle power line. It contains its own high-voltage d-c supply (0-2KV) for use with a wide variety of radiation detectors. It uses no batteries—operates from any 115-volt, 60-cycle, a-c outlet.

The RCA Count Rate Meter is the ideal testing and safety instrument for any industrial plant where radio active material may be present. As a monitor, it can be used to determine the presence of contaminated material. As an assaying device, it can be used to measure the activity of nuclear fuels or isotopes. It can be used for measuring absorption of nuclear radiation by various materials and for detecting the presence of radioactive isotopes in conjunction with tracer work. It can be used to study the characteristics of radiation detecting devices.

The instrument is complete with AN connector and six feet of coaxial cable for connection to a radiation detector. A phone jack for aural monitoring is also included. For complete information write Dept. 126F, RCA Engineering Products, Camden, N. J.

◀ **Count-Rate Meter, Type EMA-6.** *Selector switch permits choice of full scale counting rate of 10, 100, or 1000 per second.*

SCIENTIFIC INSTRUMENTS

RADIO CORPORATION of AMERICA

ENGINEERING PRODUCTS DEPARTMENT, CAMDEN, N.J.

In Canada: RCA VICTOR Company Limited, Montreal

S.S.WHITE 80X HIGH VOLTAGE RESISTOR

(½ Actual Size)

4 watts · 100 to 100,000 megohms

S.S.White 80X Resistors have many characteristics—particularly negative temperature and voltage coefficients—which make them suitable for many high voltage applications.

They are constructed of a mixture of conducting material and binder which assures adequate mechanical strength and durability. This material is non-hygroscopic and a coating of G-E Dri-Film further protects them against humidity and helps to stabilize them.

BULLETIN 4906 has full information. Write for a copy today.

S.S.WHITE INDUSTRIAL DIVISION

THE S. S. WHITE DENTAL MFG. CO. — DEPT 2 — 10 EAST 40th ST., NEW YORK 16, N. Y.

FLEXIBLE SHAFTS AND ACCESSORIES
MOLDED PLASTICS PRODUCTS—MOLDED RESISTORS

One of America's AAAA Industrial Enterprises

FOR LOWEST POSSIBLE ALPHA BACKGROUNDS!

- Background 1 count per hour.
- 25 cm^2 sample area ($2\frac{1}{4}$" dia.)
- Automatic controls.

NMC Model PC-2A
LOW-BACKGROUND PROPORTIONAL COUNTER

Ideal for bio-assay work, soil sampling, water and waste sampling and heavy-metal tracer work. Beta-counting modification soon available.

PRICE $813.50 f.o.b. Indianapolis

Subject to change without notice

WRITE FOR CATALOG NM-1

NMC nuclear measurements corporation

3339 CENTRAL AVENUE • INDIANAPOLIS 5, INDIANA

Lower Prices
On IMPROVED GEIGER TUBES

TGC-1: 3-4 mg/cm² mica end window $37.50

TGC-2: less than 2 mg/cm² mica end window $47.50

TGC-3: mica end window tube for X-rays $87.50

Tracerlab now offers the best in Geiger tubes at the lowest prices. Improved manufacturing processes have permitted substantial price reductions, together with longer life and more stable operation. A new construction is now used which consists of a thin stainless steel cathode coating evaporated on the inner surface of the glass envelope. This new method of manufacture not only improves operating characteristics, but also makes the all-glass TGC-4 and TGC-5 tubes non-photosensitive, and hence, suitable for dip counting. Our newest tube, the TGC-6 is an all-glass beta-gamma tube with a three pin base, and an overall length of 4⅞", not including the pins.

For further information write for Bulletin N-25.

TGC-4: 300mg/cm² all glass tube $12.00

30 mg/cm² all glass tubes: above—TGC-5 $14.00 right—TGC-6 $10.50

Tracerlab

TRACERLAB INC., 130 HIGH STREET, BOSTON 10, MASS.

was this call necessary?

Some "Moral Insurance" here might have avoided a serious accident

Workmen's compensation is a fine thing—but it can't replace a mangled arm.

Safety laws prevent many accidents—but they can't cover every hazard of an individual plant.

Accident prevention which goes *beyond the law* is an unwritten responsibility of every employer. It is his "Moral Insurance" for his employees welfare.

The premiums for "Moral Insurance" are not high. They do not have to be paid for in fancy safety gadgets. Their cost is simply the institution of common sense safety regulations covering all local hazards—enforced by employee committees with the full support of management.

Yes—"plant safety" is a mutual job.

DON'T FORGET—THE LIFE YOU SAVE MAY BE YOUR OWN

Published in the public interest by:

McGRAW-HILL PUBLICATIONS

Van de Graaff® TWO-MILLION-VOLT ELECTRON ACCELERATOR

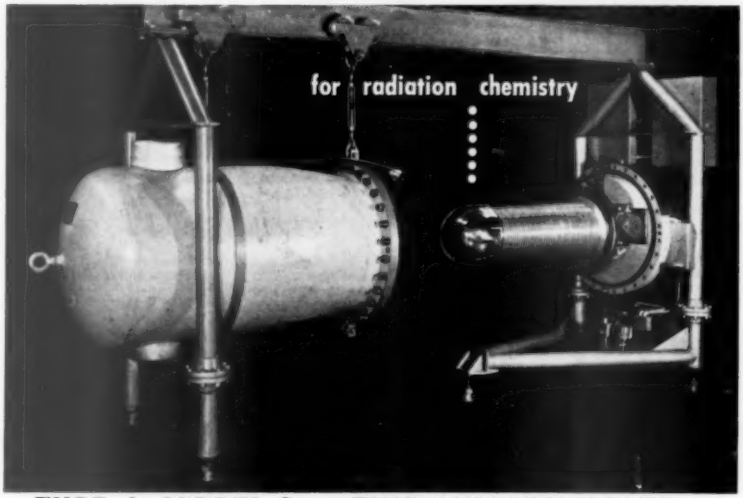

TYPE A MODEL S — TWO MILLION VOLTS

The Type A Model S electrostatic accelerator is a self-contained, self-supported unit requiring a minimum of special building facilities for its installation and use.

FEATURES

Operating potential, 0.75—2.0 million volts

Self-contained operating unit

Flexibility of operation by remote adjustment of controls for the electron source and generator

Well collimated beam of homogeneous electrons

Electron beam currents from 0.01 to 100 micro-amperes

Combination cathode-ray window and gold X-ray target for use of either electrons or X-rays

Other electrostatic accelerators can be quoted to meet your special requirements for voltage range and beam intensity. Your inquiries will receive prompt attention

HIGH VOLTAGE ENGINEERING CORPORATION

7 UNIVERSITY ROAD CAMBRIDGE 38, MASSACHUSETTS

NEW! INEXPENSIVE

with all of the features and characteristics of fine, research halogen tubes and a GUARANTEE of six months minimum shelf life, 5x10⁸ counts minimum operating life.

$10

AMPEREX
METAL WALL
BETA and GAMMA
RADIATION COUNTERS

★ *Long Life*

★ *Unchanging characteristics with use*

★ *Not damaged by excessive overvoltage*

★ *Operable over wide temperature variations*

TYPES 75N and 75NB3

Filling	Neon + quenching admixture
Operating temperature range	−55°C. to +75°C
Operating voltage	700 volts D.C.
Plateau	in excess of 150 volts
Slope of plateau	15% per 100 volts maximum
Capacity at terminals	1.5 mmf.
Dead time (approx.)	70 microseconds
Background—shielded 2" lead	50 counts per minute max.
Life expectancy in counts	unlimited by use, guaranteed $5x10^{10}$ counts, minimum
Cathode material	Stainless steel
Effective cathode dimensions	2 11/16" long x ⅝" O.D.
Cathode wall thickness	.009"-.010" (approx. 150mg/cm²)*

*A stainless steel wall 150mg/cm² thick will pass all beta radiation of energy in excess of 0.3 mev.

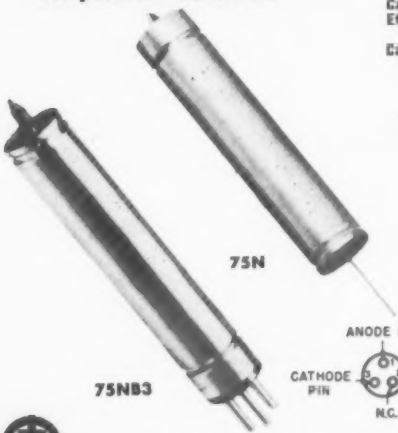

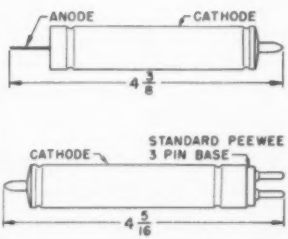

re-tube with Amperex

Pioneers and Specialists in Electronic Tube Design and Construction

AMPEREX ELECTRONIC CORP.
25 WASHINGTON STREET, BROOKLYN 1, N. Y.
In Canada and Newfoundland: Rogers Majestic Limited
11-19 Brentcliffe Road, Leaside, Toronto, Ontario, Canada

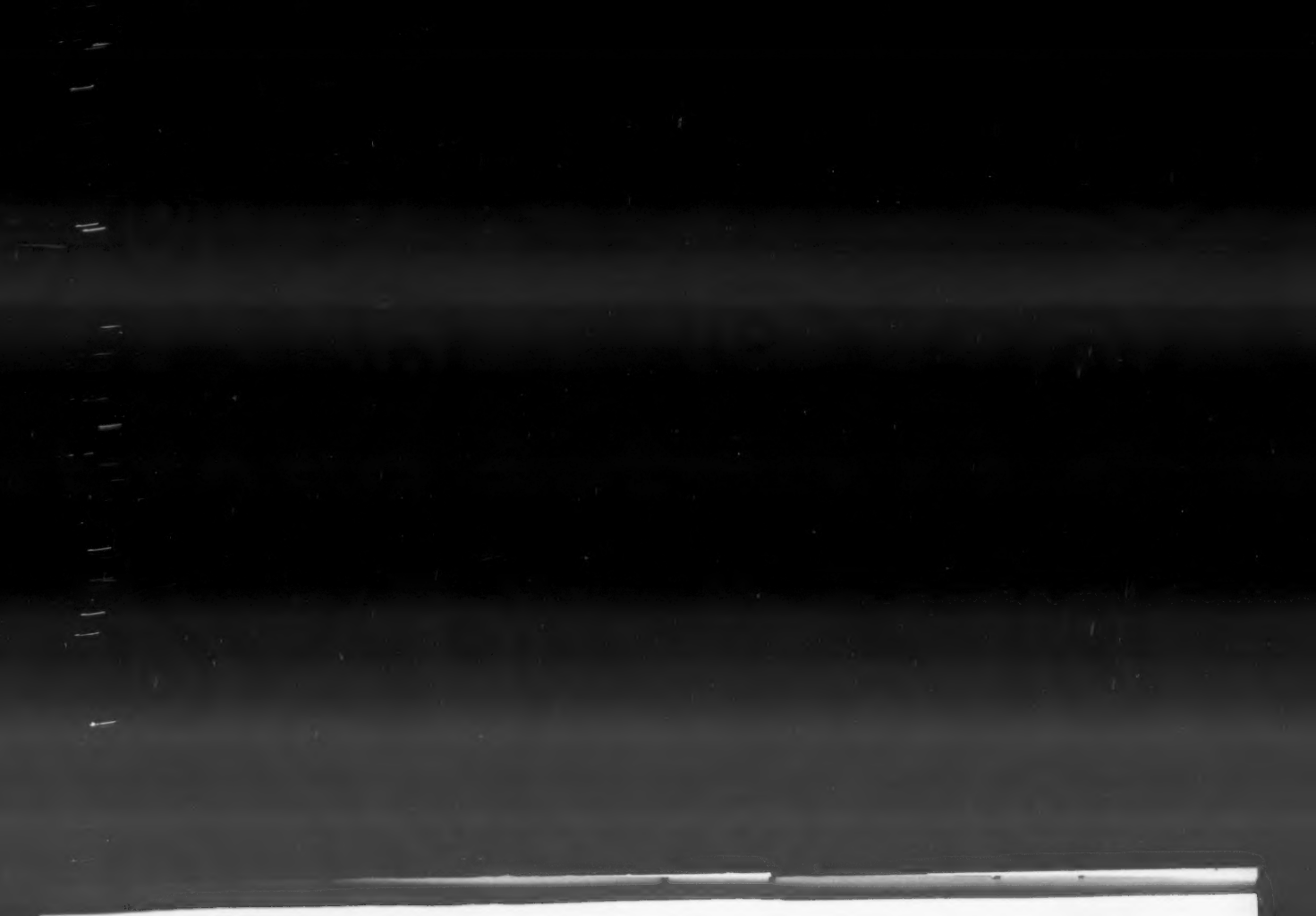

you don't need 2 pairs of hands

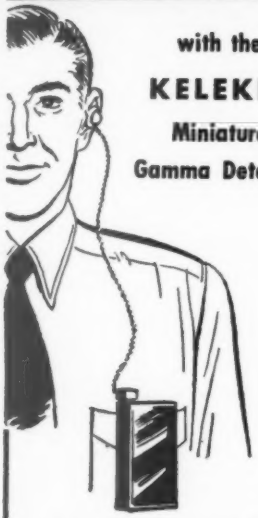

with the

KELEKET

Miniature

Gamma Detector

The Keleket K-550 is the smallest Geiger-Mueller unit made. Easily fastens to pocket, leaving hands free. Convenient, dependable for field or "lab." The versatile K-550 is the ideal choice for many Gamma detection and measurement applications. Sub-miniature detecting elements respond to Gamma and Cosmic radiation or high energy X and Beta radiation. Self-contained power supply uses two replaceable batteries. Simple "on-off" switch. Rugged components. Readily decontaminated.

SPECIFICATIONS

DIMENSIONS
4 3/4" x 2 5/8" x 1 1/8"

EARPHONE
Hearing-aid type; no head-band required.

GM TUBE
Keleket Model K-24, sub-miniature type; for gamma detection; 200 mg/sq. cm.; 300 volt.

BATTERY COMPLEMENT
1—Type C, 1 1/2 volt flashlight battery
2—Minimax, 30 volt, B cells

BATTERY LIFE
A cell: 70 hours (average use)
B Cells: Shelf-life

NORMAL BACKGROUND COUNT
10–12 pulses per minute.

CASE
Smooth black molded plastic. High impact strength. IMMERSION PROOF!

RANGE
From background up to 15R per hour.

PRICE
(F. O. B. Covington, Ky.) $85.00
Replacement GM Tube, Model K-24 . . 5.00

It's Performance that Counts

DEPEND ON THE

INSTRUMENT DIVISION . . . THE KELLEY-KOETT MFG. COMPANY

16—6 E. Sixth St., Covington, Ky.

Leading manufacturer of Instruments for the Atomic Age

Now! THE NEW nuclear "Ultra-Scaler"

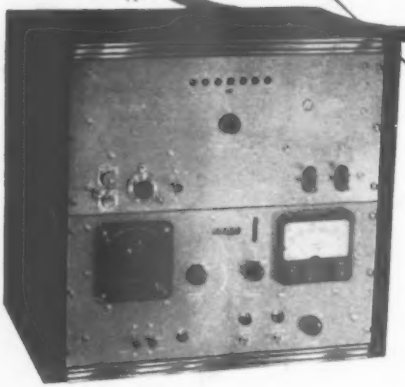

...the most versatile scaling unit available!

☆

● Geiger, proportional or scintillation counting by predetermined count, predetermined time or manual methods, plus monitoring with a probe — you can do all these with the new versatile Nuclear Model 172 "Ultra-Scaler". This wide range of adaptability allows you to do nearly every conceivable counting job, whether research or routine. Where your program is varied and unpredictable, the "Ultra-Scaler" is the right instrument to meet any and all of your counting requirements, with the same reliable accuracy for which all Nuclear instruments are noted.

The "Ultra-Scaler" represents another forward step in Nuclear's effort to provide you with the finest instruments for nuclear measurement. Write today for illustrated catalog giving full detailed information on the "Ultra-Scaler" and the rest of Nuclear's complete line.

nuclear INSTRUMENT & CHEMICAL CORPORATION

236 West Erie Street · Chicago 10, Illinois Cable Address: "Nuclear."

• Scaling Units for Every Type of Radiation Counting • Complete "Packaged" Counting Systems • Health Monitoring Instruments for Personnel Protection • Glass Wall, Mica Window, and Windowless Counters • Portable Count Rate Meters

nuclear "PRECISION INSTRUMENTATION FOR NUCLEAR MEASUREMENTS"